THE FUEL CELL - STATUS AND BACKGROUND*

by

H. A. Liebhafsky and D. L. Douglas
General Electric Co., Schenectady, New York

ABSTRACT

A few historical remarks on fuel cell development and a brief review of chemical thermodynamics as applied to fuel cells will be given. Fuel cells will be classified on the basis of fuel costs; in particular, the hydrogen-oxygen cell developed at General Electric will be used as an example to compute performance of this type of cell.

* Manuscript not received in time for preprinting.

CARBONACEOUS FUEL CELLS*

by

H. H. Chambers and A.D.S. Tantram
Sondes Place Research Institute
Dorking, Surrey, England

ABSTRACT

A brief review of work at the Sondes Place Research Laboratory on high temperature fuel cells will be presented. Particular attention is given to the problem of the operation of high temperature fuel cells on carbonaceous fuels.

* Manuscript not received in time for preprinting.

Recd 14pp ms. Aug 28, 1959 by ORB

Not for Publication

Presented before the Division of Gas and Fuel Chemistry
American Chemical Society
Atlantic City, New Jersey, Meeting, September 13-18, 1959

The Hydrogen-Oxygen (Air) Fuel Cell with Carbon Electrodes

by Karl Kordesch

Research Laboratories
National Carbon Company
Division of Union Carbide Corporation
Cleveland, Ohio

Introduction

The reversal of water electrolysis on platinum electrodes in the first hydrogen-oxygen cell was demonstrated by W. Grove in 1839.[1] Early theoretical publications appeared shortly after 1900. Very extensive competitive efforts to build practical fuel cells started after World War I, ending in the mid-thirties without practical results. The improved heat engine, in spite of the efficiency limit set by Carnot's cycle, discouraged all efforts to construct fuel battery power plants. It is beyond the scope of this paper to mention all the various fuel cell constructions tried during this period. For a comprehensive summary, see the review written in 1933 by E. Baur and J. Tobler.[2]

Practical oxygen carbon electrodes became well known from experiments with air depolarized zinc batteries. Around 1930 G. W. Heise and E. A. Schumacher at the National Carbon Company[3] constructed long lasting "Air-Cells" with caustic electrolyte, more powerful than the earlier cells operating with ammonium chloride. But not before 1943, when W. G. Berl published his studies,[4] was the peroxide mechanism of the carbon oxygen electrode accepted.

After World War II scientists became strongly aware of the need to preserve fossil fuels by obtaining higher energy conversion efficiencies and fuel cell research was revived.

Again it is impossible to mention all the progress made in recent years on many different fuel cell systems, but fortunately most communications are already collected in survey publications and papers.[5,6,7]

As far as the carbon electrode fuel cell is concerned, O. Davtyan in Russia[8] experimented with catalyzed carbon electrodes with unconvincing results. E. Justi in Germany[9] worked initially with carbon, switching later to porous metal electrodes. The lack of durable catalysts and good carbon materials was obvious. The high pressure cell of F. T. Bacon seemed to be the only prospective fuel cell.[10]

In the meantime, realizing that the simplest gas element was a carbon electrode cell operating at room temperature on air, A. Marko and the author, at the University of Vienna, investigated catalyzing procedures which led to high current oxygen electrodes for alkaline cells.[11] A short time later F. Kornfeil,[7] F. Martinola[12] and H. Hunger[13] joined the research group. The performance of hydrogen-oxygen carbon fuel cells looked very promising, but it was still difficult to obtain reliable carbon material.

In 1955 the author joined the National Carbon Company and could make use of the carbon production experience accumulated at this organization. Together

with R. R. Witherspoon and J. F. Yeager, the present fuel cells have been developed.

In the following part of this paper the fundamental principles and the performance parameters of our cells will be stressed. Technical descriptions of the performance of practical batteries have already been presented by G. E. Evans at the Twelfth and Thirteenth Annual Power Sources Conferences of the U.S. Army Signal Research & Development Laboratories.[5]

The Characteristics of the National Carbon Fuel Cell

The construction of a laboratory type hydrogen-air fuel cell with two concentric electrodes is shown in Figure 1. The electrolyte is 30 per cent KOH. The cell produces electricity as soon as hydrogen is fed into the inner carbon tube. The outer tube is exposed to air. With more cells in series a common electrolyte circulation system is provided to remove water or carbonate if necessary. It should be noted that the CO_2-pickup from the air is astonishingly slow. The larger surface of the outer tube offsets the lower current density of the air electrode. With pure oxygen-hydrogen cells we prefer equal-surface electrodes to obtain proper cell balance. Tube bundle cells or plate cells are chosen in this case.

1. The Oxygen Electrode

The transporation of oxygen through the wall of the carbon tube determines the current of the electrode. Fick's law for linear diffusion allows a calculation of the pressure drop between gas side and electrolyte side of the carbon wall.[7] Under a number of operating conditions, it amounts to several percent of the applied gas pressure, depending on the load. No gas escapes into the electrolyte in a properly operating cell. The pore structure is chosen such that a large pressure differential is required to produce gas bubbles on the electrolyte-carbon interface. Penetration of the electrolyte into the carbon is effectively stopped by a special carbon repellency treatment.

The oxygen molecule adsorbed on the carbon surface is ionized in accordance with the 2-electron transfer process:

$$O_2(ads.) + H_2O + 2e^- \rightarrow HO_2^- + OH^-$$ [10]

Using special peroxide decomposing catalysts, the hydrogen peroxide concentration is reduced beyond the sensitivity of analytical tests to an estimated value of 10^{-10} molar. Suitable catalysts for this purpose are described in the patents by Marko and Kordesch.[14] The low concentration of peroxide corresponds to the open circuit potential of 1.10 to 1.13 volts against the hydrogen electrode. The oxygen formed by decomposition of the H_2O_2 is entirely reused. This fact changes the 2-electron process to an apparent 4-electron mechanism. Only the 0.1 volt differences in the open circuit potential of the oxygen-water electrode reveals that the electrode is <u>not</u> following the equation

$$O_2 + 2H_2O + 4e \rightarrow 4OH^-$$

The hydrogen peroxide mechanism on carbon electrodes was also confirmed by E. Yeager and co-workers.[15] The temperature coefficient of the oxygen electrode open circuit potential is -1 mv/°C (negative). Under a load condition of 10 ma/cm^2 we found a positive coefficient of +0.75 mv/°C, increasing with the load.[12]

In accordance with the theory, the oxygen electrode potential must be dependent on the alkali concentration of the electrolyte. The pH function is shown

in Figure 2. The slope of the oxygen-H_2O_2-electrode curve is about 30 to 32 mv per pH unit, in good agreement with the postulated value of 29 mv for a 2-electron process. In solutions containing less than 0.01N-caustic, the potential values are not reproducible. The non-linearity at higher caustic concentration is a direct measure of the activity coefficient. The abscissa indicates normality of the KOH, determined by titration with 1-N-sulfuric acid.

The potential of the oxygen-carbon electrode follows the Nernst equation. As a result, such electrodes can be used for the determination of oxygen partial pressures. The practical usefulness of such electrodes for oxygen sensing elements is very much increased by the fact that a 1 ma/cm^2 load does not cause marked deviations from this behavior in the range between 0.1 to 10 atmospheres pressure.[16] Total pressure changes give the same indication as partial pressure changes on open circuit measurements but not under heavy load conditions. In the latter case the diffusion through the blocking inert gas causes an additional pressure drop across the carbon electrode wall.

Figure 3 shows typical pressure curves of oxygen carbon electrodes, measured against an HgO reference electrode.

The effect of hydrogen peroxide concentrations in the electrolyte has been studied by E. Yeager and co-workers[15] and recently again by W. Vielstich.[17] The influence of the pH value of the caustic electrolyte on the hydrogen peroxide decomposition with and without catalysts was studied by Hunger[13] and led to the remarkable result that a minimum half life of peroxide is observed around pH-14. Different catalysts change the half lifetime several magnitudes but the minimum stays in the same pH region. In strong caustic solutions only the best catalysts are useful. Under pH-13 no catalyst was found which prevented a rapid increase in H_2O_2 half life to values one hundred and one thousand fold that at pH-14.

2. The Hydrogen Electrode

Hydrogen is not active on untreated carbon electrodes as shown by careful experiments with carbons free of heavy or precious metals. On our hydrogen electrodes we deposit a catalyst on the electrode surface.

The reaction occurring at the catalytically active sites of the hydrogen electrode can be represented by the equation

$$H_2\,(\text{gas}) \rightarrow 2H_{(\text{ads. on catalyst})}$$

$$2H(\text{ads.}) + 2OH^- \rightarrow 2H_2O + 2e^-$$

As with the oxygen electrode, the structure of the hydrogen electrode is important for the best gas diffusion rate. A permanent three phase zone: solid/gas/liquid, has to be established by wetproofing of the carbon material. In addition we had to take precautions against "internal drowning" of the H_2-electrode by the reaction product water. As indicated by the equation above, water forms at the anode and this creates a second current-limiting situation, at least at low temperatures. (Water-removing measures will be discussed in a later paragraph.)

The hydrogen electrode also follows the theoretical pH function very closely as is shown in Figure 2. The good reproducibility of measurements makes the carbon-hydrogen electrode a tool for determination of activity coefficients. Electrode equilibria are reached in minutes instead of many hours as is required with the Pt/Pt black electrode.

It is not easy to poison our carbon hydrogen electrodes. In four years of experimental testing of hydrogen electrodes, no electrode has failed as the result of catalyst poisoning, except for experiments in which large amounts of cyanide were deliberately introduced. Oxygen is detrimental only if mixed into the hydrogen in such quantities that large amounts of water form catalytically. This catalytic recombination feature prevents accumulation of a dangerous gas mixture above the electrolyte. In case of accidental gas leakage, this is important.

The open circuit potential has a small negative temperature coefficient. Under load the voltage increases rapidly with temperature, especially in the range between 20°C and 70°C.

The pressure sensitivity on open circuit follows the Nernst equation. Under heavy load conditions, the pressure effect is magnified because of the faster gas diffusion and higher adsorption values reached under pressure.

3. Removal of Reaction Water

In principle there are four ways of disposing of the reaction water:

a. Operation at a temperature near or above 100°C, in the latter case under higher pressure.

b. Operation at low temperatures under reduced pressure; current densities even at 100 mm Hg are above 20 ma/cm^2 at 0.8 volt.

c. Use of gas circulating principle. Water from the electrolyte evaporates through the porous carbon wall especially if a temperature difference is set up. The water removal speed depends also on gas flow rates and is limited by the saturation value of water vapor. With a cell temperature of 70°C and a condenser temperature of 20°C, 180 g of water is transferred by each cubic meter of gas streaming through the electrodes. Evaporation of water occurs on both electrodes, however, we find more water at the anode if the cell is operating.

d. Operation at low cell temperatures, allowing all the water to enter the electrolyte, with concentration of the electrolyte in a separate thermal or low pressure unit. For low power applications considerable dilution of electrolyte can be tolerated. The cell operates as well in 20 per cent KOH as in 50 per cent KOH. For example, a one ampere cell can be operated for one thousand hours with the production of less than one pound of water.

4. Cell Geometry

Because of the many possible fuel cell constructions, a comparison of different electrode arrangements and cell constructions had to be made. Figure 4 shows five basic arrangements of electrodes used in fuel cell constructions. The two-electrode tube cell (A) is the laboratory test cell model, several hundreds of which have been built to investigate electrode performance. The other constructions show remarkable improvements as can be seen from the table in Figure 4. The current factor given in this comparison represents the lower average polarization achieved by a more uniform potential distribution in the cell. The influence of ohmic resistance variations is eliminated by using the pulse current technique.[19] This method made our comparison insensitive to the distance between the electrodes.

The improvement factor in respect to current output per unit volume or weight is more spectacular than the mentioned polarization drop. Cell D, for

instance, is 10 times more efficient in volume utilization than type A. The internal resistance is a major factor to be considered in high current cells. Construction E is many times better than type C at 100 ma/cm^2 current densities, but the difference is negligible at 10 ma/cm^2. These few examples show how important the engineering of fuel cells for special applications can be, independent of electrode performance.

5. Performance Characteristics

Figures 5 and 6 show the voltage/current curves of hydrogen-oxygen carbon fuel cells under different conditions. The ohmic resistance is again eliminated by means of the pulse current (interrupter) technique.[19] All curves on the graph can be compared on an equal polarization basis. To calculate actual terminal voltages in special cells the following values should be used:

Electrolyte resistance: 1.0 to 2 ohm cm. (depending on temperature and concentration)

Electrode spacing: 0.1 to 0.3 cm.

As an example, the voltage drop due to the ohmic resistance in cell components is about 0.02 volt at 100 ma/cm^2 for a parallel plate battery, the terminal voltage of the cell can then be determined by combining this internal resistance loss with the appropriate polarization value from Figures 5 or 6.

6. Life Expectancy

Low temperature, low pressure cells are not subject to electrode attack by electrolyte or oxidation. The only life limiting factor is wettability of the carbon electrodes.[18] The tendency of the electrode to wet appears to depend on the potential at which the electrode operates rather than the current density at which it operates. We have achieved two years' intermittent service on 10 ma/cm^2 and over one year continuous service on 20 ma/cm^2 at 0.8 volt, with tests still in progress. This at atmospheric pressure, between room temperature and 70°C. In the meantime better repellency treatments and more active catalysts have brought our expectations up to 30 to 50 ma/cm^2 over 0.8 volt for at least the same time period. The use of increased pressure gives us the benefit of very high currents at low temperature, at the price of more need of auxiliary equipment. The operation of completely "wet" carbon electrodes under high pressures might give us the additional advantage of reducing maintenance and control devices very considerably.

7. Special Fuels

Hydrogen is an ideal fuel. One-eighth of one pound produces 1 kwhr in a fuel cell. In liquid state hydrogen can be stored for months, with a container weight approximately that of the hydrogen weight.

For every day purposes, hydrides, decomposed by water, are more convenient choices. One pound LiH is equivalent to 1 kwhr.

A practical, widely used fuel cell must operate on air, must be inexpensive and should use a readily available fuel. Our cells operate with high current densities on air with only a small potential difference to the pure oxygen-hydrogen cell. The use of carbonaceous fuels (liquids or gases) at low temperatures is one goal which we are attempting to accomplish. The need of removing carbonate from

the alkaline electrolyte complicates this system.

Unfortunately, the present oxygen-carbon electrode does not function in acid. The use of a redox-chemical intermediate (e.g., bromine) is necessary, which complicates the system.

All halogens operate on carbon electrodes with high current densities in acid systems. As a result hydrogen chlorine fuel cells can be operated at high power outputs for extended periods. Despite the higher voltages and high current densities which can be achieved in hydrogen chlorine fuel cells, the energy output per pound of combined fuel is less than that of the hydrogen-oxygen cell (because of the low equivalent weight of oxygen).

8. Outlook

It may safely be assumed that the fuel cell will eventually become a major power source, replacing other systems in some applications. The fuel cell-operated flashlight is still a long way in the future. For the immediate present, fuel cell applications will probably be restricted to those in which the excellency of fuel efficiency, silence, freedom from fumes, simplicity of design and operation are important requirements.

REFERENCES

1. W. R. Grove, Phil. Mag.III, 14, 129 (1839)
2. E. Baur, J. Tobler, Z. Elektrochem. 39, 148-180 (1933).
3. G. W. Heise, E. A. Schumacher, Trans. Electrochem. Soc. 62, 383 (1932) ibid., 92, 173 (1947), ibid., 99, 191 (1952).
4. W. G. Berl, Trans. Electrochem. Soc. 83, 253 (1943).
5. Proceedings, Twelfth Annual Battery Research and Development Conference, U. S. Army Signal Research & Development Laboratory, 1958 Symposium on Fuel Cells. Proceedings of Thirteenth Annual Power Sources Conf. of the U. S. A. S. R & D Lab., 1959 (in print)
6. A Review of the State of the Art and Future Trends in Fuel Cell Systems, Office of Naval Research, Cont. Nonr 2391 (00), 1958, by E. Yeager, Western Reserve University, Cleveland, Ohio
7. F. Kornfeil, Survey of Galvanic Fuel Cells, AIEE Conference paper 56-327 (1956), F. Kornfeil, Dissertation, Univ. of Vienna (1952).
8. O. K. Davtyan, Bull. Acad. Sci. USSR, Dept. Sci. Techn. 1, 107 (1946) and 2, 215 (1946).
9. E. Justi and co-workers, Jahrbuch Akad. Wiss. Lit., Mainz (1955) ibid., 1956, No. 1. See alsc: H. Spengler, Angenwandte Chemie 68, 689 (1956).
10. F. T. Bacon, Beama J., 61, 6 (1954).
11. K. Kordesch and A. Marko, Oesterr. Chem. Ztg. 52, 125 (1951).
12. K. Kordesch and F. Martinola, Monatsh. Chemie 84, 1, 39 (1953).
13. H. Hunger and A. Marko, 5th World Power Conference, Vienna 1956, No. 275 (paper K/11), H. Hunger, Dissertation, Univ. of Vienna, (1954).
14. A. Marko and K. Kordesch, U. S. Pat. Nos. 2,615,932 and 2,669,598.
15. R. R. Witherspoon, H. B. Urbach, E. Yeager and F. Hovorka, Tech. Report 4, Western Reserve University, ONR Cont. Nonr 581 (00), 1954
16. K. Kordesch and A. Marko, Microchemica Acta 36/37, 420 (1951), K. Kordesch and E. M. King, BuShips Cont. Nobs 72374 (1958).
17. Wolf Vielstich, Z.f. Physikal. Chemie 15, 409 (1958)
18. H. Hunger, Proceedings, Twelfth Annual Battery Research and Development Conf. U.S.A.S.R. & D Lab., 1958.
19. K. Kordesch, Electrochem. Soc. Meeting, Oct., 1956, paper, Abstract No. 27. U.S. Pat. No. 2,662,211.

Figure 1

CONCENTRIC HYDROGEN-AIR-FUEL CELL

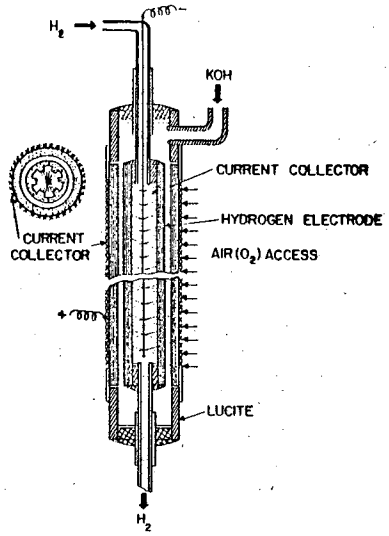

Figure 2

pH-FUNCTION OF THE OXYGEN AND HYDROGEN ELECTRODE

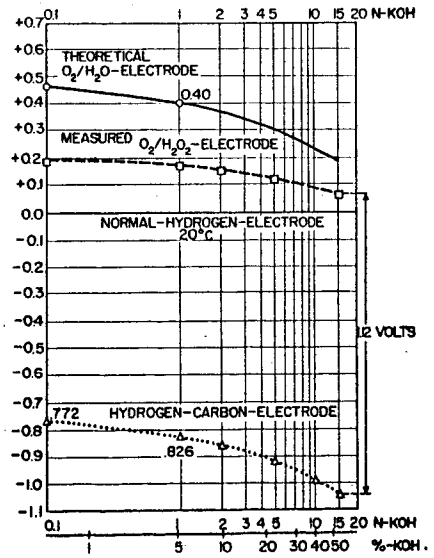

Figure 3

THE POTENTIAL OF THE OXYGEN ELECTRODE
AS A FUNCTION OF PRESSURE

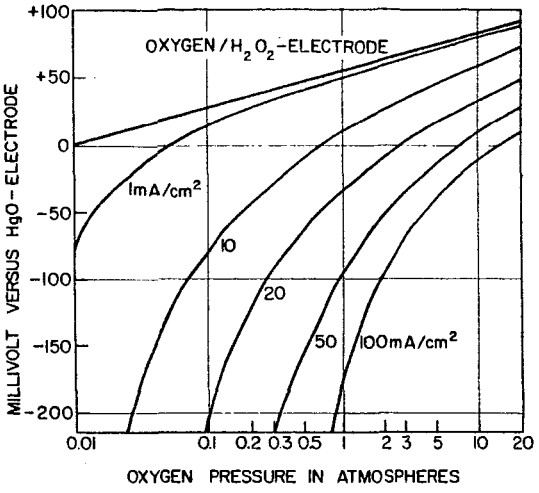

Figure 4

THE EFFECT OF CELL GEOMETRY
ON THE CURRENT OUTPUT OF A CELL

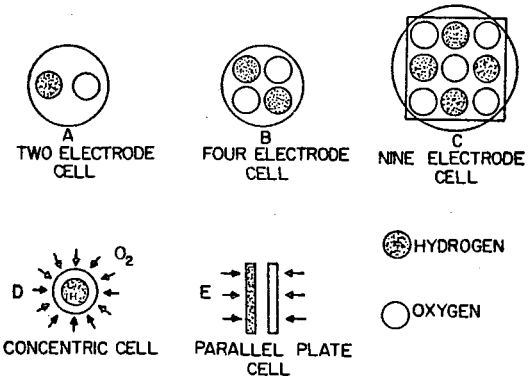

CURRENT DENSITY	CURRENT FACTORS FOR TYPES				
mA/cm²	A	B	C	D	E
10	1	1.4	1.7	1.8	1.8
50	1	1.5	1.8	2.0	2.0
100	1	1.6	2.0	2.5	2.5

Figure 5

PERFORMANCE PARAMETERS
OF NATIONAL CARBON FUEL CELLS

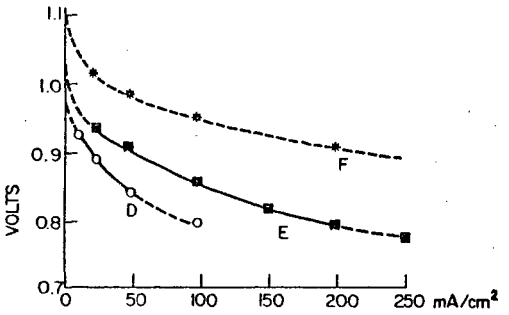

D-CELL AT 60°C O_2/H_2, ATMOSPHERIC PRESSURE(1958)
E-CELL AT 60°C O_2/H_2, 10 ATMOSPHERIC PRESSURE (1958)
F-CELL AT 60°C O_2/H_2, ATMOSPHERIC PRESSURE (1959)
---- DENOTES LACK OF LONG-TIME DATA

Figure 6

PERFORMANCE PARAMETERS
OF NATIONAL CARBON FUEL CELLS

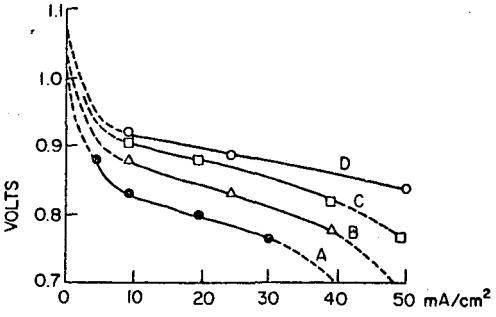

A-CELL AT 50°C O_2/H_2 PRESSURE 100 mm Hg
B-CELL AT 25°C AIR/H_2, 760mm Hg (CONCENTRIC CELL)
C-CELL AT 25°C O_2/H_2, ATMOSPHERIC PRESSURE
D-CELL AT 60°C O_2/H_2, ATMOSPHERIC PRESSURE
---- DENOTES LACK OF LONG-TIME DATA

Not for Publication
Presented Before the Division of Gas and Fuel Chemistry
American Chemical Society
Atlantic City, New Jersey, Meeting, September 13-18, 1959

CATALYSIS OF FUEL CELL ELECTRODE REACTIONS

G. J. Young and R. B. Rozelle
Catalysis Laboratory, Alfred University, Alfred, New York

Research on fuel cells over the past few years has resulted in the development of commercial prototypes of fuel gas cells operating on such gases as hydrogen, carbon monoxide, and hydrocarbons. Several considerations (1,2,3) have dictated the choice of this type of fuel cell (which includes all cells operating directly on fuel gases) over other types. Depending on projected applications and power requirements, fuel gas cells have been designed to operate at low and medium temperatures using aqueous electrolytes (4,5,6) and at higher temperatures using molten salt electrolytes (3,7).

Fuel gas cells, particularly those operating at lower temperatures, are subject to an irreversible free energy process resulting from the interaction of the reactant gases with the electrode surfaces (3,8). The reactant gases are chemisorbed by the electrode catalyst (or the electrode surface, which may act in a similar manner) and the reaction established is between the chemisorbed species and the electrolyte. The potential (free energy) developed by the cell therefore will depend on the equilibrium pressure of the chemisorbed species and has been shown (8) to be inversely proportional to the heat of chemisorption at high coverages. Thus, the catalyst surface can play a dual role in fuel cell electrode reactions - it can enhance the rate of reaction if chemical kinetics are the rate controlling factor, thus playing its usual role as a catalyst, and secondly, it can influence the potential of the cell by minimizing the free energy loss due to chemisorption.

While it is evident that the proper selection of catalysts in the design of fuel cell electrodes is essential for optimum performance, very little systematic work in this area has been published. Our present understanding of catalysis and surface physics, while far from complete, is nevertheless sufficiently comprehensive to enable a general explanation of fuel cell catalysts to be given. The present paper is concerned with a discussion of the activity of a variety of catalysts for both the fuel electrode and oxygen (air) electrode thus giving a guide to the selection of catalysts for specific cell reactions.

FUEL ELECTRODE

The role of the catalyst at the anode in a fuel gas cell is twofold: It must rapidly chemisorb the fuel gas in such a manner as to make it more susceptible to oxidation by the active species of the electrolyte and at the same time it should act to minimize the free energy loss due to chemisorption. Thus, the criteria for an active catalyst generally will be a weak, but rapid chemisorption of the fuel gas. In the selection of a catalyst these conditions must be met in addition to the requirement that the catalyst surface must preferentially

chemisorb the fuel gas species over the reaction products so as to limit self poisoning.

Hydrogen

The chemisorption of hydrogen, particularly on metal surfaces, has been studied more extensively than other fuel gases. At normal temperatures, chemisorption of the type required for high catalytic activity involves a partially covalent surface bond between hydrogen atoms and the d electrons of the metal. Thus, the general requirement for high catalytic activity of a metal in simple gas reactions of hydrogen is that it possesses d band vacancies. This limits the active metal catalysts to the transition elements, although not all of the transition metals are active catalysts even though they chemisorb hydrogen. The early members of the transition series, which have vacancies in both the first and second sub-bands, chemisorb hydrogen strongly and are not particularly good catalysts in hydrogen reactions. The later members of the three transition series, which have vacancies only in the second sub-band, exhibit the lowest heats of chemisorption at the surface coverages involved in heterogeneous reactions, and are recognized as highly active catalysts for hydrogen reactions. Thus, it would appear that the most active metal catalysts for fuel cell electrode reactions where hydrogen is the fuel gas should be selected from those transition metals with d-band vacancies only in the second sub-band- e.g. the group VIII metals.

Confirmation for the views stated above is given by Figure 1 where the open circuit potentials for the hydrogen half-cell are plotted as a function of the approximate number of d-band vacancies of the 5d transition metals and their alloys when used as catalysts at the hydrogen electrode. These data were obtained with a low temperature fuel cell (27°C) employing an aqueous sodium hydroxide electrolyte and porous graphite electrodes which were impregnated with the metal catalysts. In general the catalytic activities of the metals appear to parallel their open circuit potentials e.g. a small free energy loss due to chemisorption generally implies a high catalytic activity. Tungsten and rhenium both have relatively low open circuit potentials and high heats of chemisorption. Tungsten and quite probably rhenium have vacancies in the first d sub-band. The open circuit half cell potential of osmium is intermediate between the latter metals and platinum and iridium. The alloys of platinum-iridium appear to exhibit a maximum in catalytic activity at about one d band vacancy. As the vacancies in the d band of platinum are filled by the s electrons of gold upon alloying, the fuel cell potential decreases sharply until the 60% Au - 40% Pt alloy after which the potential appears to remain relatively constant.

Table I lists the open circuit, hydrogen half-cell potentials for the group VIII transition metals and the neighboring Ib metals. The same trend in catalytic activity is observed in the three transition series, the potential reaching a maximum between the last two transition metals and falling sharply for the following Ib metal. The irreversible free energy loss in chemisorption is larger for the group VIII metals of the first series (Fe, Co, Ni) than for the metals in the second and third series. Also, these metals of the first series are more susceptible to poisoning by impurity gases such as sulfur compounds. Platinum and

Palladium are probably the best catalysts for hydrogen electrodes in fuel gas cells. Although, a maximum in activity is obtained with alloys of certain of these metals the slight increase in potential over the pure metals would probably not justify the difficulties of alloying in commercial practice.

Table I

OPEN CIRCUIT HYDROGEN HALF CELL POTENTIALS FOR GROUP VIII AND Ib METAL CATALYSTS

Fe	Co	Ni	Cu
533	703	693	323
Ru	Rh	Pd	Ag
740	763	743	243
Os	Ir	Pt	Au
603	733	753	263

The results given in Table I for low temperature fuel cells, using aqueous hydroxide electrolyte, in general are paralleled by high temperature cells employing molten salt electrolytes, although the free energy loss on chemisorption often decreases with increasing temperature and consequently is of less importance. For example, palladium and platinum catalysts give higher open circuit potentials with hydrogen as a fuel gas than does nickel, iron, etc. in a variety of molten salt electrolytes. At relatively high temperatures (Ca 500-800°C) the nature of the hydrogen chemisorption changes for several of the group VIII metals. Quite probably, hydrogen forms d s p hybrid bonds with the metal. Indeed, in some cases the catalyst can be poisoned by being heated to a high temperature and then cooled in hydrogen. Presumably, this leaves a strongly bonded form of chemisorbed hydrogen on the surface which is not active in the electrode reaction since the activity of the catalyst can be restored by heating and cooling in helium.

Acetylene and Ethylene

The catalytic activities of the group VIII and Ib metals in the oxidation of ethylene and acetylene in a fuel cell appear to be similar to their activities with hydrogen, i.e. a high catalyst activity is favored by vacancies in the d band of the metal. However, these reaction systems are fundamentally more complex than those of the hydrogen cell. The reactions which occur at the anode are complicated by two factors (i) the nature of the chemisorbed complex, which is in doubt, since either carbon-carbon or carbon-hydrogen bonds may be broken in chemisorption and (ii) the amount of self-hydrogenation at the surface.

The reaction species may be alike in some instances since the fuel cell potentials, for both ethylene and acetylene on certain catalysts, are very similar.

The fuel cell employed for studies of acetylene and ethylene was similar to the cell used for hydrogen except that the electrolyte was a 40% aqueous solution of K_2CO_3. The reactive species in solution may be either the carbonate ion, bicarbonate ion, or the hydroxyl ion. All three ions are present in the solution in reasonable concentrations. Preliminary experiments, however, appear to favor the bicarbonate ion. The products of the reaction at the fuel electrode are in doubt, but first analyses seemed to indicate the presence of aldehydes and carbon dioxide.

The most active catalysts among the metals studied are the group VIII metals of the first transition series along with palladium and iridium as illustrated in Table II.

Table II

Metal	Half Cell Potential (millivolts) Ethylene	Acetylene
Fe	780	790
Co	675	715
Ni	605	595
Cu	410	475
Ru	205	475
Rh	365	535
Pd	710	705
Ag	095	095
W	405	460
Os	425	570
Ir	610	625
Pt	380	570
Au	190	185

The maximum in catalytic activity appears at a different place in each transition series. The group Ib metals, although possessing some activity, are in general poor catalysts for these reactions.

The catalytic activities of these metals in the ethylene and acetylene oxidation reactions at the anode are quite sensitive to the state of the catalyst surface as was the case with hydrogen. This is especially true for the group VIII and Ib metals of the 2nd and 3rd transition series. If, after reduction, these metals are exposed to the atmosphere only momentarily their catalytic activity is decreased

considerably. This is illustrated in Figure 2 where the lower curves represent catalysts with surface oxides. Although the members of the first transition series are susceptible to oxygen poisoning the effect on catalytic activity is much less accentuated.

The most active catalysts are produced by 'in situ' reductions where the surface, after reduction, is not exposed to the atmosphere but remains constantly under hydrogen until the electrode-electrolyte contact is made.

As in the case for hydrogen, a low heat of chemisorption in either ethylene or acetylene will minimize the irreversible free energy loss at the fuel electrode and, hence, produce a higher potential in the fuel cell. There are two factors which determine the heat of chemisorption of ethylene and acetylene: (i) a geometric factor, i.e., interatomic distances in the catalyst lattice, and (ii) an electronic factor. The most favorable interatomic distance, for ethylene hydrogenation, according to Beeck (9), is 3.75 Å as observed in catalyst activity in ethylene hydrogenation reactions. Our results can neither support nor refute this, since the crystal planes exposed are not known and, thus, the more active spacings cannot be predicted. Probably the more important factor is the electronic character of the catalyst. Our results and the results of other investigators support this view (10). Only transition metals or near transition metals catalyze these reactions. Although surface reactions of acetylene have been investigated only to a limited extent, the results of this paper indicate they follow a pattern similar to that of ethylene.

The slight activity shown by the Ib metals in these reactions can be attributed to either their small d-s electron promotion energies (11), which give rise to vacancies in the d band or σ bonding by the metals to these molecules which can be achieved by a rearrangement of the metallic orbital together with the formation of a bond by overlap of the filled d-orbitals with the antibonding orbitals of the adsorbate(12).

Carbon Monoxide

The same type of fuel cell was used for studies on carbon monoxide as with ethylene and acetylene, the electrolyte being a 40% aqueous K_2CO_3 solution.

The catalytic activities of the transition metals investigated in this cell for the anodic oxidation of carbon monoxide are shown in Table III. The variation in the half cell potential among the transition metal catalysts are small with the exception of Palladium which appears to be the most active catalyst for the reaction. The activities of the Ib metals are low as for the fuel gases previously mentioned. This would indicate the necessity of vacancies in the d band of the metal catalysts for a high activity.

The chemisorption of carbon monoxide may take place by a number of different mechanisms. On certain metals, such as palladium and platinum, it chemisorbs with a one site attachment forming a surface layer similar

Table III

HALF CELL POTENTIALS (MILLIVOLTS) FOR CARBON MONOXIDE

Fe	Co	Ni	Cu
-	440	495	190
Ru	Rh	Pd	Ag
475	540	825	225
Os	Ir	Pt	Au
520	510	545	150

in structure to the metal carbonyls, i.e., M = C = O (13). The second mode of chemisorption is a two site sorption with the carbon monoxide complexes covering two surface sites as indicated in the following diagrams (14).

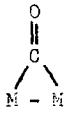

Two site chemisorption probably takes place on rhodium (13) in this manner. The two types of two site mechanisms cannot be differentiated since the lattice geometry required in the metals for chemisorption falls in quite narrow limits, otherwise, the valence angles would be prohibitive. All of the transition metals studied probably expose crystal planes suitable for both mechanisms.

Again the activities of the Ib metals may be due to the small energies required for d-s electron promotion.

OXYGEN (AIR) ELECTRODE

The general requirements of a catalyst at the oxygen electrode of a fuel gas cell are essentially the same as for the fuel electrode catalyst except that negative ion formation is the process under consideration. In cells employing aqueous hydroxide electrolytes, the oxygen must be chemisorbed in such a manner as to lead to the rapid formation of peroxide and hydroxide ions in the presence of water. A further role of the catalyst in this case is to aid in the decomposition of the peroxide.

The most active catalysts, among those investigated, for the electrode reaction of the oxygen half-cell in aqueous hydroxide electrolytes are the oxides of the group Ib metals: copper, silver, and gold. Copper and silver oxides are known to be active oxidation

catalysts (e.g. they must chemisorb oxygen in a state that will readily take part in oxidation reactions) and their presence presumably also promotes decomposition of peroxide ions formed under current drain. Gold films, however, have been reported to be inert toward the chemisorption of oxygen up to 0°C (15). Possibly O_2^- ions are formed on the gold surface as an intermediate step in the reduction of oxygen. Such a species, if present in small amounts, might not be detected in chemisorption experiments since it would be readily removed from the surface on outgassing. The activities of the Ib metal oxides are in the order: copper silver gold.

Cobalt and nickel oxides possess an activity only slightly greater than unactivated graphite which may indicate that these metals are essentially inactive; while iron oxide has a reasonable activity. The open circuit half-cell potentials for the 3d transition oxides and oxides of cobalt-nickel and nickel-copper alloys are shown in Figure 3. As copper is added to nickel, a slight increase in potential starts after the 60% copper- 40% nickel alloy (oxide) is reached and then a rapid increase is observed as pure copper oxide is approached. A similar behavior is found for palladium-silver alloys (oxides) in the 4d transition series.

The activity of oxides as catalysts at the oxygen electrode may be varied considerably by the introduction of a defect structure. It is well known that heterogeneous reactions proceeding by negative ion formation can be profoundly altered by the defect state of the catalyst surface.

ACKNOWLEDGMENT

The authors wish to gratefully acknowledge the financial assistance given by the Office of Naval Research to support this work.

REFERENCES

(1) Liebhafsky, H.A. and Douglas, D.L., Paper 59-SA-22 published by the Am. Soc. of Mechanical Eng. (1959).

(2) Young, G.J. and Rozelle, R.B., J. Chem. Ed. 36, 68 (1959).

(3) Broers, G.H.J., "High Temperature Galvanic Fuel Cells", Ph.D. Thesis, University of Amsterdam, 1958.

(4) Evans, G.E., Proceedings of the Twelth Annual Battery Conference, p. 4 (1958).

(5) Bacon, F.T., Beama, J. 61, 6 (1954).

(6) Bacon, F.T., British Patent 677,298 (1952).

(7) Gorin, E. and Recht, H.L., Paper 58-A-200 published by the Am. Soc. of Mechanical Eng. (1958).

(8) Rozelle, R.B. and Young, G.J., J. Phys. Chem., in press.

(9) Beeck, O., Rev. Mod. Physi. 17, 61 (1945).

(10) Trapnell, B.M.W., "Chemisorption", p. 228 Butterworths Scientific Pub. London, England 1955.

(11) Ibid. p. 74.

(12) Dowdin, D.A. "Chemisorption" p. 9, Butterworths Scientific Pub. 1957.

(13) Trapnell, B.M.W., "Chemisorption", p. 181, Butterworths Scientific Pub. 1957.

(14) Ibid. p. 182.

(15) Ibid. p. 61.

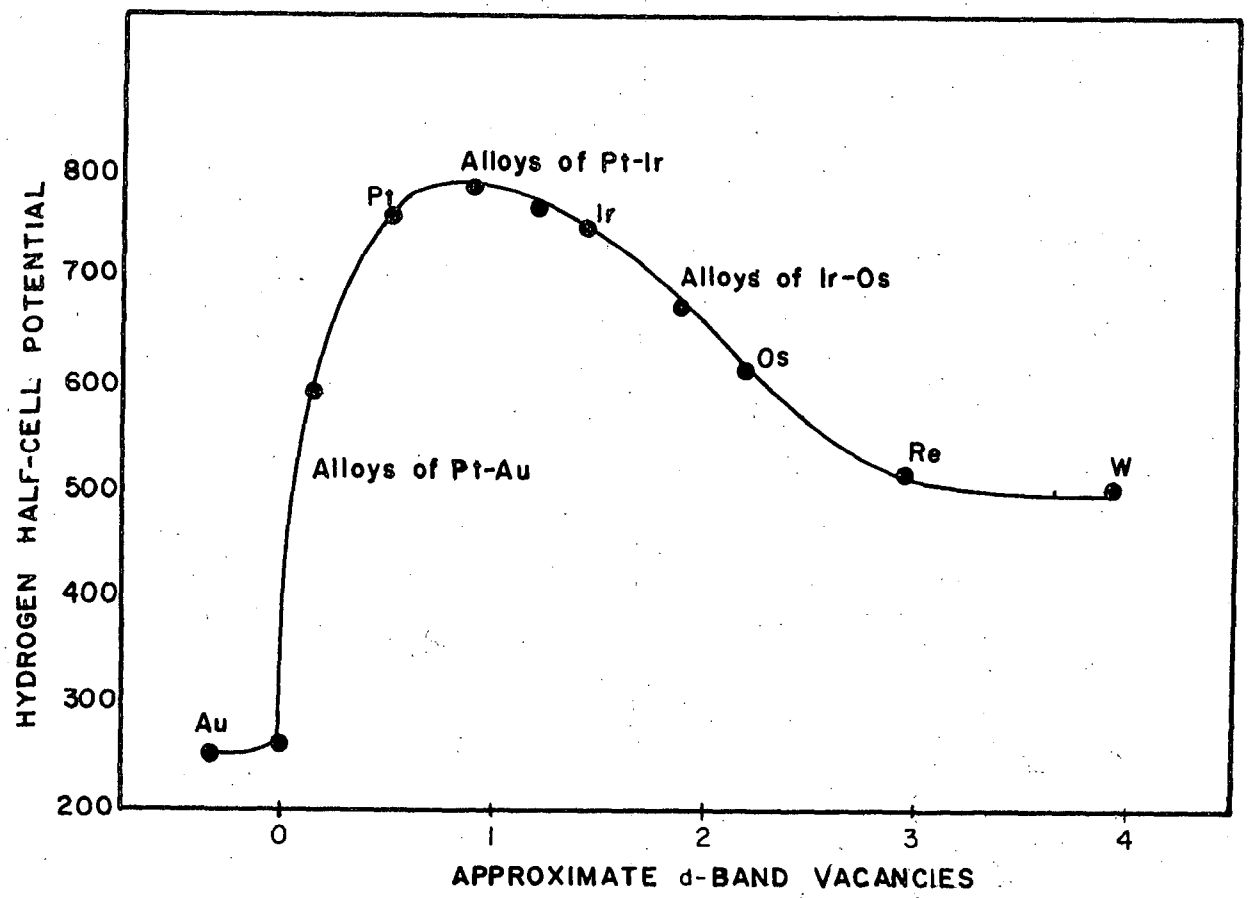

Figure I Hydrogen Half Cell Potentials as a function of d band Vacancies for the 5d Transition

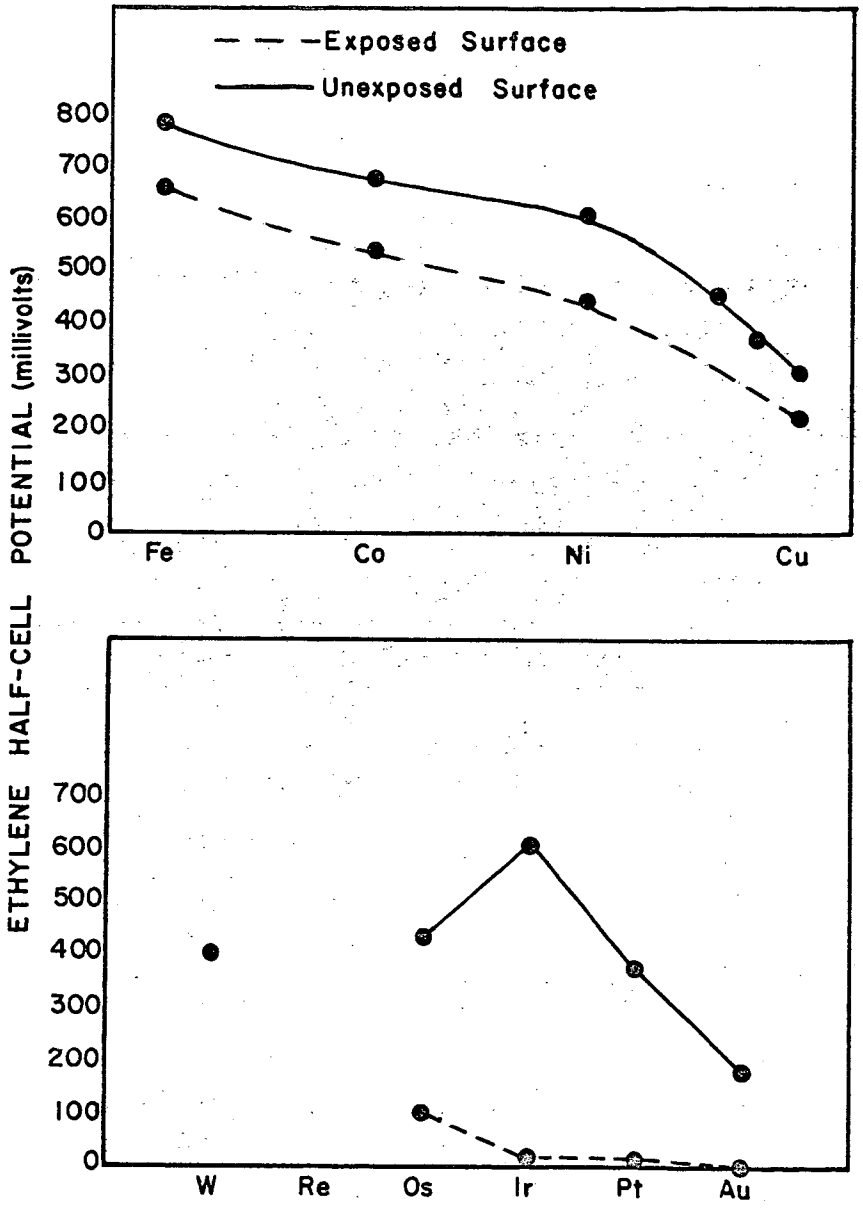

Figure II Ethylene Half Cell Potentials for the 3d and 5d Transition Metals

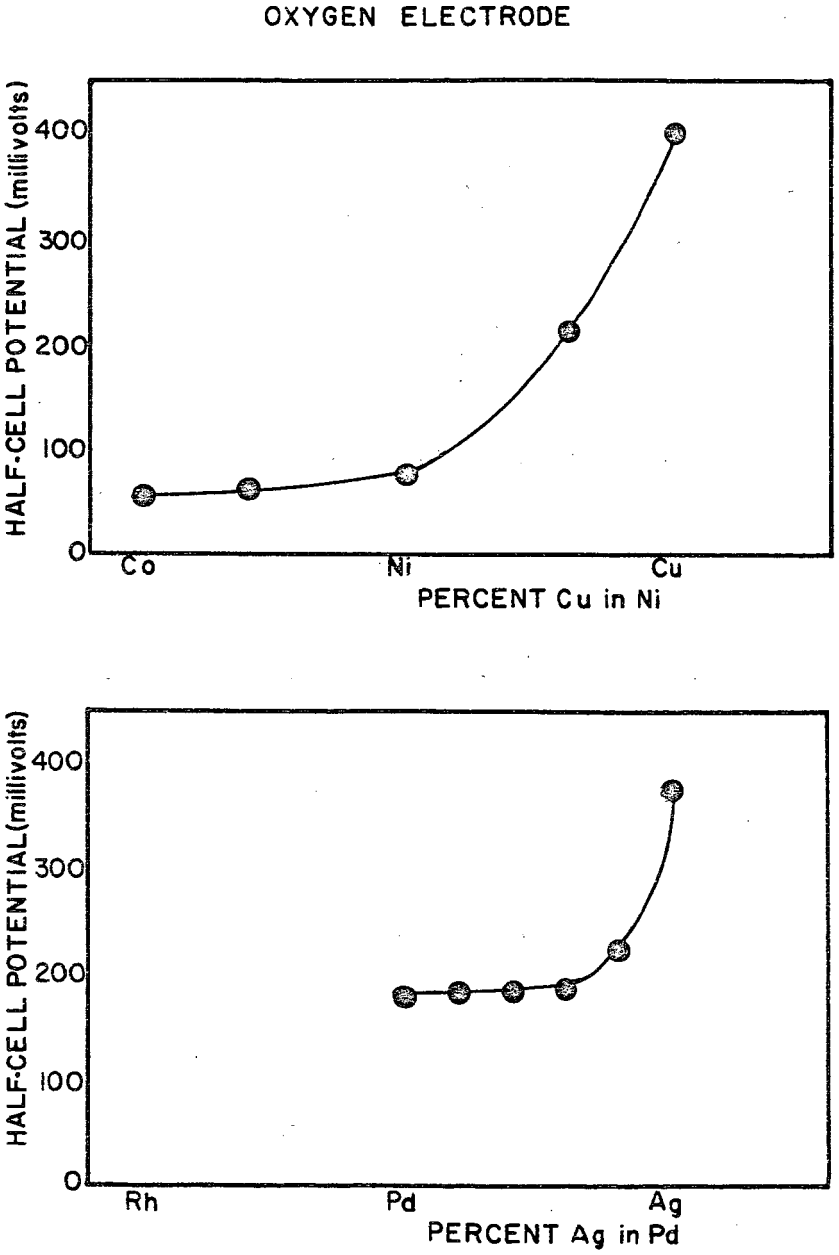

Figure III Oxygen Electrode Half Cell Potentials

Not for Publication

Presented Before the Division of Gas and Fuel Chemistry
American Chemical Society
Atlantic City, New Jersey, Meeting, September 13-18, 1959

The Fundamentals of Electrode Kinetics as They Apply to Low Temperature Hydrogen Oxygen Fuel Cells

L.G. Austin

Fuel Technology Department
The Pennsylvania State University
University Park, Pennsylvania

INTRODUCTION

In a short paper such as this it is impossible to do more than briefly summarize and explain some of the fundamental equations of irreversible electrode kinetics. It is believed, however, that there is a need for such a presentation since many of the workers becoming interested in the field of fuel cells will not be familiar with the terms and concepts involved. The subject is treated with respect to the well known [1] low temperature hydrogen oxygen fuel cell employing porous conducting electrodes.

DISCUSSION

Basic Formulae

The following thermodynamic formulae form the basis of the more specific formulae derived later and are presented for convenience. In any process

$$aA + bB + \cdots\cdots \rightleftharpoons mP + nQ + \cdots\cdots$$

the change in free energy per mole of reaction from left to right is given by

$$\Delta G = -RT \ln K_p + RT \ln \frac{(P)^m (Q)^n \cdots}{(A)^a (B)^b \cdots} \quad (1)$$

a, b, m, n are the number of molecules involved, (A), (B), (P), (Q) are the activities of the reactants and products and K_p is the equilibrium constant of the reaction.

For some arbitrary definition of a standard state where the activities are unity

$$\Delta G_o = -RT \ln K_p \quad (2)$$

where ΔG_o is known as the standard state free energy change. For a substance going from one activity, a_1, to another, a_2, $K_p = 1$, and

$$\Delta G = RT \ln a_2/a_1$$
$$a_2 = a_1 e^{\frac{\Delta G}{RT}} \qquad (3)$$

The rate of an activated chemical reaction in one direction is given by

$$v_1 = k_1 (A)_1^a (B)_1^b ( ) \cdots ( ) e^{\frac{-\Delta G_o^*}{RT}} \qquad (4)$$

where v_1 is the rate of reaction, $(A)_1$, $(B)_1$ are the activities of reactant at the reaction condition, ΔG_o^* is the free energy of activation at the standard state used to define the activities and k_1 is a constant for the reaction.

The electrical potential, E, involved for a change of free energy ΔG is given by

$$\Delta G = -nFE \qquad (5)$$

where F is the Faraday and n is the number of electrons involved in the reaction. A consistent system of units must be used.

Open Circuit Potentials

Hydraulic Analogy

At open circuit, when no current is drawn from the cell, the potential obtained from the cell is equal to the corresponding free energy change in transporting reactant to product under these ideal reversible conditions. Figure 1 shows a hydraulic analogy of a fuel cell at open circuit. Since it is impossible to measure the potential of a single electrode it is necessary to have two electrodes, represented by the two U-tubes of the figure. The difference in levels of the liquid in each arm of a U-tube (h_1 say) represents the free energy change between the reactant and the product for a half cell. For a fuel cell in which reactant is supplied continuously to each electrode and product removed continuously, the hydraulic analogy requires infinite reservoirs at the liquid levels; one of these is shown at A for illustration.

It is impossible to measure the voltage corresponding to h_1 but if the right hand U-tube is considered as a reversible standard state hydrogen half cell, h_2 is arbitrarily taken as zero, and Δ_p corresponds to the half cell potential (with respect to the standard hydrogen half cell) of the left hand electrode. With valve V closed, that is, no flow through the system, $\Delta_p \equiv h_1$, and the open circuit potential, E_r (infinite external resistance is comparable to the valve being closed) is equivalent to ΔG. It is clear from this picture that the potential change <u>through</u> the electrode-electrolyte surface is zero at zero current drain; the potential drop, Δ_p, exists <u>across</u> the external electrode to electrolyte connection. In an electrode process at open circuit, at the instant of electrode immersion ions pass into solution across the

electrode-electrolyte interface. The charge remaining on the electrode produces an attractive electric field holding back further dissolution, while the charge of opposite sign produced in the electrolyte also produces an electric field opposing further dissolution. These forces are equivalent to the p_1 (suction) and p_2 (pressure) in the analogy.

Hydrogen half cell with catalyzed porous carbon electrode and alkaline electrolyte

The half cell reaction can be represented as

$$H_2 + \text{active site} \rightleftharpoons 2[H]_{\text{chemisorbed}} \qquad (6)$$

$$[H] + OH' \rightleftharpoons H_2O + e + \text{active site} \qquad (7)$$

At equilibrium let the fraction of the active sites occupied by chemisorbed hydrogen be θ_e. The fraction of unoccupied sites is then $1-\theta_e$ and the chemisorption equilibrium of reaction (6) can be represented (2) by

$$p(1-\theta_e)^2 i = \theta_e^2 j \qquad (8)$$

where i and j are rate constants and p is the pressure of hydrogen. Thus, from equations (1) and (2), the free energy change on chemisorption is

$$(\Delta G)_c = (\Delta G_o)_c + RT \ln \theta/(1-\theta)p^{\frac{1}{2}} \qquad (9)$$

For reaction (7), the free energy change from the chemisorbed state to product, $(\Delta G)_{C\text{-}H_2O}$, is given by

$$(\Delta G)_{C\text{-}H_2O} = (\Delta G_o)_{C\text{-}H_2O} + RT \ln \frac{(H_2O)(1-\theta)}{(\theta)(OH')} \qquad (10)$$

Substituting for $\theta/1-\theta$ from (9)

$$(\Delta G)_{C\text{-}H_2O} = (\Delta G_o)_{C\text{-}H_2O} + (\Delta G_o)_c - (\Delta G)_c + RT \ln \frac{(H_2O)}{(OH')\,p^{1/2}}$$

Now at equilibrium in the chemisorption process, equation (1) shows that $(\Delta G)_c$ is zero; further $(\Delta G_o)_{C\text{-}H_2O} + (\Delta G_o)_c = (\Delta G_o)_{H_2\text{-}H_2O}$, therefore

$$(\Delta G)_{C\text{-}H_2O} = (\Delta G_o)_{H_2\text{-}H_2O} + RT \ln \frac{(H_2O)}{(OH')\,p^{1/2}} \qquad (11)$$

where $(\Delta G_o)_{H_2\text{-}H_2O}$ is the overall standard state free energy change from hydrogen

to product. From equation (5)

$$nFE_r = nFE_o + RT \ln \frac{(H_2O)}{[OH^-]P^{1/2}} \qquad (12)$$

Thus, at open circuit, the reversible potential E_r should be independent of the chemisorption step and hence independent of the surface or catalyst used. Young and Rozelle [3,4] have presented evidence to show that this is not true, and they ascribe the loss of potential on open circuit as being due to loss of free energy on chemisorption. This immediately raises the question as to why, when hydrogen is allowed to stand in contact with the catalyst surface, a normal adsorption equilibrium fitting a Langmuir or Tempkin isotherm is not reached? Equation (8) can be expressed as

$$\theta = \frac{aP^{1/2}}{1+aP^{1/2}} \qquad (13)$$

where a is a constant at a given temperature. This indicates that the surface is saturated, and hence irreversible, only at infinite pressure. A similar result is obtained by the use of the Tempkin isotherm[5]. The theory of these isotherms states that, providing θ is not continually removed as some other product of reaction, then the gas surface reaction is reversible and will reach an equilibrium state. The modification of the Freundlich adsorption isotherm suggested by Taylor and Halsey[6] gives θ as

$$\theta = (a_o P)^{\frac{RT}{q_m}} \qquad (14)$$

where a_o, q_m are constants. Clearly when $P = 1/a_o$, θ is 1, and hence $1/a_o$ represents a saturation pressure p_s, beyond which further increase in gas pressure (and hence gas free energy) produces no further free energy increase in the surface, and the system is irreversible. The loss of theoretical open circuit voltage, assuming that the Langmuir isotherm (equation 8) has fair numerical agreement with the Freundlich isotherm up to the saturation pressure[7] is approximately

$$E_r - E_{actual} = \frac{RT}{nF} \ln \frac{P}{P_s} \quad , P \not< P_s \qquad (15)$$

Raising the temperature of the cell should bring the cell nearer to reversibility since p_s increases with temperature. Different catalyst surfaces may have different values for p_s.

Young has attempted to correlate the loss of open circuit potential with heats of chemisorption[4]. However, such heats are free energy changes obtained on raising the pressure and consequently have little significance for an equilibrium process. Indeed these heats are often calculated using isotherms derived by assuming that an equilibrium state exists in which the transfer of an infinitesimal quantity of gas to the surface involves no free energy change.

There are other possible explanations for the open circuit voltage loss. It may be that a pseudo equilibrium is reached in which stray currents

are sufficiently large to disturb the equilibrium on a poorly catalyzed surface. Again the attainment of equilibrium may be slow, especially if the activation energy for chemisorption is high and θ_e tends to one. The rate of chemisorption is proportional to $(1-\theta)^2 \exp(-\Delta G_a^*/RT)$.

Under these circumstances it would be expected that the potential of the half cell would increase slowly with time. In general, if such irreversibility exists, it should be difficult to obtain consistent results for open circuit potentials.

Loss of Potential During Current Flow

The polarization or loss of potential during current flow is obviously of prime importance in the design of fuel cells. To obtain good fuel efficiency the cell must be operated at a maximum internal voltage loss of about 20 to 30% of the open circuit voltage. If the current flowing per sq. cm. of electrode area or per pound of cell is small, then the cell will be bulky and uneconomic. The theoretical analysis of polarization is an attempt to show which factors must be varied to obtain optimum conditions.

Activation polarization across the electrode-electrolyte surface

Consider the hydraulic analogy discussed previously. The transfer of ions across the electrode-electrolyte interface, being a chemical reaction, is activated, and the potential energy curve through the surface at open circuit can be visualized as in Figure 2. The energy is composed of the original chemical free energy and the electrical field energies which counterbalance the chemical energy to give zero free energy change across the interface. Stated more precisely, the activities of the reactants and products at the surface change to bring the reaction into dynamic equilibrium. This produces a concentration of electrons in the electrode surface and a concentration of positive ions at the plane of closest approach in the electrolyte; the open circuit potential is due to this double layer. Reducing the external resistance from infinity is comparable to partially opening valve V and allowing flow. Clearly a small flow will increase p_1 slightly and reduce p_2, Δp will decrease, and a pressure gradient is set up across B. In the electrical case this is equivalent to reducing the retaining electric fields and consequently the energy curve on the left in Figure 2 rises and that on the right falls. (See broken curves in Figure 2). The change in free energy through the surface on flow is clearly not available for outside potential and E_r is reduced to E. The rest of the overall free energy change of the reaction is carried through the external circuit by the electrons involved and the reaction can proceed only as fast as the external resistance will allow the current to flow, with Ohm's Law applying.

Let the change in free energy through the surface be $d(\Delta G)$. Then

$$\eta_a = E_r - E = \frac{-d(\Delta G)}{nF} \qquad (16)$$

η_a is called the activation polarization at the given current flow. At short circuit, if there were no other resistances to flow present, then the drop of free energy through the surface would be the total free energy change and $\eta_a = \frac{-\Delta G}{nF} = E_r$ where ΔG is the total free energy change of the reaction.

At open circuit a dynamic equilibrium exists across the interface,

$$[H] + OH' \rightleftharpoons H_2O + e +$$

Let $(a_H)_e$ be the activity of the chemisorbed hydrogen at equilibrium, $(a_{OH})_e$ be that of OH', $(a_{H_2O})_e$ be that of water, and $(a_s)_e$ be activity of active sites. Then from equation (4)

$$\text{forward reaction rate} \quad v_{1e} = k_1 (a_H)_e (a_{OH})_e e^{\frac{-\Delta G_{01}^*}{RT}}$$

$$\text{back reaction rate} \quad v_{2e} = k_2 (a_s)_e (a_{H_2O})_e e^{\frac{-\Delta G_{02}^*}{RT}}$$

The rate may be expressed as amps per sq. cm. of active area, and at equilibrium $v_{1e} = v_{2e} = I'$. Under non-equilibrium conditions, from equation (3)

$$(a_H)(a_{OH}) = (a_H)_e (a_{OH})_e e^{\frac{\Delta G_1}{RT}}$$

where ΔG_1 is the free energy change from equilibrium activities to those considered. A similar expression can be written for the back reaction with a free energy change of ΔG_2. Clearly the free energy changes represent the loss in free energy through the surface due to current flow and

$$-\Delta G_1 + \Delta G_2 = d(\Delta G) = -nF\eta_a$$

Let α be the fraction of η_a aiding the reaction from left to right. Then

$$\Delta G_1 = \alpha n F \eta_a$$

The new reaction rate from left to right is

$$v_1 = k_1 (a_H)(a_{OH}) e^{\frac{-\Delta G_{01}^*}{RT}}$$

$$= k_1 (a_H)_e (a_{OH})_e e^{\frac{-\Delta G_{01}^*}{RT}} e^{\frac{\Delta G_1}{RT}}$$

$$= I' e^{\frac{\alpha n F \eta_a}{RT}} \qquad (17)$$

I' is the equilibrium current corresponding to rate in either direction at equilibrium. Similarly, $\Delta G_2 = -(1-\alpha) nF\eta_a$ where $1-\alpha$ is the fraction of η_a decreasing the reaction from right to left, and

$$v_2 = I' e^{\frac{-(1-\alpha) n F \eta_a}{RT}} \qquad (18)$$

Thus the net current flow from left to right is

$$i' = I' \left(e^{\frac{\alpha n F \eta_a}{RT}} - e^{\frac{-(1-\alpha) n F \eta_a}{RT}} \right) \qquad (19)$$

In general, part of the polarization measured in equation (19) exists through the diffuse part of the double layer [8] extending from the plane of closest approach into the electrolyte. The structure of the double layer can be changed by the presence of salts in the electrolyte, specific adsorption on the electrode surface and electrolyte concentration. Thus I' in equation (19) is changed by these factors. It is easily shown[9] that I' may be represented as

$$I' = (I)_c \, e^{\frac{Fz\psi}{RT}(\alpha n - z)} \qquad (20)$$

where ψ is the potential drop in the double layer and z is the number of electrons involved in transfer through the layer. $(I)_c$ is an equilibrium current which is more nearly characteristic of the reaction, while the term involving ψ can be used to explain the effects of modification of the double layer [10]. For the type of cell considered here the composition of the electrolyte is usually dictated by other considerations and providing specific adsorption is avoided the factor involving ψ is predetermined.

In equation (19), the value of i' was derived per sq. cm. of active site area. Normally, current is expressed per sq. cm. of geometric electrode area and

$$i = (\text{constant}) \quad N_s A_e i' \qquad (21)$$

where N_s is the number of sites per unit effective area and A_e is the effective area per unit geometric electrode area. Then

$$\begin{aligned} i &= k N_s A_e I' \left(e^{\frac{\alpha n F \eta_a}{RT}} - e^{\frac{-(1-\alpha) n F \eta_a}{RT}} \right) \\ &= I \left(e^{\frac{\alpha n F \eta_a}{RT}} - e^{\frac{-(1-\alpha) n F \eta_a}{RT}} \right) \end{aligned} \qquad (22)$$

I is called the exchange current density as it is the equilibrium forward and reverse currents flowing at open circuit. This term is sometimes reserved for the equilibrium current for standard state conditions, I_o, but it is easy to convert from one to the other knowing the cell pressures and concentrations.

As η_a becomes large in equation (22) (and if α does not alter in value) then the reverse reaction becomes negligible and

$$i = I \, e^{\frac{\alpha n F \eta_a}{RT}} \qquad (23)$$

or

$$\begin{aligned} \eta_a &= \frac{2.3RT}{\alpha n F} \log i - \frac{2.3RT}{\alpha n F} \log I \\ &= a + b \log i \end{aligned} \qquad (24)$$

where

$$a = \frac{2.3RT}{\alpha n F} \log \frac{1}{I}$$

$$b = \frac{2.3RT}{\alpha n F}$$

This is known as the Tafel equation. It applies when the polarization is greater than about 100 millivolts. For a required current the polarization is small as I is large. Neglecting double layer effect

$$I = k N_S A_e e^{\frac{-\Delta G^*_{01}}{RT}} \quad \text{(terms in equilibrium activities)} \qquad (25)$$

To obtain low polarization it is desirable to have as much effective surface per unit geometrical area as possible. This is accomplished by having a system of small pores with a high surface roughness in contact with the electrolyte. Thus when using porous carbon electrodes it is sometimes necessary to "activate" the carbon by reaction with air or steam. This burns open pores which were closed and increases the surface roughness. Again, since the reaction takes place at an area of contact of gas, solid and liquid, saturation of the surface with electrolyte will greatly increase polarization.

The function of the catalyst impregnated on the surface is to decrease the activation energy ΔG^*_{01} of the reaction. The standard state free energy change during the reaction is illustrated in Figure 3. Considering the chemisorption step,

$$\Delta G^*_{cf} = \Delta H^*_{cf} - T\Delta S^*$$

The desorption step gives

$$\Delta G^*_{cb} = \Delta H^*_{cb} - T\Delta S^*$$

Therefore

$$\Delta G^*_{cb} - \Delta G^*_{cf} = \Delta H^*_{cb} - \Delta H^*_{cf} = q$$

where q is the exothermic standard state heat of chemisorption[11]. When comparing catalysts, the catalyst with the smaller q should have a smaller ΔG^*_{01} and hence less activation polarization at a given current.

Increase in temperature increases I, but it also reduces the other term in equation (22). Normally the polarization is markedly decreased by increase in temperature. The effect of the quantity of catalyst is governed by N_S. As the quantity is increased from zero the polarization is decreased, but a saturation state is reached when the surface is completely covered with the optimum quantity of catalyst.

Increasing the gas pressure on the cell increases the equilibrium activities and should thus decrease polarization.

Activation polarization of chemisorption.

Equation (22) was derived specifically for the reaction

$$[H] + OH' \rightleftharpoons H_2O + e + \text{active site}$$

However, it is possible that the preceding chemisorption of hydrogen is slow during current flow. If this is true, the electrochemical reaction comes into balance with the chemisorption and an additional polarization is introduced, due to free energy changes on chemisorption. Considering the reaction

$$H_2 + \text{active site} \rightleftharpoons 2[H]$$

the activities may be represented as p, $(1-\theta)^2$ and θ^2. In a similar manner to the derivation of equation (22)

$$i = k N_S A_e p (1-\theta_e)^2 e^{\frac{-\Delta G_c^*}{RT}} \left(e^{\frac{\alpha n F \eta_a}{RT}} - e^{\frac{-(1-\alpha) n F \eta_a}{RT}} \right)$$

$$= I \left(e^{\frac{\alpha n F \eta_a}{RT}} - e^{\frac{-(1-\alpha) n F \eta_a}{RT}} \right)$$

where the rate constant, value of activation energy and exchange current are for the chemisorption process. When the cell is supplying current, θ must decrease to allow more chemisorption. If θ is near 1, a small decrease in θ produces much extra chemisorption but virtually no change in the back reaction; therefore the polarization completely aids the reaction from left to right and $\alpha = 1$. Since $n = 2$, the slope b of the Tafel line under these circumstances is

$$b = \frac{2.303RT}{2F} \simeq 0.03 \text{ volts, at room temperature.}$$

If the chemisorption is fast compared to the electrochemical step the value of θ does not change much and the value of (θ_H) in equation (17) can be considered constant; α is about 1/2, n is 1 and the slope of the Tafel equation is about 0.12 volts[12]. Thus the slope of the Tafel equation gives a means of determining whether the chemisorption step or the electrochemical step is predominantly rate controlling. For chemisorption rate controlling, the function of the catalyst is to lower the activation energy of chemisorption. Activation and chemisorption activation polarization are considered in more detail by Parsons[13].

At sufficiently large current flows, θ tends to zero, α tends to zero and η_a tends to infinity. This expresses the fact that the reaction cannot proceed faster than chemisorption on to an almost bare surface. Thus the complete polarization versus current curve is as illustrated in Figure 4. If θ is not near 1 at open circuit, the curve will start at E_T but its shape will be that of the right hand portion of Figure 4.

Concentration Polarization

Concentration polarization is the loss of potential during current flow due to mass transport limitations in the cell. During current flow reactant has to be transported to the reaction site and energy is thus used in overcoming the resistance to flow which is always present.

Gas transport polarization

Gas transport through a porous carbon electrode is illustrated in Figure 5. If the reversible potential of the cell is for a pressure of p_1, then as the reaction proceeds and p_2 becomes less than p_1, the cell e.m.f. will fall.

If the fall is η_c at a current of i

$$\eta_c nF = RT \ln \frac{P_1}{P_2} \qquad (26)$$

Assuming the carbon has an effective diffusion coefficient D_{eff}, independent of pressure [14] and that the electrode is in the form of a slab

$$\text{Rate} = D_{eff} \frac{(P_1 - P_2)}{\Delta L} \quad \text{per sq. cm.} \qquad (27)$$

ΔL is the thickness of the electrode. Equation (27) may be expressed as

$$i = B (P_1 - P_2)$$

where B includes a conversion factor. Then

$$\eta_c = \frac{RT}{nF} \ln \frac{P_1 B}{P_1 B - i}$$

Since the maximum value of $P_1 - P_2$ is P_1, BP_1 represents a limiting current, I_ℓ say, and

$$\eta_c = \frac{RT}{nF} \ln \frac{I_\ell}{I_\ell - i} \qquad (28)$$

When i is small compared to I_ℓ, η_c is linearly dependent on i, and as i approaches I_ℓ, polarization becomes very great. Thus it is desirable for I_ℓ to be large. The thickness of the electrode cannot in practice be reduced beyond a certain limit. Due to the inhomogeneous nature of the pore system, reducing the thickness tends to give either gas leakage from the surface or flooding of the pore system by the electrolyte. Thus it is desirable to have an electrode which has a high diffusion coefficient, high internal area or roughness factor and which is as homogenous in pore structure as possible. In operation, since p_2 has to be maintained sufficiently high to prevent electrolyte flooding, p_1 would have to be raised as concentration polarization becomes appreciable.

Electrolyte concentration polarization

In a similar manner to that above the concentration polarization due to mass transfer of ions is

$$\eta_c = \frac{RT}{nF} \ln \frac{i_\ell}{i_\ell - i}$$

where the limiting current i_ℓ is given by

$$i_\ell = \frac{D_i z F a_1}{(1 - t_i)\delta} \qquad (29)$$

D_i , a_i, t_i are respectively the diffusion coefficient, bulk activity and transport number of the ion and δ is the effective thickness of the diffusion layer adjacent to the electrode surface. This type of polarization is well described by Kortüm and Bockris [15].

The effect of concentration polarization can be introduced into equation (22) by writing

$$\alpha_1 \eta_o = \alpha \eta_a + \eta_c$$

where η_o is the overall polarization and η_c is the concentration polarization in the same direction as $\alpha\eta_a$. Considering just this direction

$$\begin{aligned} i &= I\, e^{\frac{\alpha n F \eta_a}{RT}} \\ &= I\, e^{\frac{\alpha_1 n F \eta_o}{RT}} e^{\frac{-nF\eta_c}{RT}} \\ &= I\, \frac{C_r}{C_{ro}}\, e^{\frac{\alpha_1 nF\eta_o}{RT}} \end{aligned} \qquad (30)$$

where C_r is the effective activity and C_{ro} is the original bulk activity of the reactants. $C_r/C_{ro} = I_e - i/I_l$ thus i appears on both sides of equation (3). The general form of the equation is similar to that in Figure 4. The introduction of concentration polarization in equation (22) must be made for all of the steps in the reaction which give appreciable concentration polarization.

Ohmic Resistance

In addition to the polarization already described an internal loss of potential, η_r , occurs due to the electrical resistance of the electrolyte. By Ohm's Law

$$\eta_r = i r$$

r is low for high concentration of ions in the electrolyte. It is of interest to note that if penetration of electrolyte into the pore system occurs, then the effective conductivity for ionic conduction is [16]

$$C_{eff} = \frac{\epsilon}{q} C_{free} \qquad (31)$$

where ϵ is the porosity of the carbon and q is a tortuosity factor. For porous carbon electrodes ϵ is of the order of 1/3. q may be very high[17] but is often[18] about 2 to 3 Thus a penetration of 1 mm will usually give as high an electrical resistance as about 1 cm of the free electrolyte between the electrodes.

The Oxygen Alkali Half Cell

If the oxygen half cell reaction were

$$\tfrac{1}{2} O_2 \rightleftharpoons [O] \quad , \quad [O] + H_2O + 2e \rightleftharpoons 2\,OH'$$

then the standard state potential of an hydrogen oxygen fuel cell should be about 1.23 volts at room temperature. However, it has been shown[19,20] that the half cell reaction is

$$[O_2] + H_2O + 2e \rightleftharpoons HO_2' + OH'$$

Since the normal cell is not standard with respect to peroxide concentration the open circuit potential is usually not 1.23 volts. It is easily shown that if the peroxide ion is rapidly decomposed to its equilibrium value with respect to oxygen (in the electrode) and hydroxyl then the cell voltage would again be 1.23 volts. Even if peroxide decomposing catalysts are employed it appears that, at room temperatures, the decomposition is not sufficiently rapid for this equilibrium to be reached near the electrode surface and a loss of ideal potential occurs[21].

CONCLUSION

In studying the polarization of the type of fuel cells considered here it is important to determine the contribution of each type of polarization to each half cell. If such determinations are made, they will indicate what can be done to improve the performance of the cell. The various techniques for determining each polarization are described in the literature[12,15,22]. However, even if optimum conditions for minimum polarization are obtained, there are still many mechanical and technological difficulties to overcome in the construction of operating fuel cells.

REFERENCES

1. Evans, G.E., Proceedings, Twelfth Annual Battery Research and Development Conference, U.S. Army Signal Research and Development Laboratory, 1958 Symposium on Fuel Cells.
2. Trapnell, B.M.W., "Chemisorption", Butterworth's Scientific Publications, London (1955), p.111.
3. Young, G.J. and Rozelle, R.B., Journal of Chem. Education, 36 (1959) 68.
4. Young, G.J. and Rozelle, R.B., Private Communication (1959).
5. Trapnell, B.M.W., "Chemisorption", Butterworth's Scientific Publications, London (1955), p.126.
6. Halsey, G. and Taylor, H.S., J. Chem. Phys. 15 (1947) 624.
7. Trapnell, B.M.W., "Chemisorption", Butterworth's Scientific Publications, London (1955), p.118.
8. Frumkin, A.N., Bagotskii, V.S., Iofa, Z.A., and Kabanov, B.N., "Kinetics of Electrode Processes", Moscow University Press, Moscow (1952), 177.
9. Berzius, T. and Delahay, P., J. Am. Chem. Soc. 77 (1955) 6448.
10. Frumkin, A.N., Trans. Faraday Soc. (London) 55 (1959), 156.
11. Trapnell, B.M.W., "Chemisorption", Butterworth's Scientific Publications, London (1955), p.209.
12. Potter, E.C., "Electrochemistry", Cleaver-Hume Press Ltd., London (1956), p.133.
13. Parsons, R., Trans. Faraday Soc. (London) 54 (1958), 1053.
14. Walker, P.L. Jr., Rusinko, F. and Austin, L.G., "Advances in Catalysis", Vol. XI, Chapter on Gas Reactions of Carbon, Academic Press Inc., New York, 1959, in press.
15. Kortüm, G. and Bockris, J. O'M., "Textbook of Electrochemistry", Vol. II, Elsevier Pub. Co., New York (1951), p.400.
16. Carman, P.C., "Flow of Gases Through Porous Media", Academic Press Inc., New York (1956), p.46.
17. Dutcheon, J.M., Longstaff, E. and Warner, R.K., Preprints of Conference on Industrial Carbon and Graphite (London), 1957, "Flow of Gases Through Fine-Pore Graphite".
18. Wiggs, P.K.C., Preprints of Conference on Industrial Carbon and Graphite (London), 1957, "Gas Permeability and Pore Size Distribution".
19. Berl, W.G., Trans. Electrochem. Soc., 83, (1943) 253.
20. Witherspoon, R.R., Urbach, H., Yeager, E. and Hovorka, F., Technical Report No. 4, Electrochemistry Research Laboratory, Western Reserve University (1954).
21. Kordesch, K., and Marko, A., Oesterr. Chem. Ztg. 52 (1951) 125.
22. Broers, G.H.J., Ph.D. Thesis, University of Amsterdam (1958).

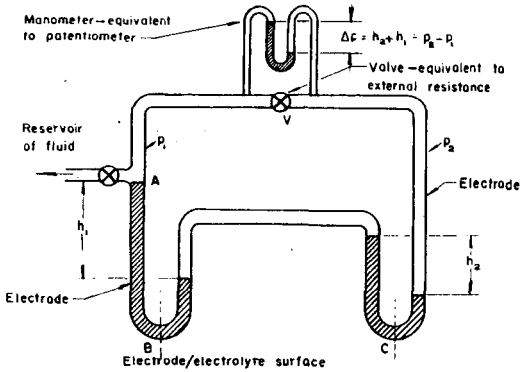

FIG. 1 Hydraulic analogy of a hydrogen–oxygen porous electrode fuel cell.

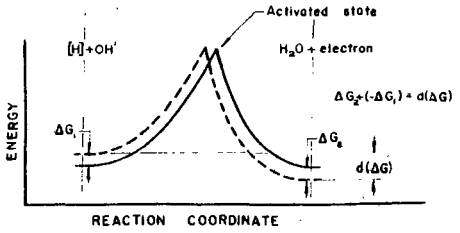

FIG. 2 Representation of energy state of reaction across electrode – electrolyte interface

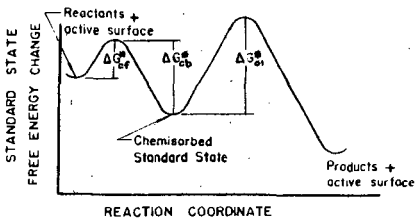

FIG. 3 Illustration of standard state free energy changes during reaction.

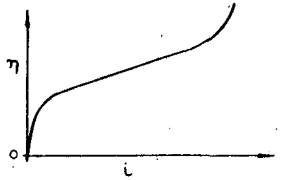

FIG. 4 Illustration of variation of chemisorption polarisation with current flow.

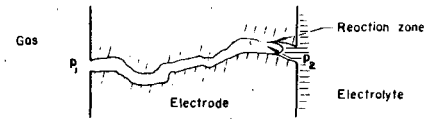

FIG. 5 Illustration of gas transport process in a porous electrode.

Not for Publication

Presented before the Division of Gas and Fuel Chemistry
American Chemical Society
Atlantic City, New Jersey, Meeting, September 13-18, 1959

THE HIGH PRESSURE HYDROGEN/OXYGEN FUEL CELL

F. T. Bacon, M.A., A.M.I.Mech.E.
Marshalls' Flying School, Ltd.
Cambridge, England

1. Introduction.

The hydrogen/oxygen cell is particularly attractive, when compared with other types of fuel cell, for a number of reasons; it has always appeared likely that a practical unit could be developed working at low or medium temperatures, and it raises the interesting possibility that it could be used as a kind of electrical storage battery, the two gases having been previously generated by the electrolysis of water, using power produced on a large scale.

Moreover, when the author first became interested in fuel cells in 1932, a search through the available literature soon showed that the most promising results had in fact been obtained with this type of cell. The cell was first described by Sir William Grove in 1839(i), and in 1889, particularly good results were recorded by the great chemist Ludwig Mond and his associate Charles Langer (ii), they achieved a current density of 6A/ft.^{2}(6.5m A/cm^2) at 0.73 V., using either oxygen or air, and they also showed that the best results were obtained when the platinized platinum electrodes were kept substantially dry on the gas side. Further progress was prevented largely because of the high cost of the platinum electrodes.

Since the end of the second World War, a great deal of interesting work has been done in many countries on the hydrogen/oxygen cell, and this need not be referred to in detail here. Particular reference, however, should be made to the work of Davtyan(iii) and Kordesch(iv) and his associates.

2. Types of Cell Investigated.

In 1938 a small cell similar to Grove's original gas battery was constructed, and fair results obtained; but when activated nickel gauze electrodes were used, in conjunction with an alkaline electrolyte of potassium hydroxide, the results were poor, even when the temperature was raised to the boiling point of the liquid.

It was next decided that the problem would have to be attacked essentially from an engineering point of view, and that with this type of cell operation under pressure could not be avoided if high current densities were to be obtained, in conjunction with comparatively cheap materials of construction such as nickel. So in 1939 a cell was designed which would stand a pressure of 3000 p.s.i. and any reasonable temperature (Fig.1).

The electrolyte was a 27% solution of potassium hydroxide and the cylindrical electrodes were of nickel gauze, activated by alternate oxidation in air and reduction in hydrogen; they were separated by a diaphragm of asbestos cloth. Other metals, such as platinum, palladium, silver and copper were tried, but were discarded in favour of nickel, partly because of cost and corrosion difficulties, but mainly because of the superior performance shown by nickel under these circumstances. The cell was tested by alternately charging it from an external source of direct current and discharging it through an ammeter and variable resistance at a constant current. It was found finally that a current density of 12.2 A/ft.^{2} (13.1m A/cm^2) of the external surface of the inner electrode could be maintained for 48 minutes at about 0.89 V., with a temperature of 100°C; many thicknesses of gauze and fairly high pressures were used to get these results. Curiously enough, no advantage was obtained by using higher temperatures than 100°C., and this was tentatively ascribed to the irreversible anodic oxidation of the oxygen electrode during the charging period.

The next stage was to construct two cells, one acting as an electrolyser for generating the two gases and the other being the current-producing cell (Fig.2). The gases produced in the electrolyser were carried separately up into the cell in solution in the electrolyte, the liquid returning to the electrolyser through separate pipes. Activated nickel gauze electrodes and asbestos diaphragms were again used, but this time in the form of flat discs.

It was found that the performances of this cell improved continuously with increasing temperatures and pressures up to 240°C. and 1075 p.s.i., the highest tried. The highest current density obtained at 240°C. was 75A/ft.^{2} (81m A/cm^2) at 0.65 V. with six gauze electrodes on each side of the cell. The current density appeared to be limited by the rate at which fresh gas could be brought up to each electrode in solution in the electrolyte. The materials and methods of construction used proved to be reasonably satisfactory.

3. The Present Cell with Diffusion Electrodes.

At this stage it was still considered that the performance was not good enough for any practical application, bearing in mind that high pressures inevitably lead to higher container weights than would be necessary with a fuel cell working at atmospheric pressure. So it was decided that a new apparatus should be built with the gases confined to the backs of porous nickel electrodes; this design has been used with very little change ever since.

The details of the construction of the cell have often been described before (v), but it is probably best to recapitulate them briefly here.

A single cell is illustrated diagrammatically in Fig.3. The electrodes are made of porous sintered nickel, and the main cell parts are of nickel-plated steel or pure nickel; the electrolyte is strong potassium hydroxide solution, between 37 and 50% concentration. The normal operating conditions are 200°C. and 300-600 p.s.i.. At the present time a pressure of 400 p.s.i. is normally being used. The porous nickel electrodes, which are about one sixteenth of an inch thick, have a pore size of about 30 microns or more, on the gas side, with a thin layer of much smaller pores on the liquid side; a small pressure difference is

set up in the apparatus across each electrode, so that the liquid is expelled from the large pores on the gas side, but the gas cannot bubble through the smaller pores on the liquid side owing to the surface tension of the liquid. The interior of the 30 micron pores, which are wetted throughout with electrolyte, presents a large surface for absorption of gas. The oxygen electrodes are subjected to a pre-oxidation treatment at a high temperature in air, and this protects them from corrosion by the high pressure oxygen and electrolyte. Lithium atoms are incorporated into the crystal lattice of the nickel oxide, thus converting the ordinary green nickel oxide, which is an insulator, into a black double oxide of nickel and lithium, which is a good semi-conductor.

With this arrangement, the gases are of course supplied from cylinders in the normal way; other advantages over previous designs are that the gas sides of the electrodes are coated with only a very thin layer of electrolyte, giving a very short diffusion path for the gases in solution before reaching the active surface of the electrodes, the useful surface area of the electrodes is greatly increased, and the asbestos diaphragm is eliminated.

4. Electrode Design.

A good electrode design is of course of the utmost importance, and several different designs have been tried. The largest electrodes made so far are 10 in. effective diameter, though this does not by any means represent the limit in size; they are sintered directly onto a flat circular perforated sheet of nickel or nickel-plated steel, about one sixteenth of an inch thick; this provides adequate strength, and serves also to conduct away the current generated. Electrodes up to 5 in. diameter were previously made without a backing plate of solid metal, but it was considered unlikely that larger ones would be satisfactory, without adequate support. Separators, in the form of narrow vertical strips of p.t.f.e., have to be used with 10 in. diameter electrodes, to prevent internal short-circuits when the pressure difference is applied.

An alternative from of electrode which has been employed comprises a bipolar structure with recesses machined on either side of a solid metal plate, each recess then being filled with porous sintered nickel for a hydrogen and oxygen electrode respectively. A thin dimpled perforated plate is first sintered into each recess, and this leaves a narrow space for leading the gas from ports in the rim to all parts of the porous metal. When bipolar electrodes of this type are assembled in series, with gaskets of insulating material between each, they form a series of cells which do not require any external current connection except at each end of the battery. This electrode construction is attractive in many ways, and leads to a very compact battery, but it has temporarily been abandoned in favour of the simple unipolar design, mainly owing to difficulties in manufacture.

The coarse pore layers of hydrogen electrodes are made from Grade B carbonyl nickel powder (average particle size 2-3 microns) mixed with about 20% by weight of 100-240 mesh ammonium bicarbonate which acts as a spacing agent during sintering; it is pressed lightly in a rubber press, and then sintered for about $\frac{1}{2}$ hour at 850°C. in a reducing atmosphere. The fine pore layer is then applied as a suspension of Grade A carbonyl nickel powder (average particle size 4-5 microns) in alcohol; this is sintered for $\frac{1}{2}$ hour at 800°C., any leaks being repaired by further thin applications of A nickel as before.

The coarse pore layers of oxygen electrodes are now usually made from Grade D carbonyl nickel powder (average particle size 7-9 microns) mixed with 15-20% of 100-240 mesh ammonium bicarbonate; it is pressed lightly and sintered for $\frac{1}{2}$ to 1 hour at 1000°-1150°C. in a reducing atmosphere. The fine pore layer is again of Grade A nickel, sintered for $\frac{1}{2}$ to 1 hour at 950-1000°C. Alternatively, the coarse pore layers of the oxygen electrodes may be made from a coarse nickel powder, about 200-250 mesh, without a spacing agent; but in this case a higher compressing pressure and a higher sintering temperature (1150°C. as a minimum) are required to get a really strong compact.

Finally the oxygen electrodes are pre-oxidised after impregnation with a dilute solution of lithium hydroxide and drying; air is used for oxidation, and a satisfactory thickness of oxide is formed in $\frac{1}{4}$ to 1 hour at 700°-800°C.

Hydrogen electrodes are activated by impregnation with a strong solution of nickel nitrate, followed by a roasting treatment in air at 400°C. and finally reduction in hydrogen at about the same temperature. Work is proceeding on the activation of oxygen electrodes, but a standard treatment has not yet been arrived at.

Typical microsections of hydrogen and oxygen electrodes are shown in Figs. 4 and 5.

5. Prevention of Corrosion of Oxygen Electrodes.

When porous nickel electrodes were first put into use, serious trouble arose with the gradual corrosion of oxygen electrodes, leading first to a drop in output and finally to complete breakdown. This trouble has now been largely overcome by the pre-oxidation treatment already described. It was first found that samples of nickel pre-oxidised in air at about 800°C. were extremely resistant to corrosion when subsequently exposed to strong KOH solution and oxygen under similar conditions to those in the cell. But the green oxide layer produced during pre-oxidation is an electrical insulator, so an electrode protected in this way would be useless in the cell. However, it was ascertained that if lithium atoms are incorporated into the crystal lattice of the nickel oxide, a black double oxide of nickel and lithium is produced, which is a good semiconductor(6); and the corrosion resistance is unimpaired, or even enhanced. Using this technique, oxygen electrodes have been in operation in the cell for periods up to 1500 hours at 200°C. without failure, and with only a very small drop in performance. Specimens of pre-oxidised nickel have been exposed to oxygen under pressure and potassium hydroxide solution at 200°C. for more than 10,000 hours without visible deterioration; and accelerated corrosion tests at a higher temperature have shown that considerable improvement on this figure should be possible. It should be mentioned here that before the pre-oxidation treatment had been introduced, experiments were made with various corrosion inhibitors which were dissolved in the electrolyte; potassium silicate and potassium aluminate were particularly successful in arresting corrosion of oxygen electrodes, but they also reduced the performance of the cell to a serious extent. It is believed that this provides the explanation for the curious fact that no corrosion of oxygen electrodes was observed when using the previous cells with nickel gauze electrodes; these earlier cells all had diaphragms of asbestos cloth, and it is to be expected that the electrolyte would therefore become somewhat contaminated with potassium silicate or aluminate. It is interesting also that a small amount of copper, added to the KOH in the form of copper oxide, was also effective as a corrosion inhibitor and in all cases led to the formation of a black oxide on the nickel.

The results of some accelerated corrosion tests on samples of nickel pre-oxidised in the presence of lithium hydroxide, and exposed to 65% KOH and oxygen at 300°C. and 800 p.s.i. total pressure, are shown graphically in Fig.6. The samples were placed in oxidized nickel crucibles, which were set up in autoclaves; the samples were half in and half out of the KOH solution. The gas space was filled with oxygen under pressure, and readings of temperature and pressure were recorded periodically. The autoclaves were opened at intervals and the samples washed in distilled water, dried and weighed; the extent of corrosion was indicated by the weight change. Fresh KOH solution was used in each run. These curves emphasize the importance of a sufficiently thick oxide layer, in order to obtain really good durability. It is estimated that an oxide layer about 3 microns thick can be obtained by coating the nickel with 2 g. of lithium hydroxide per square metre of surface and oxidising in air at 800°C. for 16 minutes.

In Fig. 7 some results of tests at 200°C, 260°C. and 300°C. have been plotted together. These samples are not exactly comparable due to differences in the initial thickness of the oxide coating and in the conditions under which the corrosion tests were carried out. It is possible to say, however, that similar samples corrode at 200°C. much more slowly than at 260°C.. Also a further considerable increase in corrosion rate is produced if the temperature is raised to 300°C.. By pre-oxidising the samples to produce an increase in weight of 5g/metre^2 instead of 2-3g/metre^2, the rate of corrosion at 300°C was reduced considerably as shown in Fig.6. It seems reasonable to suppose that if the samples oxidized, with lithium present, to give an increase in weight of 5g/metre^2 were tested at 200°C., they would give a life many times longer than those already tested at this temperature (Fig.7). Even if it were to prove impossible to produce such a thick oxide layer on the oxygen electrode, a thinner layer of 2g/metre^2 will protect an electrode for more than 10,000 hours at 200°C.

6. Jointing Material.

There must be at least one electrically insulating gasket per cell, and at the present time, using unipolar electrodes, four gaskets must be used per cell..

Many different materials have been tried, but at the present time nothing has been found which is superior in all respects to ordinary compressed asbestos fibre jointing, which is mainly composed of asbestos fibre and rubber (generally neoprene). This has a number of disadvantages, the principal one being that the rubber content is gradually oxidised where exposed to the high pressure oxygen; this finally leads to loss of strength and leakage to atmosphere. However, runs as long as 800 hours have been achieved without failure, and runs greatly exceeding this should be possible with a superior design. One other fault is that substances given off when the rubber decomposes on heating, poison the hydrogen electrode and tend to reduce the output of the cell.

The most attractive alternative to CAF jointing would appear to be p.t.f.e. loaded with asbestos fibre, or possibly loaded with powdered glass, but these materials are only now in process of development in England; and the metal surfaces would certainly have to be specially roughened to prevent slip. End pressure on the gaskets could no doubt be reduced by the use of a pressure cylinder or tank, in which the whole cell pack is contained under pressure, but this line of development is not being pursued at present in England, owing to the extra complication involved.

7. Cell Performance.

The performance of the cell improves with both temperature and pressure, but in order to attain a long life it will probably prove desirable to limit the working temperature to 200°C or slightly higher. The best performance obtained so far with a 10" dia: cell at 200°C and 400 p.s.i. is shown in the table, and plotted as a voltage-current density characteristic in Fig.8; the diameter of the sinter is somewhat less than 10", and is approximately 9⅞", but it is felt that it is more precise to base the figures for current density on the internal diameter of the body of the cell.

TABLE.

Current Density	A/ft.^{2}	0	10	50	100	200	300	440
	mA/cm^2	0	11	54	107.6	215	323	473
Voltage, V		1.04	1.005	0.93	0.885	0.82	0.755	0.68

These figures were taken from one cell in a 10-cell battery, and using 37% KOH as electrolyte; both these factors contribute to the rather low open-circuit voltage obtained. Under the above conditions of 0.68 V. and 440 A/ft^2 (or 240A), the power output per unit of internal volumn corresponds to 8.2 kW/ft^3.

The current efficiency has been measured over a period of some hundreds of hours in a 5 in diameter unit with two cells in series, and works out at 98%. This means that the energy efficiency, based on the free energy of the reaction, will approximate at any useful current density to the voltage efficiency; e.g. at 0.9V and 200°C and 600 p.s.i. the energy efficiency will be $\frac{0.9}{1.20} \times 100 = 75\%$; at 0.8V. it will be 66%, and at 0.6V. it will be 50%.

When the cell is on load, the losses which appear in the form of heat, are mainly due to the irreversibility of the electrode reactions, or what may be called activation polarization; a smaller proportion of the losses are due to resistance and concentration polarization. On open circuit, and at low current densities, there will in addition be a 'lost current' due to diffusion of the two gases in solution through the electrolyte, followed by combination on the opposite electrode.

A graph showing the relative proportions of polarization due to each electrode and to the electrolyte is shown in Fig.9. Ordinary C&F jointing was used, so the hydrogen electrode was somewhat "poisoned". Assuming that activation of the hydrogen electrode can easily reduce polarization from this source to a negligible amount, while electrolyte resistance and oxygen electrode polarization are less easily improved, then a curve showing the best easily obtained performance to be expected from a cell can be drawn (see Fig.9). This shows that 223A/ft.^{2} (240 mA/cm^2) at 0.8 V. and 650 A/ft.^{2} (700 mA/cm^2) at 0.6V can reasonably be expected at 200°C. and 620 p.s.i..

The experimental method has been improved by the measurement of purely resistive polarization in the cell circuit using a commutator technique in conjunction with a cathode ray oscilloscope, so that individual electrode performance can be studied precisely. This is particularly important in the case of the hydrogen electrode, where both resistance and activation polarization have the same linear dependence on the current passing. The use of a reference electrode, in the form of a small resting (i.e. unloaded) hydrogen electrode of porous nickel, situated in the electrolyte space, about halfway between the main hydrogen and oxygen electrodes, has made it possible to study the polarization in each electrode separately; a reference electrode of this kind is used fairly regularly in cell operation, even when the commutator technique is not being employed. This has shown that the polarization of the hydrogen electrode at 200°C., when plotted against current density, gives approximately a straight line; at lower temperatures, the behaviour becomes logarithmic (see Fig.10). In the case of the oxygen electrode, however, the behaviour is logarithmic even up to the highest temperature yet tried the shape of the curve which it gives at 200°C, can be seen in Fig.9. The difference in the shape of the polarization curves shown by hydrogen and oxygen electrodes at 200°C. can be explained by the fact that the exchange current is much less in the latter case, or in other words the oxygen electrode is much less reversible than the hydrogen one; in addition to this, the surface area of the oxygen electrode is much less than that of the hydrogen one. But even an oxygen electrode of large surface, made from Grade B nickel, will polarize more than a hydrogen one made from the same powder and having the same surface area. To improve the performance of oxygen electrodes, a very large increase in surface area will be required; this can probably best be obtained by some form of activation.

Since electrodes have been made with a backing plate, it has been possible to test hydrogen and oxygen electrodes as thin as 1/32 in. The performance of these thin electrodes is within 20% of that of the previous electrodes which were $\frac{1}{8}$" - 5/32" thick. If the electrodes are made 1/16 inch thick, there does not appear to be any sacrifice in performance. A number of other hydrogen and oxygen electrodes of varying structures have been tested, but so far none has shown a striking improvement in performance when compared with the standard types.

8. The Effect of Cell Conditions on Performance.

(8.1). Pressure.

The effect of temperature and pressure on the reversible voltage of the hydrogen/oxygen cell can be seen in Fig.11. Measurements of electrode and cell performance at varying pressures of gas (the electrolyte vapour pressure having been measured, see Fig. 12) show that small variations in pressure have only a small effect. A tenfold change in gas pressure from 30 atmospheres to 3 atmospheres (441 to 44 p.s.i.) approximately halves the cell performance at normal operating voltages (see Fig. 13). A theoretical analysis done fairly recently shows that for a given power output, and assuming that the gases are both stored in high tensile steel cylinders at 3,000 p.s.i., the overall weight of the battery and storage cylinders would not be increased if the operating pressure were reduced from 600 to 300 p.s.i.; the efficiency would be slightly reduced, however; this calculation allows for the "dead" fuel left in the cylinders when the battery is discharged, and also for the reduction in weight of the battery itself.

(8.2). Temperature.-

The maximum cell temperature is limited by the materials used in it's construction. Thus, p.t.f.e. is found to corrode relatively quickly at 250°C. undercell conditions, where in contact with porous nickel; and the nickel-lithium oxide of the oxygen electrode breaks down fairly quickly at 300°C.. Between 100° and 250°C. the cell output at normal operating voltage increases rapidly with rise in temperature, as the hydrogen electrode changes from logarithmic behavious at 100°C. to linear behaviour. After 200°C. the output does not increase as rapidly as it does between 100° and 200°C.. Taking 100°C. as unit performance, that at 150°C. is roughly 4, at 200°C. it is 10, and at 250°C. it is 15. The actual maximum power available (at a low efficiency) rises increasingly steeply with increasing temperature, and is roughly doubled with each 50°C. rise in temperature.

(8.3). Electrolyte Concentration.

The effect of the vapour pressure of the electrolyte on the reversible voltage of the hydrogen/oxygen cell at a temperature of 200°C. is shown in Fig.14. This assumes that the total pressure is kept constant at 600 p.s.i.. It has been necessary to plot the vapour pressure of the electrolyte, rather than the concentration, as the relationship between concentration and vapour pressure of very strong KOH solutions has not been measured, as far as is known.

It has been assumed that the disposable energy in the formation of water vapour at a constant pressure of one atmosphere is 219.4 kilo-joules per gramme formula weight, at 200°C. At other values of pressure the disposable energy is increased by an amount

$$\frac{0.5\ R\ T \log_n (P_{H_2}{}^2 . P_{O_2})}{P_{H_2O}{}^2}$$

the pressures being measured in atmospheres.

The theoretical voltage is obtained by dividing the disposable energy by 2F, where F is the Faraday, 96,500 coulombs.

Increasing the concentration of the potassium hydroxide electrolyte to 35% by weight, increases the cell output progressively, but further increase from 35% to 45% has a smaller effect. Operation at higher concentrations than 45% leads to practical difficulties with the KOH electrolyte going solid on cooling down. Long continuous operation of cells on load for periods of 50-100 hours has shown that the very high concentrations of KOH lead to build-up of concentration polarization (absence of water in the oxygen electrode is the most probable cause), so that a concentration of about 35% KOH seems likely to be the optimum at present. If later it proves feasible to condense out twice the water formed from the hydrogen electrodes, and then return one half of this, in the form of steam mixed with the oxygen, to the oxygen electrodes, this difficulty should disappear and stronger concentrations could be contemplated.

The values obtained for specific conductivities of a range of electrolytes at various temperatures are shown in Fig.15; these have been obtained by measuring cell resistance with two different inter-electrode distances using the commutator technique mentioned previously; they are only approximate. Results for 36% KOH are particularly erratic, and the measurement of conductivity using an a.c. bridge and high temperature conductivity cell should provide accurate results.

The values predicted by T.M. Fry[7] are also plotted; these were obtained by using the relationship between conductivity and viscosity, and using an estimated value of viscosity; also values quoted for KOH by C.E. Bowen[8] (deduced from work by Kohlrausch in 1898); a general agreement is observed.

The contribution of electrolyte resistances to cell operation will be approximately 0.25 ohm/cm^2 of apparent electrode surface, for $\frac{1}{8}$ in. electrode spacing using electrodes of the types described. For a current density of 250 mA/cm^2, this would give a polarization of 0.0625 V., i.e. a voltage drop corresponding to about 5% of the total free energy available.

(8.4). Shunt currents in Multi-cell Packs.

A six cell pack of 5 in. diameter electrodes was constructed in 1954 and fair results were obtained.

Measurements of the shunt currents along the common eletrolyte ports, and a theoretical treatment, suggest that the magnitude of the shunt currents will depend largely on the dimensions of the axial electrolyte ports through the pack.

If V = the open circuit voltage of one cell
n = the number of cells in the pack
R = the resistance of one pair of axial ports in one cell, and
r = the resistance of one pair of radial ports in one cell,
then the shunt current = $\frac{(n-1)\ V}{2r + (n-1)\ R}$

For large packs, where distribution of liquid may be important, it might be better to have a number of axial ports serving groups of cells, rather than one large port serving all the cells.

9. Use of Other Gases.

It has often been suggested that a cell of this type could be used as a genuine fuel cell for generating power on a large scale, using hydrogen produced from coal by ordinary chemical methods, and oxygen from the air. This is, of course, a very ambitious project and cannot honestly be envisaged at present, owing to the high cost of pure hydrogen produced in this way; pure oxygen is also expensive.

Nevertheless, it is obvious that the scope of the whole project could be greatly widened if it were found to be possible to make use of a liquid fuel which could be converted into some gas which is electrochemically active in the cell; in this way it would become possible to compete on rather more level terms with the internal combustion engine.

A number of experiments have been carried out using other gases, and with mixtures of gases, and the conclusions can be summarized as follows :-

1. No other fuel gas, apart from hydrogen, has been found to be electrochemically active on a nickel electrode at temperatures which it would be practicable to use in a cell of this type. Carbon monoxide, methane and methanol were tried and were all unsuccessful.

2. Both carbon monoxide and carbon dioxide are soluble in caustic potash and would lead to the eventual carbonation of the electrolyte.

3. Complete carbonation of the electrolyte would lead to a serious loss in performance, amounting to a reduction to one quarter of the normal performance; this is partly due to loss in oxygen electrode performance and partly to increased cell resistance.

4. Hydrogen containing inert diluents, such as nitrogen or methane, can be used with a high volume percentage of inert gas, as long as provision is made for exhausting the residue; some hydrogen would no doubt be wasted in the exhaust, but the amount lost is not likely to be serious.

5. Possibly because of its solubility in hot caustic potash solution, carbon monoxide does not poison the fuel electrode, but it may attack the nickel pipe-work leading gas into the cell. No poisoning was observed with other gases used.

6. Experiments using nitrogen-oxygen mixtures showed that air could be used in place of oxygen, as long as the nitrogen left over was continuously removed, and the carbon dioxide extracted before entry into the cell.

The above conclusions show that the presence of any gases, apart from hydrogen and oxygen, may lead to rather awkward problems which it would probably be wise to avoid at present. On the other hand, small percentages of inert gases would do no harm to the cell, provided adequate means were worked out for exhausting them to atmosphere from time to time, before they had built up to large proportions inside the electrodes. A small purification plant could no doubt be designed for continuously purifying a slightly carbonated electrolyte.

The additional polarization at the oxygen electrode, caused by using air instead of pure oxygen, can be seen in Fig.16; this also shows the effect of oxygen pressure on polarization. Fig.17 shows the effect of various fuel gases on the polarization at the fuel electrode; the curve for technical hydrogen, and also for the mixture of 90% hydrogen plus 10% carbon monoxide is identical with that for pure hydrogen, over short periods of time. The "technical hydrogen" is the gas which is produced as a by-product in oil refineries, from the "platforming process".

10. Present Design.

In 1957, the National Research Development Corporation of Great Britain agreed to finance the development and construction of a unit developing 5-10 kW., complete with all automatic controls, and a contract for this work was placed with Marshall of Cambridge, England.

It was decided that a 10 in. diameter cell should be constructed, and this has been in operation since March 1958. The present electrode design has already been described; axial ports for the admission of the two gases and the electrolyte are drilled in the rim, as shown in Fig.18; when these electrodes are bolted up together in the correct order, with rings to provide space for the electrolyte and with flat discs of metal to separate the hydrogen from the oxygen in the adjacent cell, they form a battery, the voltage of which depends upon the number of cells connected in series. Radial ports for admitting gas or electrolyte from the axial ports to each cell are provided simply by slotting the gaskets. A distributor plate for leading the gases and electrolyte into and out of the battery is provided either at one end, or else in the centre of the cell-pack. The whole assembly is bolted up between two ribbed end plates, with powerful bolts, with electrical insulation between the ends of the pack and the end plates. Electrical connections are silver-soldered onto each electrode, and the inter cell connections are made externally; the main connections are of course made to the electrodes at each end of the pack.

Up to 30 cells in series have been operated so far (see Fig.19), and no special difficulties have been encountered with, for example, sealing of the joints, excessive shunt currents between cells, excessive electrolysis in the electrolyte ports, etc. But more experience will have to be obtained with large multi-cell packs before reliable results can be quoted.

11. Development of Control Gear.

Control of gas admission has always been a problem, as a very delicate pressure balance has to be maintained between the two gases in the battery. A system has now been worked out whereby as a basis the pressure of the oxygen remains constant under all conditions of load; this is achieved with a standard two-stage reducing valve. The hydrogen then has to be admitted at precisely the correct rate, so that the two gas pressures are balanced to within a few inches water gauge; this is done by fitting an accurate differential pressure meter, which actuates a power-operated valve admitting the hydrogen, the valve-opening being controlled by a servo mechanism operating with compressed air. A fair amount of experience has been obtained with this gear which works extremely well. Figure 20 shows various items which made up this control gear, mounted on the front of the protective framework enclosing the cell pack.

Much thought has also been given to the problem of the removal of water, at the same rate at which it is formed. Previously this has been achieved by circulating the hydrogen steam mixture by thermosyphonic action, the steam being condensed out in a small vessel outside the lagging. In order to do this in a large battery, very large hydrogen circulating pipes and ports would be needed, so it was decided that a small hydrogen blower would be used; it was considered that a glandless form of drive would be necessary, in view of the difficulty of preventing hydrogen leakage with a standard type of gland. A magnetically driven pump using a sealing shroud of thin non-magnetic metal has been successfully employed for some time; it can be seen mounted underneath the battery in Fig.19. The rate at which the condensate is removed from the system is controlled by switching the blower on and off at intervals, the switch being controlled by a second differential pressure meter which operates on the pressure difference between the hydrogen in the system and the electrolyte. In this way, the removal of water is controlled by the total volume of electrolyte which should of course be kept approximately constant. The condensate collects in a small vessel, from which it is released periodically by a level-sensing device such as a capacitor probe. The main parts of this gear, which can be also seen in Fig.20, have been in operation and appear to work perfectly well.

Until more experience with this gear is obtained, the main level gauges will be retained in use, but eventually it should be possible to remove them.

The initial heating of the battery is accomplished by electrical heaters mounted on the end plates and round the main body of the battery inside the lagging. Various plans have been suggested for maintaining the battery at a constant temperature when on load, but the simplest is undoubtedly to allow cold air to circulate round the battery, inside the lagging, the amount of cold air introduced depending on the temperature of the cell pack.

Lastly, there is the problem of removing gas from the electrolyte system; it is difficult to prevent entirely some generation of hydrogen and oxygen by electrolysis in the common electrolyte ports, although insulation with p.t.f.e. helps considerably in this respect. Moreover, there is always the possibility that an electrode may start leaking, thus allowing gas to get into the electrolyte system. This is taken care of by a level-sensing device, which will release any gas which may collect at the top of the electrolyte system, by means of a solenoid operated valve.

All these controls may seem somewhat complicated and expensive, but there is no doubt that they can be made to work, and with a larger battery they should not be any more complex and would then represent only a small proportion of the cost of the whole plant.

12. Advantages and Applications.

From what has been said, it will be seen that it is unlikely that this kind of battery could be competitive with existing types of accumulator in small sizes, owing to the high cost of the control gear in comparison with the overall cost of the plant. And in very small sizes it would be difficult to keep the cells up to the working temperature unless they were on load continuously and unless very efficient heat insulation were employed. It is difficult to quote exact figures for minimum sizes until more experience is obtained, but a power output as small as 100 watts is believed to be feasable with really good lagging.

One other factor that must be appreciated is that it could not compete with say lead accumulators on a weight basis unless the length of time of discharge is greater than about 1 hour; however, for longer times than this, the saving in weight should become increasingly important, as shown in Fig.21. The figures for conventional accumulators are a few years out-of-date, but the general picture to-day is undoubtedly roughly the same. It is on a weight basis that the hydrogen-oxygen battery should be able to show it's principal advantage over conventional accumulators. A curve for a Diesel engine with fuel is also included, and this serves to show that it will always be difficult to compete on a weight basis with a power generator which can draw it's oxygen from the atmosphere. However, it is as well to bear in mind that both accumulators and internal combustion engines have a great many years of careful development behind them, whereas the fuel cell is still in its infancy.

The fuel cell weight of 50 lb./kW shown in Fig.21 was worked out for a large battery developing about 44 kW.; this weight to power ratio will not be achieved in the small experimental unit now being built, and it would be unwise to hazard a guess about this until it is completed. The first requirement has been that it should work, rather than that it should have minimum weight or volume.

As regards power per unit volume, the figure of 8.2 kW/ft.^{3} of internal cell volume has already been quoted for a cell voltage of 0.68; a figure of 3kW/ft.^{3} for the whole battery without control gear, was quoted by an independent body some years ago, for a cell voltage of 0.8.

It has always been hoped that some specialised application will arise first, an application for which a fuel cell is particularly suited. In this connection, the possible use of fuel cells in satellites and space vehicles is of great interest. Then, when further experience has been obtained, it should be possible to enter the commercial field in competition with storage batteries which have already been developed to a high pitch.

It would seem that fuel cells of this type are most suitable for traction purposes, both road and rail; the combination of battery and direct current series wound motor provides an ideal propulsion unit for many types of vehicle, the limiting factor so far being the weight of the battery. The gases would probably be generated by electrolysis of water, and in this connection the development of an efficient high pressure electrolyser in Germany is of great interest. It is well known that the cost of electrical power from the National grid is considerably less than that of power produced in a petrol engine, and this is of special importance where the vehicle is subject to repeated starts and stops.

Further, if finally most of the power is generated on a large scale from nuclear energy, the cost of the electricity will be mainly due to the capital cost of the plant rather than to the cost of the nuclear fuel; and the need for some kind of large scale storage will become increasingly important, as little will be saved by shutting down the plants during times of light load.

Other advantages of this kind of fuel cell are that it is able to take large overloads at reduced efficiency without damage, it is silent and free from vibration in operation, it has very few moving parts and the "exhaust" is only water; moreover, the "charging" process would merely consist of refilling with the two gases, a very rapid process.

With the advent of new methods of storing hydrogen and oxygen, either in liquid form, or else in the former case as a compressed gas at a very low temperature, it would seem conceivable that vehicles could be propelled over really long distances with fuel cells; and in view of the rapid depletion of the world's oil supplies, the development of a practical fuel cell should, in the author's opinion, be given a high priority.

The author would like to thank his colleagues who have given invaluable help in the preparation of this paper; and in particular Dr. R.G.H. Watson, now at the Admiralty Materials Laboratory, Holton Heath, England.

He would also like to thank the Electrical Research Association and the Ministry of Power for valuable financial assistance over many years of research; also Messrs. Marshall of Cambridge, who are now providing facilities for the development work and who have given all possible advice and help; and specially the National Research Development Corporation who are now financing the development work, and who have kindly given permission for the publication of this paper.

REFERENCES.

(1) Grove. W.R., PhilMag. (3), 1839, 14, 139.

(2) Mond. L. and Langer. C., Proc.Roy.Soc.Lond., 1889, 46. 296-308.

(3) Davtyan. O.K., Direct Conversion of Chemical Energy of Fuel into Electrical Energy (in Russian), Academy of Sciences, Moscow. 1947; E.R.A. Translation Ref. Trans./IB.884(1949).

(4) Kordesch. K. and Marko. A., Osterreichische Chemiker - Zeitung, July 1951, 52, 125-131, etc.

(5) Bacon. F.T., B.E.A.M.A. Journal, 1954, 61, 6.
" " and Forrest, J.S., Trans. Fifth World Power Conference (Vienna), Div. 3, Section K, paper 119K/4.
Watson, R.G.H., Research, 1954, 7, 34.

(6) Verwey, E.J.W., Semi-Conducting Materials, Butterworths Scientific Publications Ltd., 1951, 151-161.

(7) Fry. T.M., private communication.

(8) Bowen, C.E., J.I.E.E.Eng., 1943, 90, 473.

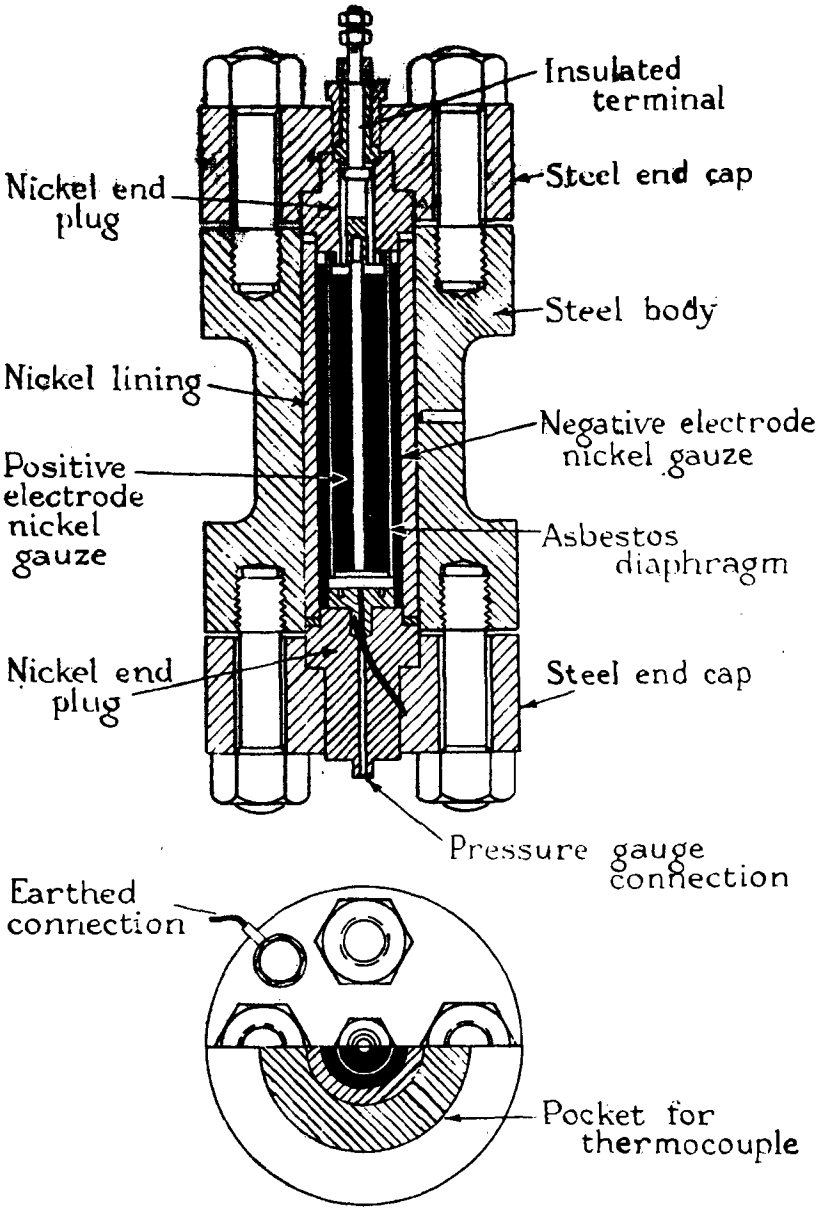

FIG. 1. APPARATUS FOR USING COILS OF GAUZE AS ELECTRODES. GAS SUPPLY BY INITIAL ELECTROLYSIS

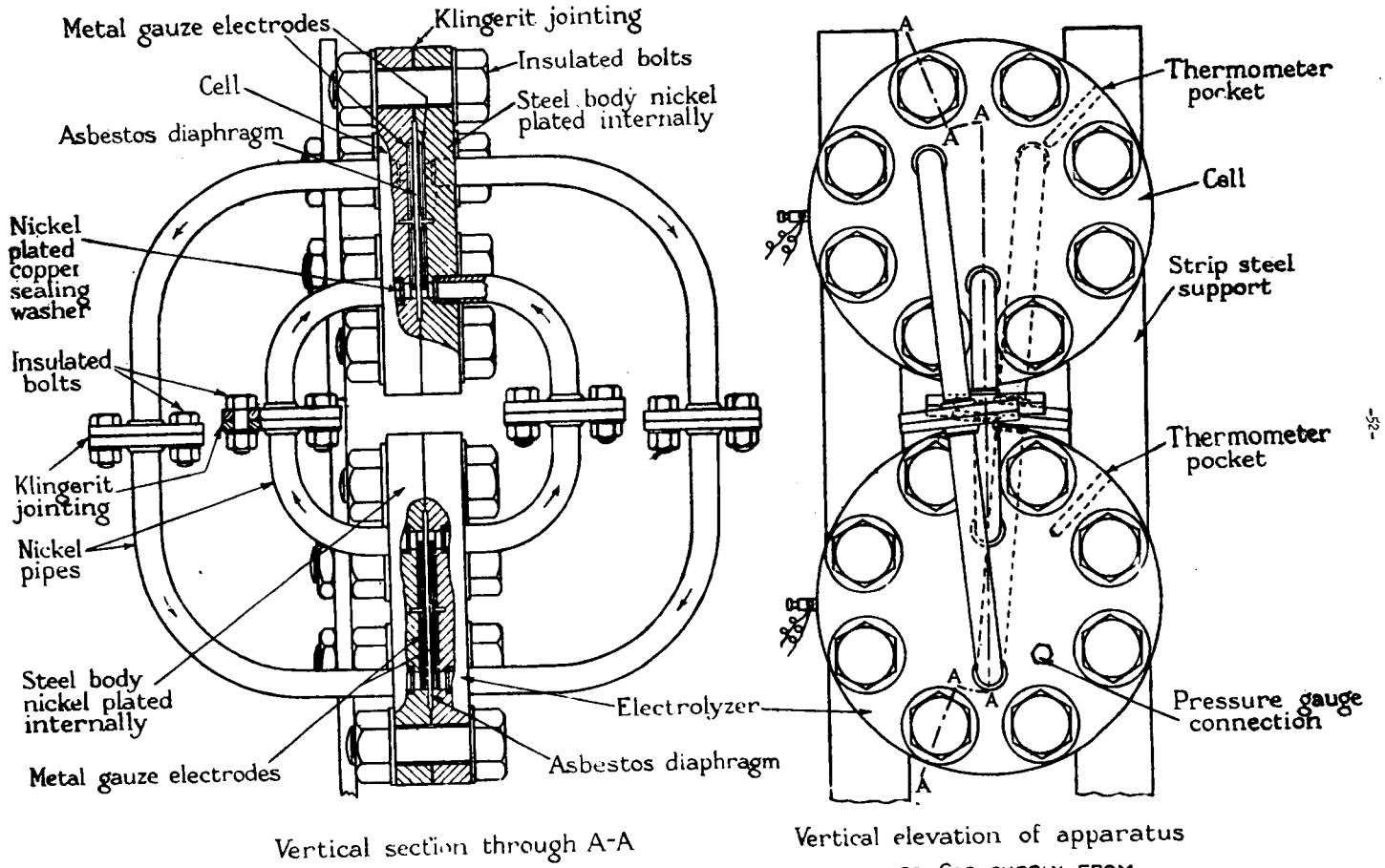

Vertical section through A-A

Vertical elevation of apparatus

FIG. 2. APPARATUS USING FLAT DISCS OF GAUZE AS ELECTRODES. GAS SUPPLY FROM SEPARATE ELECTROLYZER.

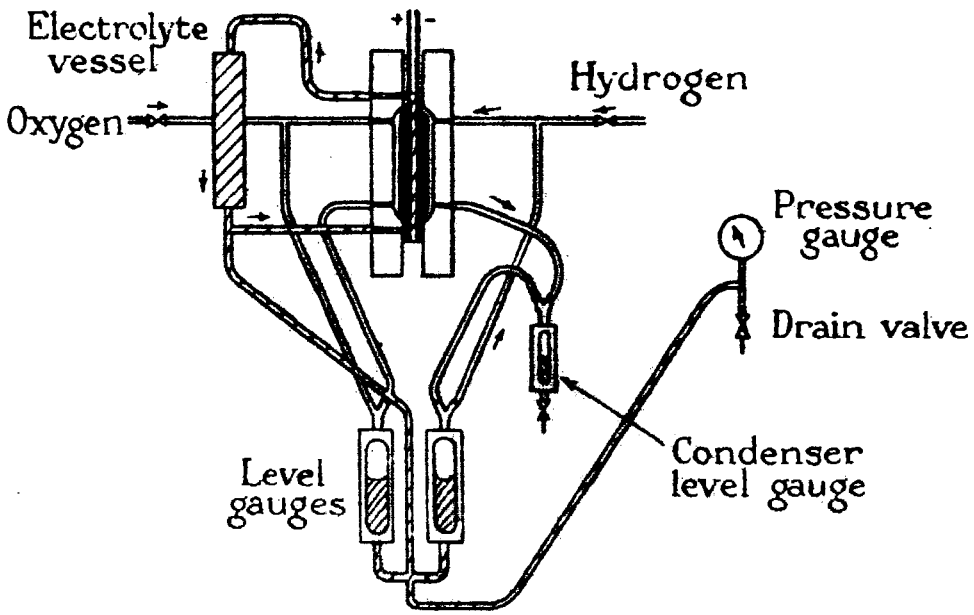

FIG. 3 APPARATUS EMBODYING CELL WITH POROUS DIFFUSION ELECTRODES.

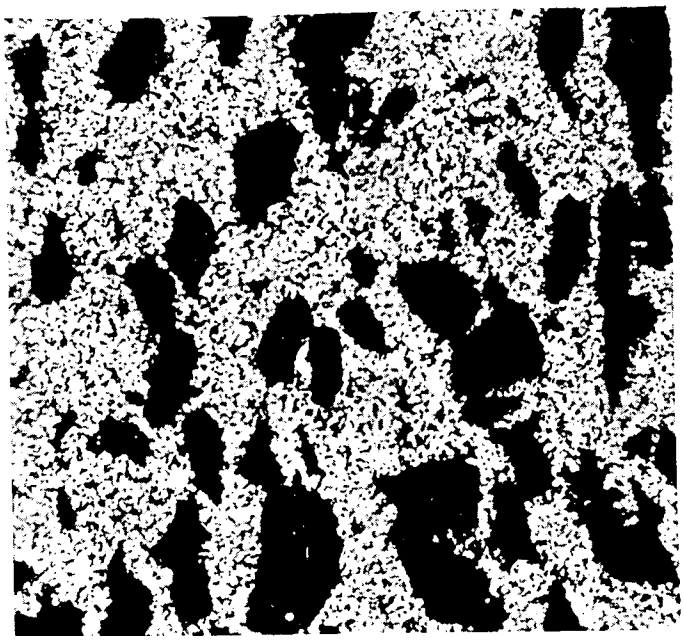

FIG. 4. MICROSECTION SHOWING COARSE PORE SIDE OF HYDROGEN ELECTRODE (x 150)

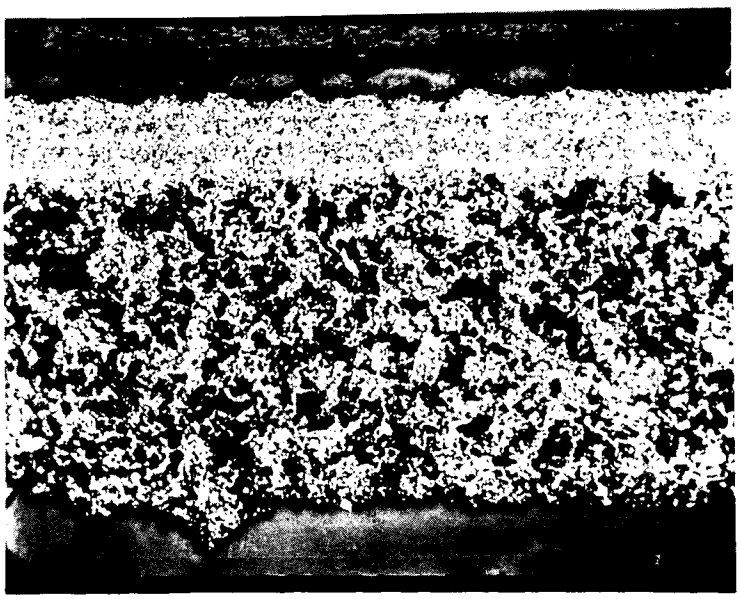

FIG. 5. MICROSECTION SHOWING COARSE AND FINE PORE LAYERS OF OXYGEN ELECTRODE (x 38)

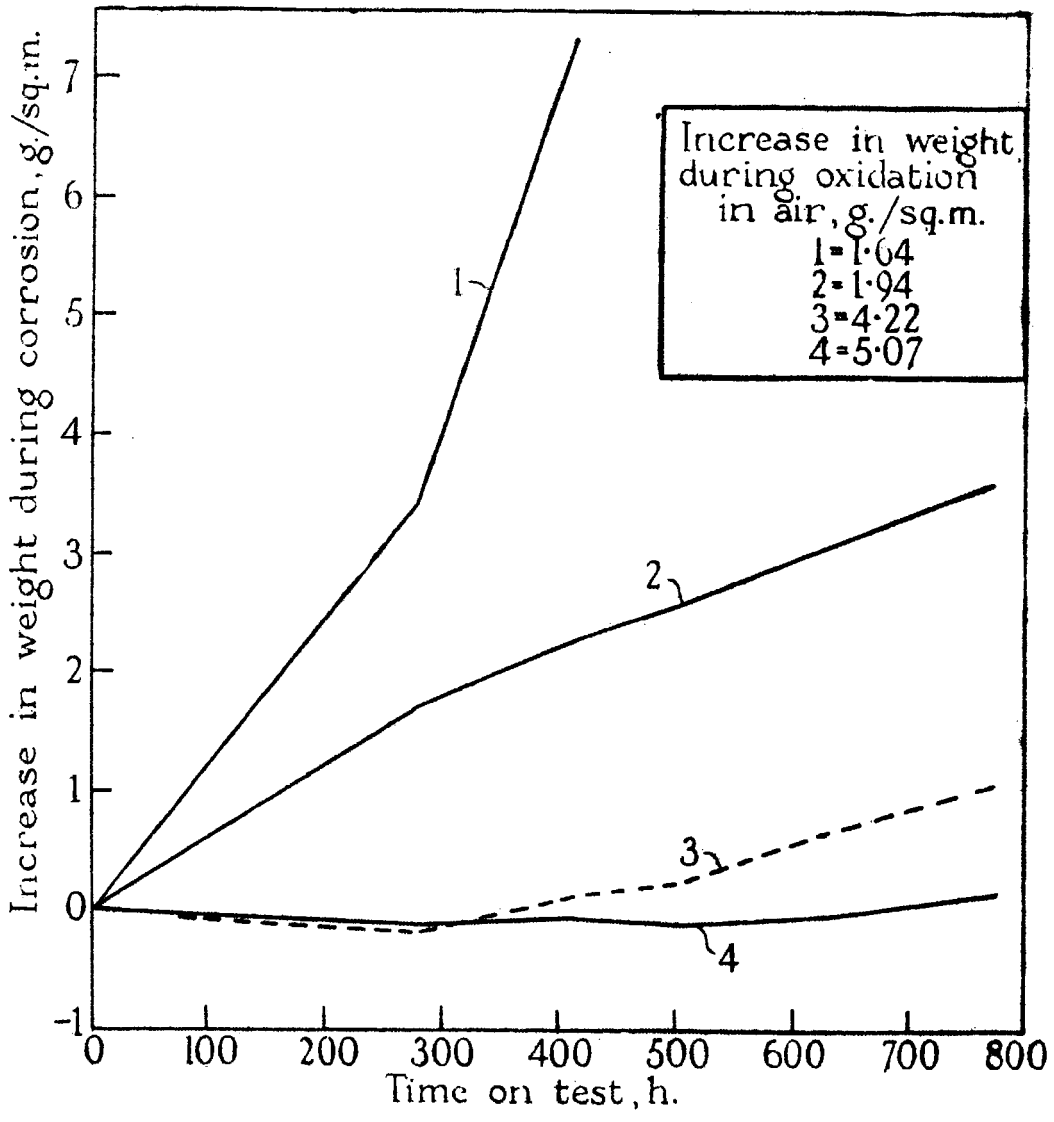

FIG. 6 CORROSION OF SAMPLES OF NICKEL PREOXIDIZED IN THE PRESENCE OF LITHIUM HYDROXIDE AND EXPOSED TO 65 % KOH AND OXYGEN AT 300°C. AND 800 lb./sq. in. TOTAL PRESSURE.

Each curve represents a pair of samples.

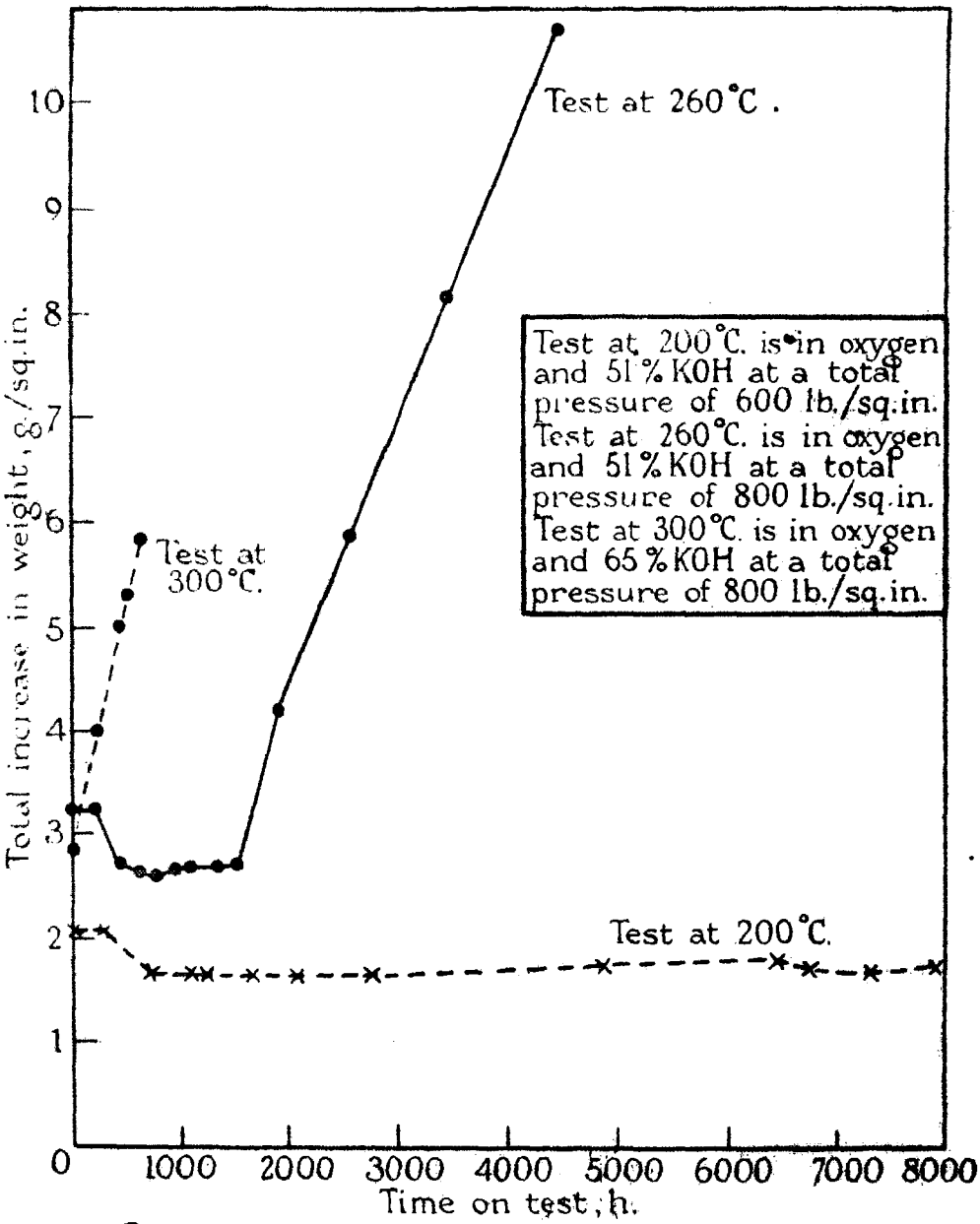

FIG. 7 CURVES SHOWING THE EFFECT OF TEMPERATURE ON CORROSION RATE

Values plotted are averaged from a series of samples coated with a protective oxide containing lithium, the oxide layers being of similar thickness.

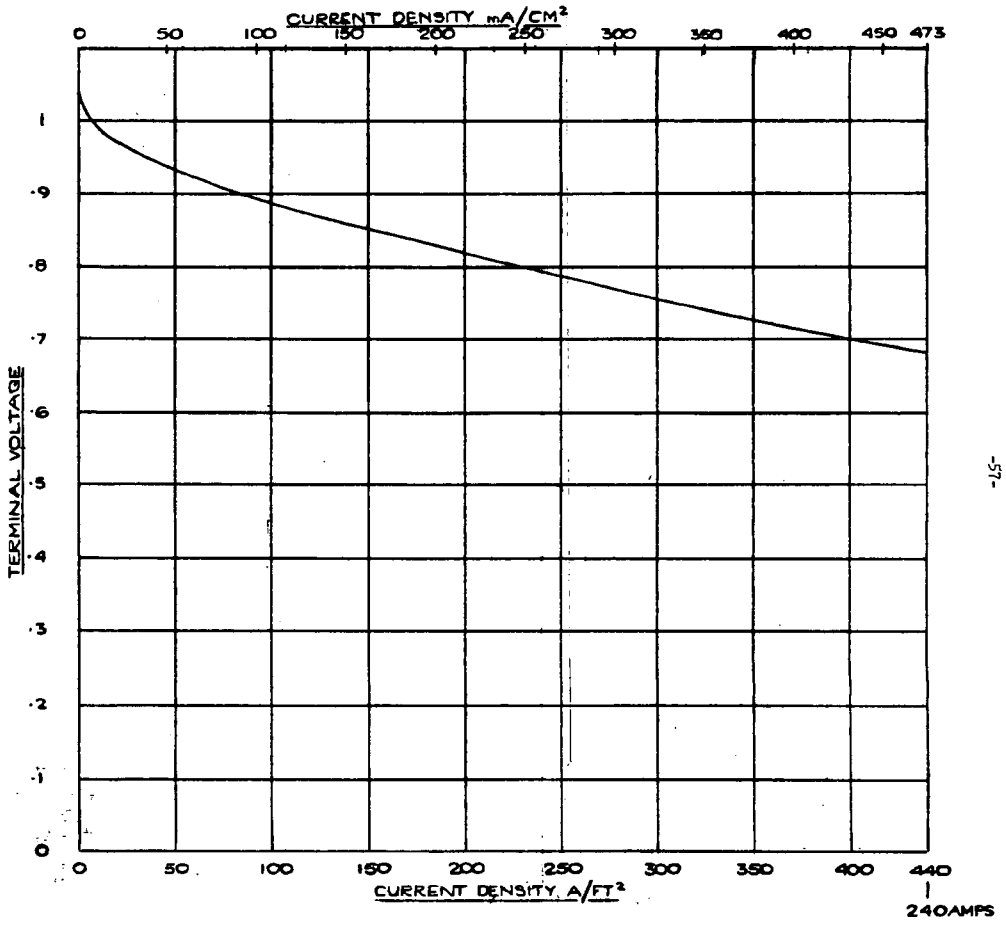

FIG.8 BEST PERFORMANCE OBTAINED SO FAR WITH 10" DIA CELL (MULTI-CELL PACK.)
(200°C; 400 P.S.I; 37% KOH)

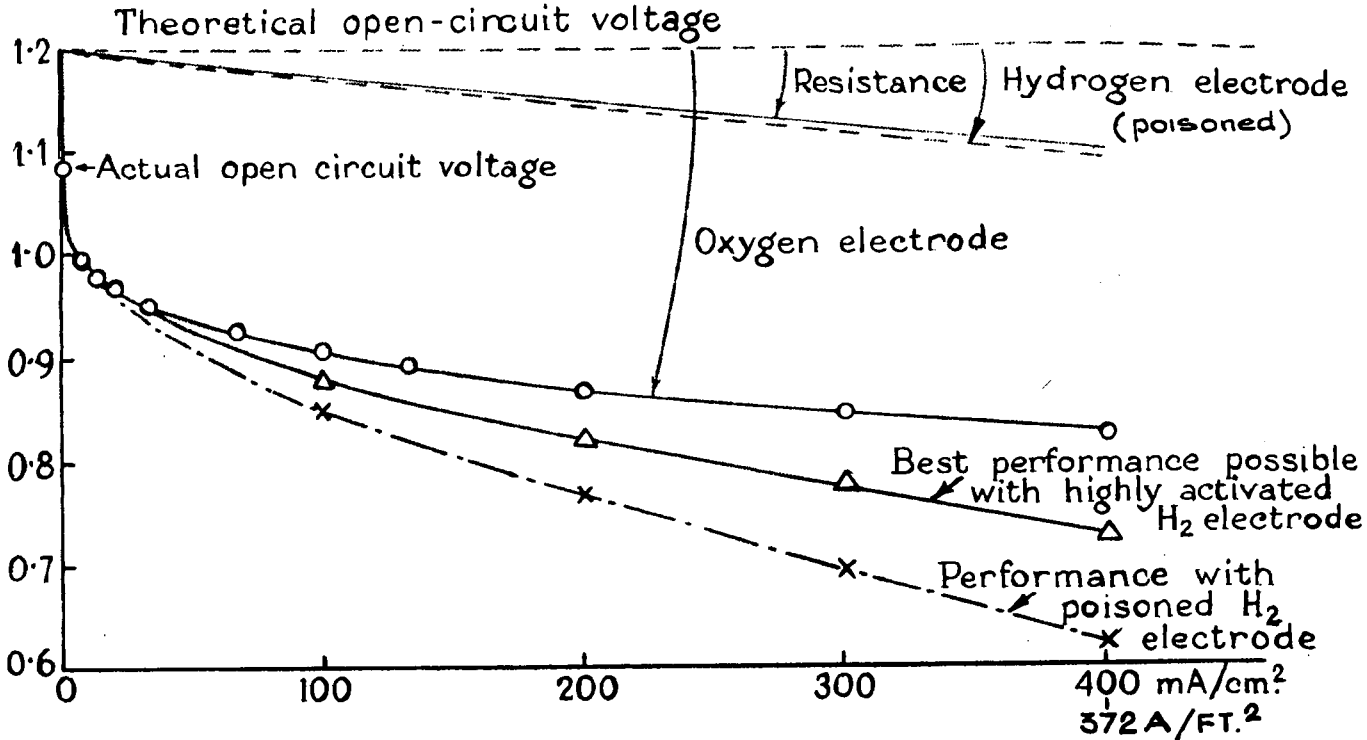

FIG. 9. PERFORMANCE OF CELL IN TERMS OF EACH ELECTRODE AND RESISTANCE 40% KOH ; 200°C ; 620 lb./sq. in.

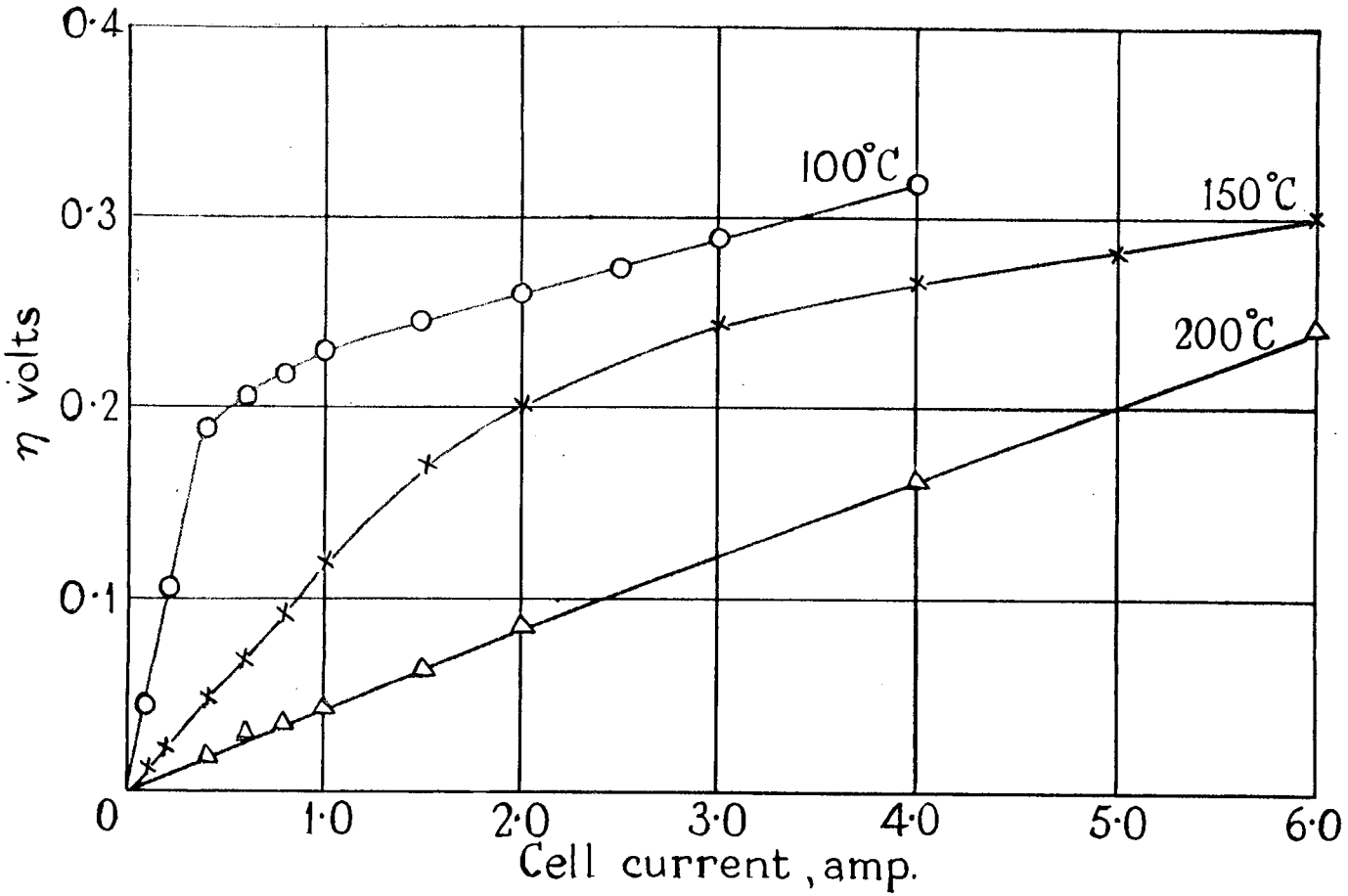

FIG. 10. POLARIZATION OF HYDROGEN ELECTRODE AT VARYING TEMPERATURE IN 5 N, KOH SOLUTION.

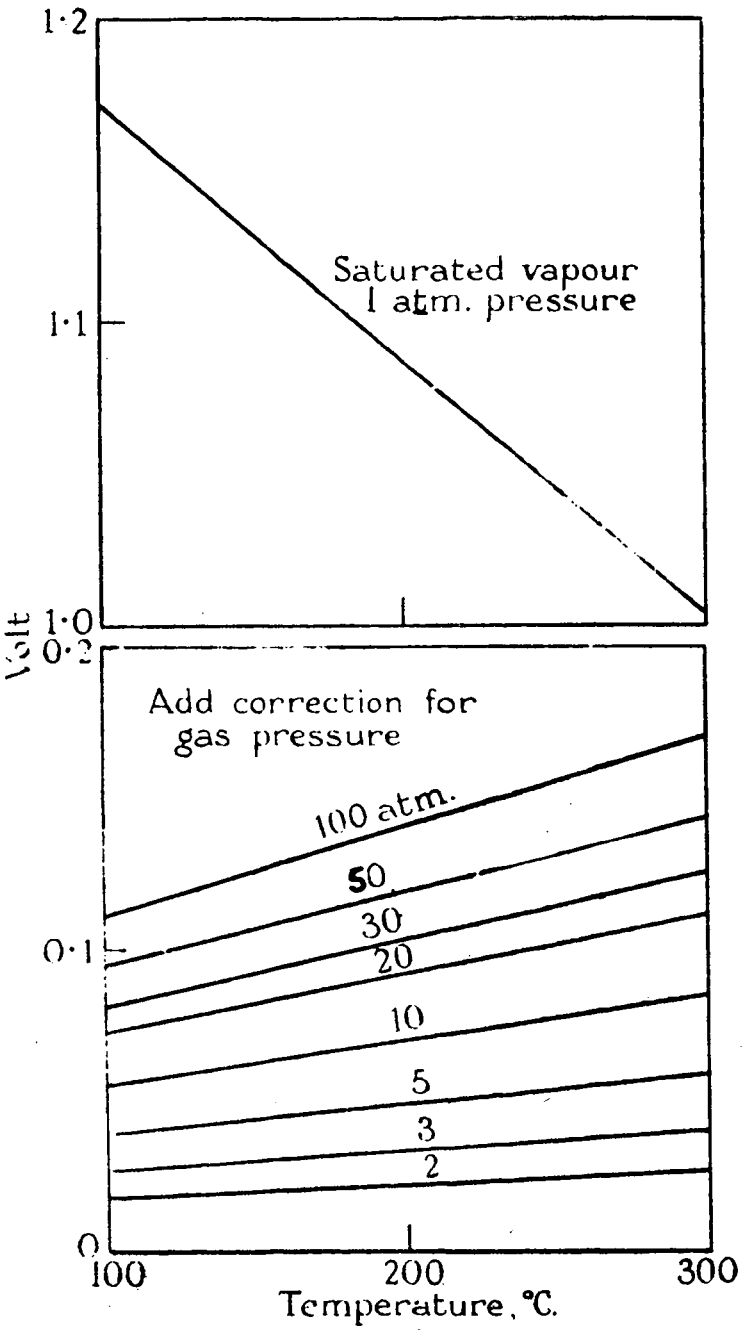

FIG. 11. REVERSIBLE VOLTAGE OF HYDROGEN-OXYGEN CELL

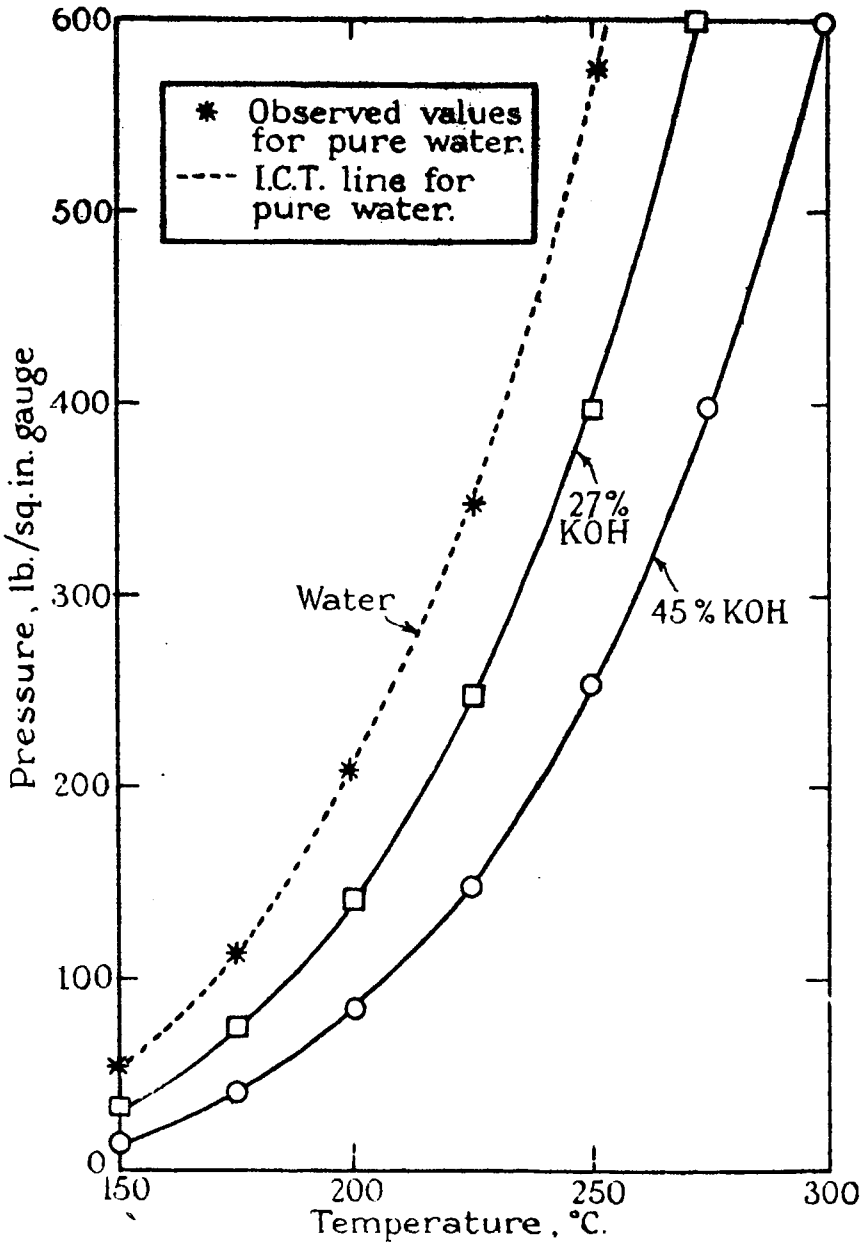

FIG. 12. VAPOUR PRESSURE OF ELECTROLYTES.

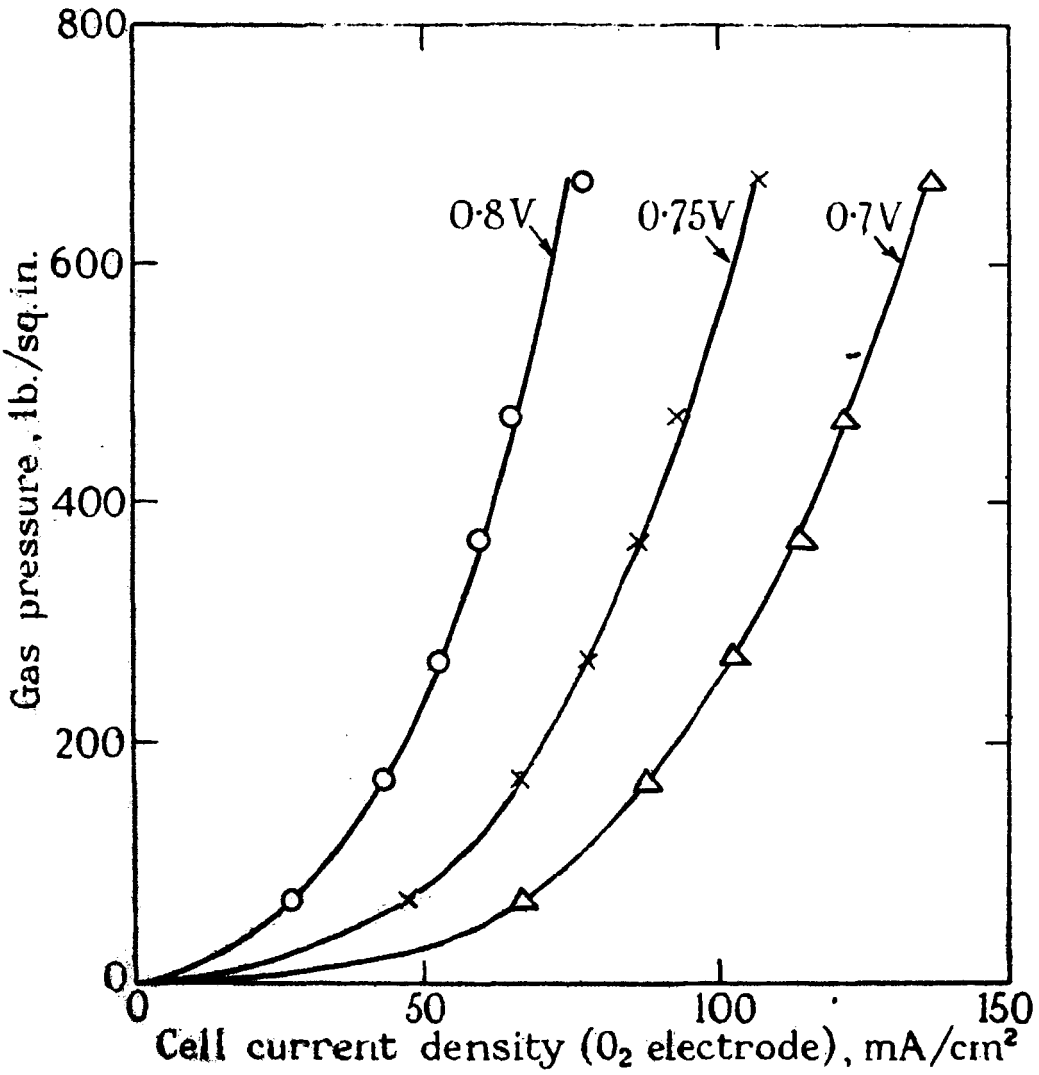

FIG. 13. VARIATION OF CELL OUTPUT WITH GAS PRESSURE FOR VARIOUS VOLTAGES.

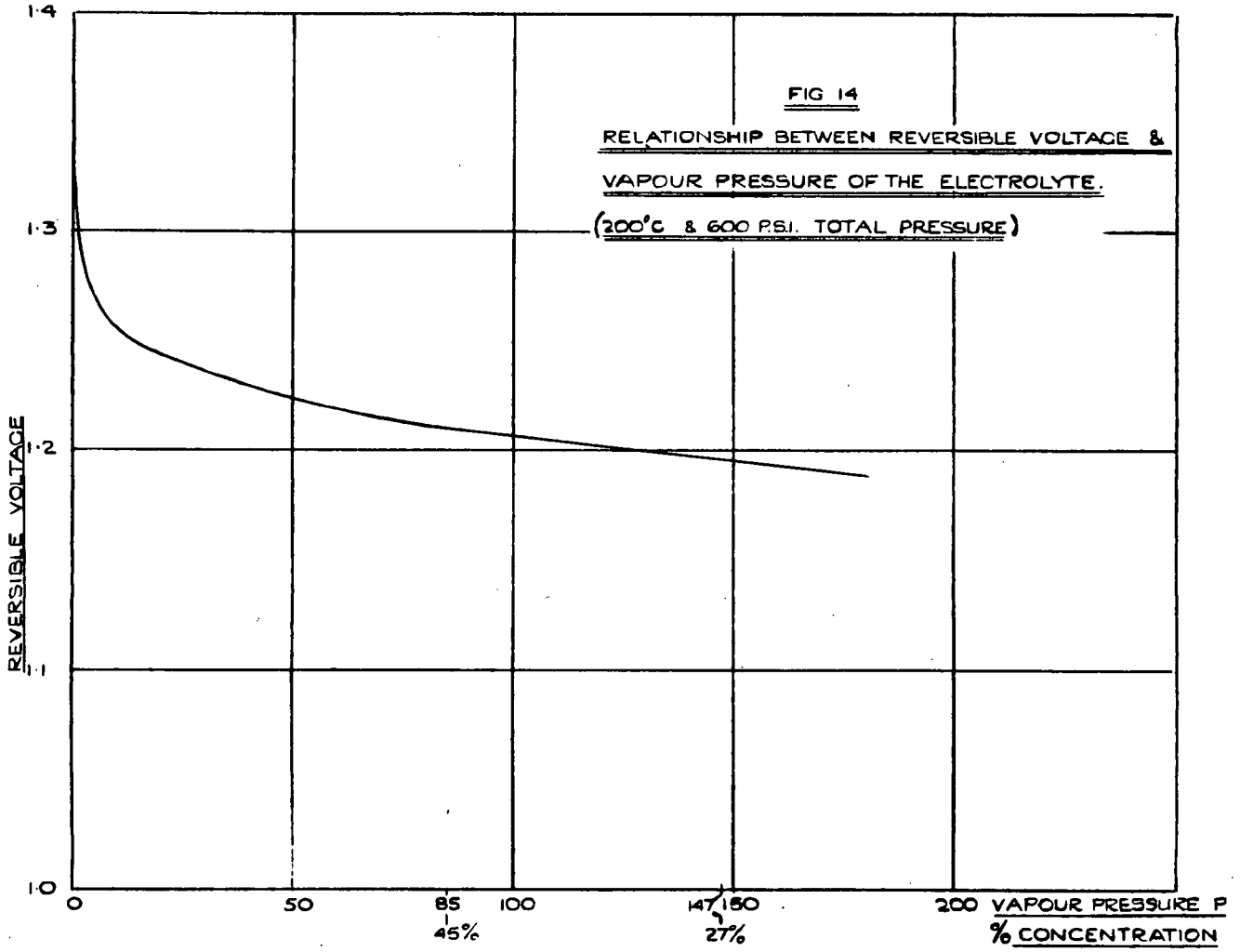

FIG 14

RELATIONSHIP BETWEEN REVERSIBLE VOLTAGE & VAPOUR PRESSURE OF THE ELECTROLYTE.

(200°C & 600 P.S.I. TOTAL PRESSURE)

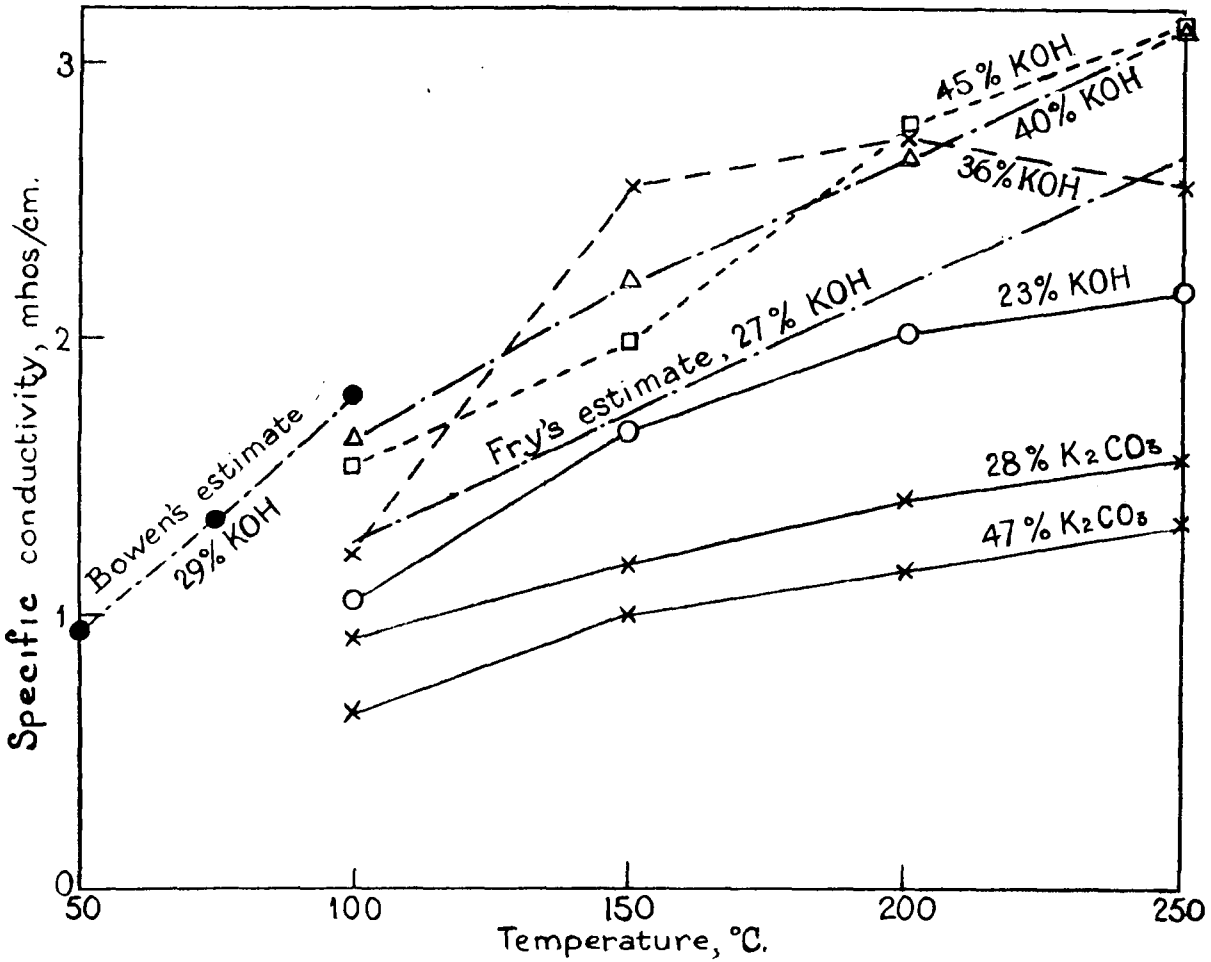

FIG. 15. VARIATION OF ELECTROLYTE CONDUCTIVITY WITH CONCENTRATION AND TEMPERATURE.

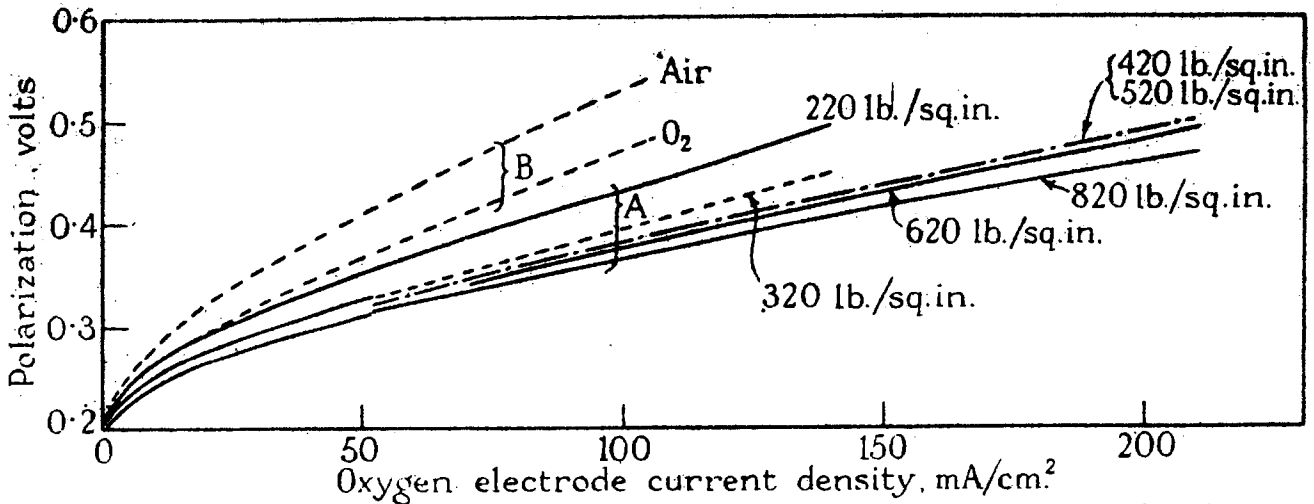

FIG. 16 THE EFFECT OF PRESSURE ON POLARIZATION AT THE OXYGEN ELECTRODE (A) 5 N. KOH, 200°C. G.31. (B) 5 N. KOH 200°C. E.183

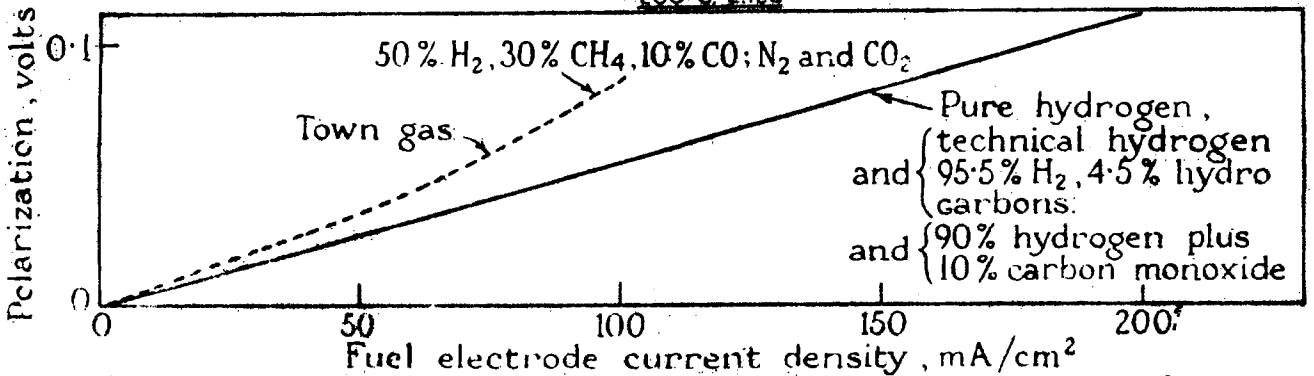

FIG 17 THE EFFECT OF VARIOUS FUEL GASES ON THE POLARIZATION AT THE FUEL ELECTRODE, 200°C. 5 N. KOH. 620 lb/sq.in.

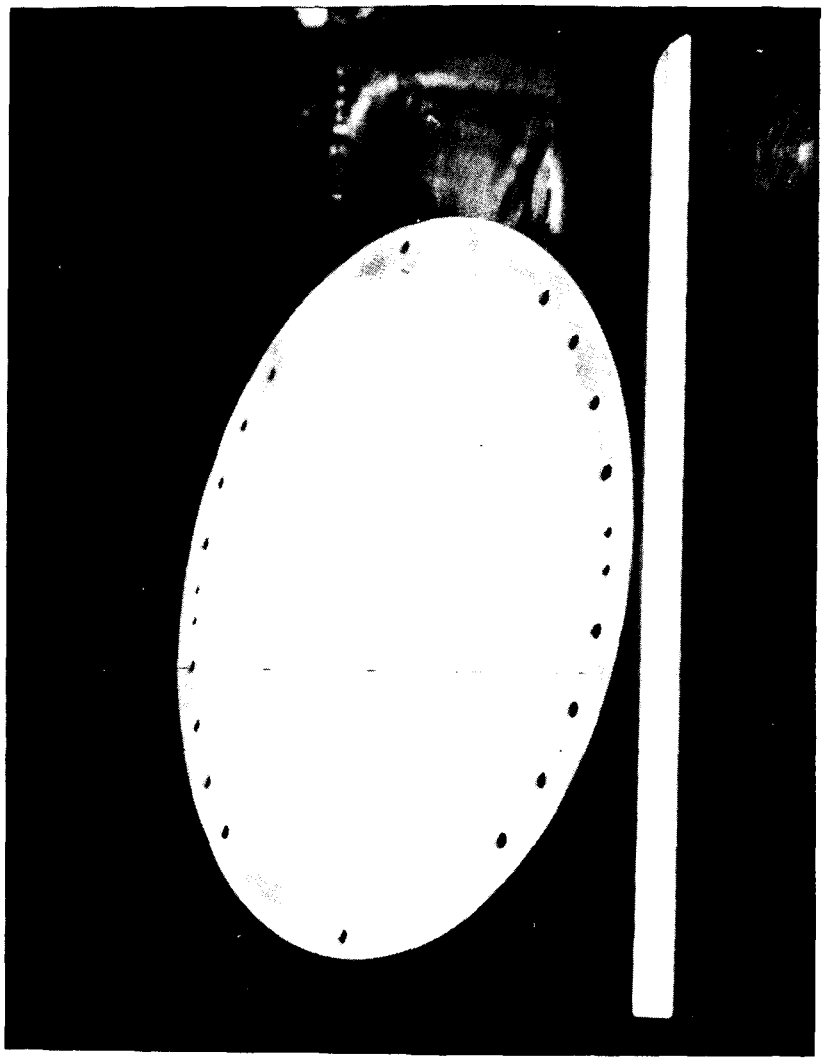

FIG. 18. ELECTROLYTE SIDE OF 10-INCH DIAMETER ELECTRODE

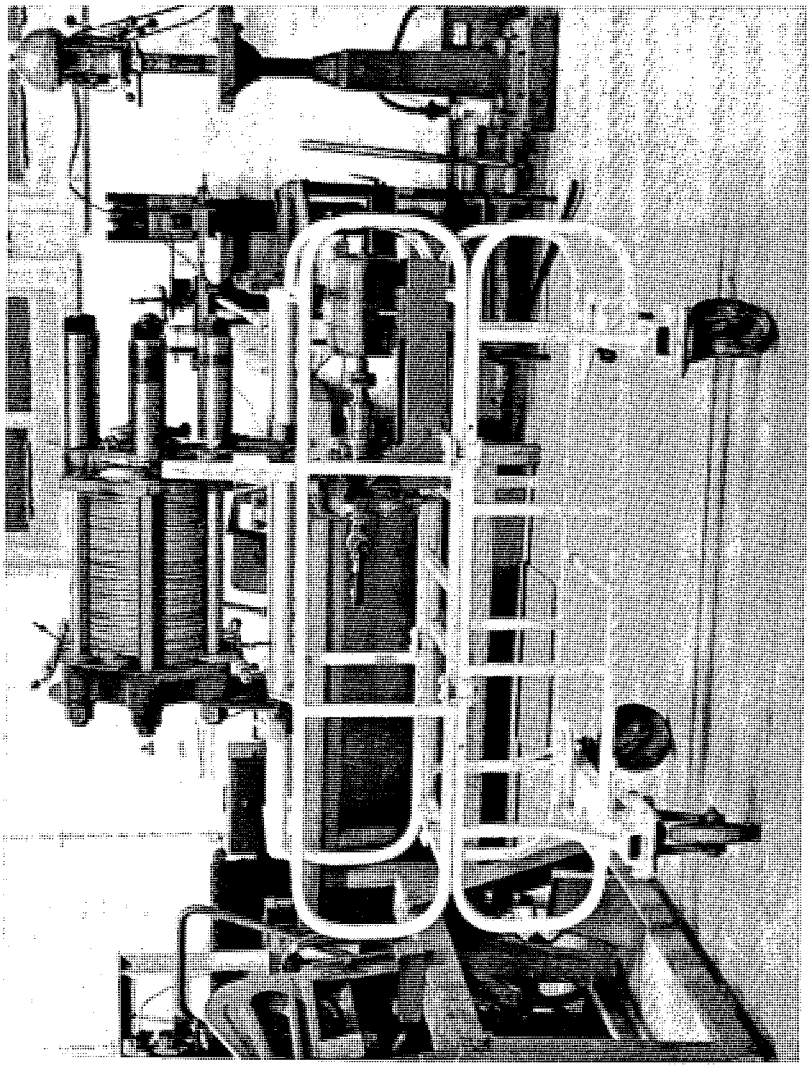

FIG. 19. 30-CELL BATTERY MOUNTED ON TROLLEY; HYDROGEN BLOWER MOUNTED UNDERNEATH

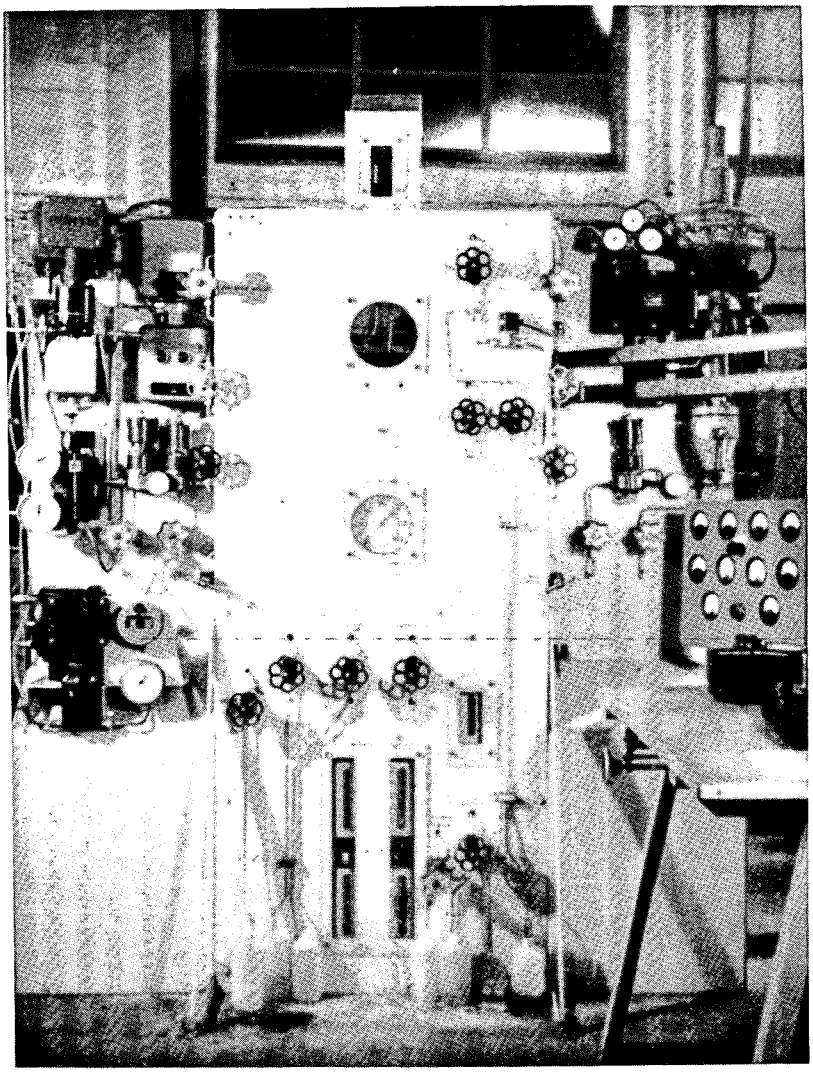

FIG. 20. CONTROL GEAR MOUNTED ON FRONT
OF PROTECTIVE FRAMEWORK

HYDROGEN/OXYGEN CELL (FIG 21)

RELATIONSHIP BETWEEN WEIGHT & ENDURANCE FOR 44 KW CELL

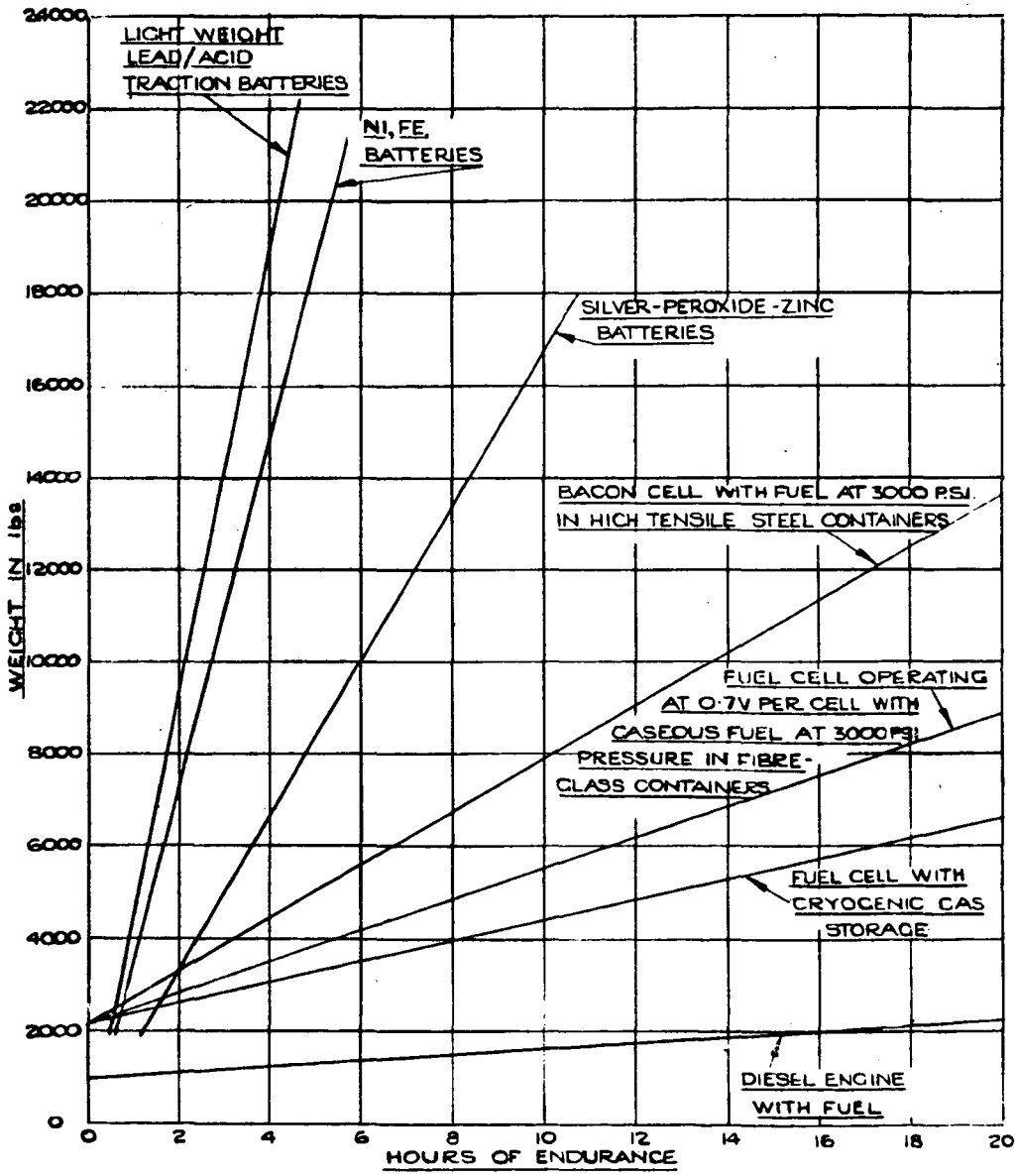

HIGH TEMPERATURE GALVANIC FUEL CELLS*

by

G.H.J. Broers
Central Technical Institute, The Hague, Netherlands

ABSTRACT

Stability of electrolytes for high temperature fuel cells will be discussed. Of all electrolytes investigated, only fused carbonates appear to be stable. The development of laboratory model magnesium oxide - carbonate cells and interpretation of their characteristics will be described. Performance results with regard to electrode gases and stability are surveyed.

* Manuscript not received in time for preprinting.

Not For Publication
Presented Before the Division of Gas anf Fuel Chemistry
American Chemical Society
Atlantic City, New Jersey, Meeting, September, 1959

The High Temperature Fuel Cell And the Nature of the Electrode Process

E. Gorin and H. L. Recht

CONSOLIDATION COAL COMPANY
Research and Development Division
Library, Pennsylvania

INTRODUCTION

Considerable activity has been generated in recent years on fuel cell research. The work has encompassed many different types of cells. The major portion of the work, however, has been concentrated on the low[1] and medium temperature[2] hydrogen oxygen cells and on the so-called high temperature gas cell.

No attempt will be made to review the rather voluminous literature in this field since many excellent review papers are available[3].

The high temperature cell may arbitrarily be defined as a gas cell which operates at atmospheric pressure and at temperatures in the general range of 500-900° C. It operates either with hydrogen or mixtures of hydrogen and carbon monoxide as fuel gas and usually with air as the oxidant. This is the type of cell which has excited most interest as a potential source of Central Station power.

Work on the high temperature fuel cell is now underway at quite a few laboratories throughout the world. The most extensive and probably the most successful work has been carried out at the University of Amsterdam under the direction of J. A. A. Ketelaar[4]. Broers[5] in particular has recently published an extensive account of the work carried out at Amsterdam.

Work has been conducted until recently on the high temperature cell at the laboratories of the Consolidation Coal Company. Recent publications[6] have described some of the experimental results as well as methods that could be employed for effecting the integration of the cell operation with the gas manufacturing process. Such integration is essential to realize the potential advantage of the fuel cell in achieving a high efficiency for power generation.

The high temperature cell[7] utilized in this work has been similar in most respects to that used by Broers[5]. The electrolyte used was mixed alkali carbonates disposed on a specially prepared pure porous magnesia matrix. In addition to the metal gauzes used by Broers, porous sintered metals have been used as the fuel electrode and a semi-conducting lithiated nickel oxide refractory as air[8] electrode. Likewise, metal gauzes, and in particular nickel and silver have been found to operate satisfactorily without the powdered metal activators used by Broers.

The basic problems that remain to be resolved before the fuel cell can attain commercial stature are the attainment of a system of acceptable life and power output. The resolution of these problems could be considerably expedited if a better understanding of the manner in which the cell functions were available.

The purpose of this paper is to present some thoughts with regard to the mechanism of the cell action. The experimental work carried out to date has not been sufficiently extensive to provide positive confirmation of the theories presented. The mechanism is put forth, therefore, without adequate experimental proof, in the hope that it may prove useful to other workers in the field.

EXPERIMENTAL METHOD AND RESULTS

The construction of the fuel cell, the method of fabrication of the components and the operating procedure have been described previously and will not be repeated here[7]. Likewise, some of the experimental results[6,7] have been presented before although in somewhat different form.

The data presented here serve as a basis for discussion of the mechanism of cell action. Most of the data given here revolve about the use of hydrogen as fuel gas. Considerable data have been accumulated also on carbon monoxide-carbon dioxide mixtures as fuel gas. The power outputs achieved are, in general, considerably lower than with hydrogen. These data are not included since the discussion revolves largely about the mechanism of the hydrogen and air electrodes only.

It is felt that the utilization of hydrogen will be the determining factor in any potential practical fuel cell system. All fuel gases that would be utilized in practice would be rich in hydrogen. Due to the relatively poor performance of the carbon monoxide electrode, the major portion of the carbon monoxide would likely be utilized indirectly through conversion in situ to hydrogen by means of the water gas shift reaction. The major distinction in practice between the low temperature and high temperature cells would be the ability of the latter to utilize the carbon monoxide even if it is only indirectly as discussed above.

Operating data obtained with the carbonate type cell are summarized in Tables IA and IB.

The electrolyte employed in the work reported here was an equimolar mixture of sodium and lithium carbonates throughout. Carbon dioxide was always added to the air stream as a depolarizer. The amount used is specified in Table IA.

The results given in the table are, except for individual cases noted, smoothed results. The method of least squares was used for this purpose based on the assumption of a linear drop in cell voltage with current drain. In order to apply this method it was necessary to correct for the decrease in open circuit voltage due to change in gas composition as a result of accumulation of reaction products with current drain. The theoretical voltage was calculated by the application of the Nernst equation. This figure is listed in Column 4) of Table IB. It is noted that the theoretical voltage with no current drain could not be calculated since it is effected by the very small but unknown amount of carbon dioxide in the hydrogen fuel gas.

The application of the statistical method to the treatment of the results is illustrated in Figures 1 and 2. The dotted lines present the field in which the experimental data should fall within a confidence limit of 95 percent.

The fit suggests that the cell operates without substantial electrode polarization at 700-750° C with porous nickel fuel electrode and either silver gauze or lithiated nickel oxide as the air electrode.

The above statement must be qualified, however, by the area as shown for the confidence limits. A polarization of up to .06 volts is permitted at 750° C and of up to .08 volts at 700° C.

Another check for polarization is the agreement between the cell resistance as measured directly by an A. C. bridge and that determined by the least squares analysis. The agreement is excellent for Run Ag2b at 750° C. Broers[5], likewise, reports excellent agreement between calculated and measured resistance even at lower temperatures. In the 700° C runs, however, the calculated resistance is definitely higher than measured. This does not necessarily indicate polarization, however, as will be shown later.

No realistic comparison could be made between measured and calculated resistance in many of the runs shown. This is because the open circuit voltage falls in some cases below the theoretical value. This is attributed to limited mixing of the fuel gas and air through microscopic cracks in the electrolyte matrix. Such cracks were observed after the runs were completed.

A few other interesting observations can be made. Silver is seen to be a fair hydrogen electrode although not nearly as good as nickel. It is practically worthless, however, as a carbon monoxide electrode.

Iron does not appear to be as good a hydrogen electrode as nickel. The data presented are not conclusive on this point. Numerous other data not presented here all point, however, to the same conclusions.

The above discussion is generally in accord with the findings of Broers[5].

Internal Resistance of the Cell

The high internal resistance of the cell during operation is noteworthy. Separate conductivity measurements were made to determine whether this could be attributed to some peculiar property of the electrolyte matrix. Measurements were made with the matrix loaded with an excess of the mixed carbonate melt. Two flat silver gaskets were used as electrodes. An average value of the resistance/cm^2 of 0.7 ohm was found in the temperature range of 700-800° C. The expected value from the thickness and porosity of the matrix, 0.2 cm and 28% respectively, and the specific conductivity of the melt 2.9 ohm^{-1} cm is only 0.25 ohm. Even so, the measured value is smaller by a factor of 7-10 than that observed during cell operation. Broers also found a similar high resistance during cell operation.

The high ratio between the resistance measured during cell operation and the inherent resistivity of the electrolyte matrix can be taken to have

the following significance. The melt inventory must be adjusted until a small area of contact is maintained between the electrode and the electrolyte. This may be required to maintain proper access of the gas to the electrode surface, and greatly increases the effective resistance of the electrolyte if the contact area is sufficiently small.

Consider, for example, an idealized model where the electrode maintains symmetrical square areas of contact having individual areas Δ^2 and a spacing between contact area d as shown in Figure 3.

The effective resistance of a cell containing two such identical infinite plane square mesh electrodes separated by an electrolyte of thickness ℓ may be calculated by a solution of Lapluces equation which relates the potential V to the position in the electrolyte

$$\nabla^2 V = 0$$

The calculation desired is the potential drop across such an electrode system as a function of the current density $\bar{I}$ and the specific resistance $\bar{R}$. This can then be compared with the potential drop across plane flat electrodes. The appropriate boundary conditions and solution of the above partial differential equation for this particular case was given previously[ab] and is omitted here for the sake of brevity. The solution is shown graphically in Figure 4 where the ratio R_{eff}/R is plotted as a function of ℓ/d with Δ/d as a parameter. R_{eff}/R is the ratio of the effective resistance to the resistance obtaining in the case where one has plane flat electrodes.

It is noted, for example, that the experimentally observed ratio R_{eff}/R of about 8.0 could be explained if the spacing d is about 3.2×10^{-2} cm and $\Delta/d = 1.8 \times 10^{-2}$. The above corresponds to an ℓ/d ratio of 6.3 which is in accord with the electrolyte thickness of 2 mm used in our work. It is interesting to note that such a situation corresponds to confining the electrode reaction to only 3.2×10^{-4} cm^2 per square centimeter of electrolyte surface.

The effective resistance ratio is very much a function of the spacing between contact areas. It is clear from Figure 4 that the resistance drops markedly for constant fractional active area as the spacing decreases. The importance of this factor in optimizing cell design is obvious.

Another way of illustrating this point is to repeat the same calculation with a different geometrical pattern. This was done with a parallel wire type electrode as shown in Figure 5. Such a system would correspond to the "hypothetical" case of a wire gauze electrode where none of the cross wires made contact.

Laplaces equation for this case was solved with the following pertinent boundary conditions:

$$\frac{\partial V}{\partial x} = \frac{\bar{I}\bar{R}}{\Delta/d} \qquad \text{for } x = -\Delta/2 \text{ to } +\Delta/2$$

$$= 0 \qquad \text{for } x = -d/2 \text{ to } -\Delta/2 \text{ and } x = \Delta/2 \text{ to } d/2$$

It was assumed again for simplicity that both electrodes were identical. The solution is

$$V = V_0 + \frac{i\bar{R}l}{2} + \sum_{n=1}^{\infty} \frac{i\bar{R}d}{\pi^2 n^2 r} \sin(n\pi r) \tanh\left(\frac{n\pi l}{d}\right) \quad \text{at } z = l/2 \tag{1}$$

$$\frac{R_{eff}}{R} = \frac{V_{z=l_2} - V_{z=l_2}}{i\bar{R}l} = 1 + \frac{2}{\pi^2 \left(\frac{l}{d}\right) r} \sum_{n=1}^{\infty} \frac{\sin n\pi r}{n^2} \tanh\left(\frac{n\pi l}{d}\right) \tag{2}$$

where $r = \Delta/d$ and $\bar{R}$ is the specific resistance.

The fractional area covered in this case is Δ/d as against $(\Delta/d)^2$ for the square mesh electrode. The points therefore were plotted with this in mind such that $(\Delta/d)^{1/2}$ for the parallel wire type electrode corresponded to Δ/d for the square mesh type.

It is readily seen that the parallel wire type electrode can tolerate a much smaller contact area without a large increase in cell resistance. Again the desirability of maintaining close spacing between contact points in cell design is emphasized.

Since the actual area of contact during operation of our cell was unknown one cannot state definitely that this is the major cause of the high resistance observed. Rather it seems likely that the low melt inventory itself may be partly responsible by causing part of the electrolytic conduction to be effected through small zones of extremely thin layers of melt.

As will be shown later, however, it is possible in principle to have a relatively low resistance as measured with an A. C. bridge and an effectively high resistance during cell operation as a result of the electrode reaction being concentrated in a very small area.

Maximum Rate of Electrode Reaction

The electrode reaction as mentioned above must be concentrated in a very small area due to the difficulty of providing acess of the gas through the three phase limit where electrode, electrolyte and gas meet. The minimum area required may be estimated as follows. The electrode reaction can certainly not take place, in the limit, any faster than gas molecules striking the metal surface can be adsorbed. Fortunately, Eyring[9] has provided us with a method of estimating this rate using his theory of absolute reaction rates. For the case where gas molecules strike a surface to form an immobile dissociated adsorbed film, Eyring gives the equation

$$V_1 = \frac{1}{2} \alpha C_g \bar{C}_a \frac{\sigma}{\sigma_\ddagger} \frac{h^4}{8\pi^2 I (2\pi m k T)^{1/2}} e^{-E_1/RT} \tag{3}$$

where V_1 is that rate of adsorption in molecules/cm^2 sec and E_1 is the activation

energy of adsorption. If we use $\lambda = 4$ and $C_s = 10^{15}$ sites/cm^2 as suggested by Eyring one calculates the adsorption rate for hydrogen as

$$v_i = 2.29 \times 10^{-5} T^{3/2} p_{H_2} e^{-E_1/RT} \text{ mols/cm}^2\text{sec.} \qquad (4)$$

Thus, if E_1 is small, i.e., equal to 3000 cal/mol, the endothermic heat of solution in nickel, the rate can be as large as 130 mol/cm^2 sec at 750°C. The above rate is sufficiently large such that a current density of 100 ma/cm^2 could be achieved on a surface as small as 4.0×10^{-9} cm^2/cm^2 of electrolyte area. Such a concentration of the electrode reaction, however, would , in view of the preceding considerations, cause a very considerable increase in the effective resistance of the cell.

In the case of the air electrode, under comparable assumptions, the maximum rate of the electrode reaction would be somewhat smaller due to the lower partial pressure and the higher molecular weight and moment of inertia of oxygen. Even so a rate of the order of 1 mol/cm^2 sec is possible in this case.

The Three Phase Limit

It is obvious that some mechanism must be in force for broadening of the three phase limit. Otherwise two deleterious factors come strongly into play, i.e., activation polarization as a result of concentrating the electrode reaction on a very small area and the concomitant high effective resistance discussed above.

Three mechanisms may be cited, diffusion of the gas through a thin film in the neighborhood of the interface, permeation of gas through the bulk electrode metal and finally surface diffusion across the electrode surface.

The first seems unlikely even though data on the permeation of gases through salt melts at high temperatures is unavailable.

Some data are available, however, on the diffusion and permeability rates of hydrogen and oxygen through aqueous solutions of electrolytes. For example, the diffusion constant of hydrogen through 20% NaOH solution[10] is reported as about 10^{-5} cm^2/sec at 25°C. The solubility C_o is of the order of 2×10^{-7} mols/cc at atmospheric pressure. The rate of transport of hydrogen to the electrode surface per unit area through an electrolyte film of thickness d is thus

$$\frac{D (C_o - C_1)}{d} = \frac{i}{2 \times 96500}$$

where C_1 is the concentration at the electrode interface. The exposure of as much as 1 cm^2 of surface to a thin film of electrolyte per cm^2 of electrolyte area seems rather unlikely with electrodes of the type used in this work. Even so one calculates in the above case that the average thickness of electrolyte film would have to be less than 6×10^{-6} cm to maintain a current density of 100 ma/cm^2.

Corresponding data are absent of course under conditions where the high temperature cell operates but it is not likely that the permeability of

gases through salt melts would be any higher due to a probably very low solubility of gases in melts. It would be interesting of course to obtain such data.

Data are available, however, from which the rate of permeation of gases through metals can be calculated. Probably the best data on the solubility of hydrogen in nickel and iron are those of Armbruster[11]. Edwards[12] gives corresponding data on the diffusion constant of hydrogen in nickel. Combining the two sets of data, one finds the permeation rate of hydrogen through nickel at atmospheric pressure $P = DC_o = 1.46 \times 10^{-6} \; e^{-\frac{13100}{RT}}$ mols/cm^7 sec. The permeation rate at 750° C is thus 2.37×10^{-9} mols/cm^2 sec/cm or greater by a factor of 10^3 than the permeation of hydrogen through electrolyte solutions at room temperature.

The rest of this paper is concerned with an examination of the permeation of gases through the metal electrodes as a mechanism for broadening the three phase limit. Some consideration is given also for the last mechanism.

Permeable Metal Gas Electrodes

A simplified model can be set up of the metal electrolyte contact such that the problem of a permeable metal electrode reaction can be treated mathematically. Such an idealized model is represented graphically in Figure 6. Here a cross section of the contact between the electrode and electrolyte matrix is represented. The cross section represents either a spherical metal granule of radius r, of the porous metal electrode or of a cylindrical wire of the same radius for the case where a wire gauze electrode is used. The angle ψ, represents the portion of the cross section where contact is maintained between the electrolyte and the metal electrode surface.

It is now necessary to make assumptions relative to the rate controlling processes. These must be made primarily on a basis of "reasonableness". It is assumed, therefore, that the rate of solution of gas into the metal is controlled by the rate of penetration of the gas from an adsorbed layer of dissociated atoms. Similarly the rate of dissolution is controlled by the rate at which the gas penetrates the metal surface to form the same adsorbed layer.

Experimentally it is known the rate of solution and dissolution of gas in metals is very rapid relative to the rate of permeation through the metal bulk[12]. No information is available, therefore, on the rate determining step for adsorption and desorption. The experimental facts are also consistent with the hypothesis that the dissolved gases are present in dissociated form when dissolved in metals. The adsorbed layer may therefore also be considered as being present in dissociated form.

Two further assumptions are now required, namely, that the rate of adsorption is very rapid relative to the rate of solution such that the concentration in the adsorbed layer is in equilibrium with gas phase. Similarly, it is assumed that the electrode reaction involves the adsorbed layer and again this is very rapid relative to the rate of desorption from the metal bulk. Thus again, the equilibrium electrode potential is maintained as determined by the concentration in the adsorbed layer.

Since the electrode must be at constant potential, it follows that the concentration of the adsorbed layer must be constant at all points within the electrolyte. This concentration C_1 may be considered to be equivalent to that in equilibrium with gas at a pressure P_1 in atmosphere, i.e., $C_1 = C_0 \sqrt{P_1}$. Similarly, the concentration of the adsorbed layer in the area outside of the electrolyte Cg, must be constant and in equilibrium with pressure of gas existing in the gas phase, i.e., $Cg = C_0 \sqrt{Pg}$. C_0 is the concentration in equilibrium with 1 atmosphere of gas.

The rate of permeation of the gas through the electrode may be obtained by solution of Ficks diffusion equation. For steady flow this reduces to

$$D \nabla^2 C = 0 \tag{5}$$

The boundary conditions for solution of the above equation based on the above assumptions are:

$$D\left(\frac{\partial C}{\partial r}\right)_{r=r_1} = -k(C - C_1) \qquad \psi = 0 \text{ to } \psi_1$$

$$D\left(\frac{\partial C}{\partial r}\right)_{r=r_1} = +k(C_g - C) \qquad \psi = \psi_1 \text{ to } \pi$$

where k is the rate of desorption of the gas from solution in the metal and C is the concentration of gas in the metal.

We obtain two solutions for the two cases considered:

a) Spherical Electrode Contact

$$C = \frac{(C_g + C_1) + (C_g - C_1)h}{2} - \left(\frac{k}{2D}\right)(C_g - C_1) \sum_{m=1}^{\infty} \frac{r^m \left[P_{m-1}(h) - P_{m+1}(h)\right] P_m(x)}{r_1^{m-1}\left(m + \frac{k r_1}{D}\right)} \tag{6}$$

where $x = \cos\psi$ and $h = \cos\psi_1$

and $P_m(x)$ are the Legendre polynomials of the first kind.

$$F = \pi r_1 D (C_g - C_1) X_1 \tag{7}$$

where

$$X_1 = \left(\frac{h_1}{D}\right) \sum_{m=1}^{\infty} \frac{m \left[P_{m-1}(h) - P_{m+1}(h_1)\right]^2}{(2m+1)\left(m + \frac{h_1}{D}\right)} \tag{8}$$

The flux F above is the total flow of gas through the metal electrode surface and is obtained by the integration

$$F = -2\pi r_1^2 D \int_{\psi_1}^{\pi} \left(\frac{\partial C}{\partial r}\right)_{r=r_1} \sin\psi \, d\psi \tag{9}$$

Now the flux F must equal the current flow so that we obtain

$$N\pi h_1 P \sqrt{P_g} \left(1 - \sqrt{\frac{P_1}{P_g}}\right) \bar{X}_1 = \frac{\bar{\imath}}{96500n} \tag{10}$$

where $\bar{\imath}$ is the current density in amps/cm^2, N is the number of spheres making contact/cm^2 area, n is the number of electrons involved in the electrode process (2 in the case of hydrogen) and $P = DC_0$ is the permeability of the gas through the metal. The above equation may be used to calculate the extent of electrode polarization ΔE as determined by the slow permeation through the electrode

$$\Delta E = \frac{RT}{nF} \ln\left(\frac{P_1}{P_g}\right) \tag{11}$$

The maximum current that may be drawn is determined by the value of $\bar{\imath}$ in equation (10) when $p_1 = 0$.

The basic assumption in the above derivation is that activation polarization is absent, i.e., the electrode reaction is very rapid. It will be seen in what follows that a rapid electrode reaction is a necessity in order to obtain adequate permeation rates in any case.

An interesting feature of equation (10) is that the permeation rate decreases only as the square root of the pressure. This tends to favor this

mechanism of broadening of the three phase limit in the low pressure range. The extent of polarization is thus proportional to permeation rate of the electrode P and is, as will be seen later, relatively insensitive to the rate of the electrode process.

b) Cylindrical Wire Electrode Contact

The solutions of equation (5) are obtained in this case in exactly the same fashion as before. They are given below

$$C = C_g - \frac{\psi_1}{\pi}(c_g - c_1) - \frac{2}{\pi}\left(\frac{k}{D}\right)(c_g - c_1)\sum_{n=1}^{\infty} \frac{r^n \sin\psi_1 \cos n\psi}{r_1^{n-1} n\left(n + \frac{k r_1}{D}\right)} \tag{12}$$

$$F = D(c_g - c_1)\left(\frac{k r_1}{D}\right)\left(\frac{4}{\pi}\right)\sum_{n=1}^{\infty} \frac{\sin^2\psi_1}{n\left(n + k r_1/D\right)} \tag{13}$$

$$NP\sqrt{p_g}\left(1 - \sqrt{\frac{p_1}{p_g}}\right)\bar{X}_2 = \frac{\bar{i}}{96500\,n} \tag{14}$$

$$\bar{X}_2 = \frac{4}{\pi}\left(\frac{k r_1}{D}\right)\sum_{n=1}^{\infty} \frac{\sin^2\psi_1}{n\left(n + \frac{k r_1}{D}\right)} \tag{15}$$

The form of the above equations is very similar to the spherical case. N in this case is defined as the number of cylindrical wires of unit length in contact with 1 cm^2 of electrolyte surface.

It is noted that in all cases the flux factor X in the above equations is determined only by the term ($\frac{k r_1}{D}$). The rate constant for the electrode reaction k is unknown.

However, it is possible to make some deductions from the experimental data as to the permissible range of this rate. It is implicit in the above derivation that the rate of the electrode process k (C_g - C_1) must be less than the rate of adsorption from the gas phase.

Consider now porous nickel as a hydrogen electrode. It was shown previously that a maximum value for the adsorption rate at 750°C is of the order of 130 mols/cm^2 sec. For hydrogen in nickel D = 6 x 10^{-5} cm^2 sec^{-1} and C_o = 3 x 10^{-5} mols/cc at 750°C. Thus for a particle of 65 microns diameter mean particle size of the metal granules in the electrode used

$$k(c_o) < 130 \qquad \frac{k r_1}{D} < 2 \times 10^8$$

It is therefore clear that for the present very large values of ($\frac{k r_1}{D}$) are not ruled out. Computations of the flux factor X, however, become very laborous for values of ($\frac{k r_1}{D}$) > 500. Computed values of the flux factor as a function of the contact angle ψ_1 and the flux factor are shown in Figure 7. It may be shown from the behavior of equation (8) that as $\frac{k r_1}{D}$ increases indefinitely so does the flux factor. It is seen from Figure 7 that X may be extrapolated to higher values of ($\frac{k r_1}{D}$) by use of the empirical relationship

$$X_1 = A \left(\frac{k r_1}{D} \right)^n$$

The polarization curves calculated in this way for several assigned values of ($\frac{k r_1}{D}$) and for several immersion angles are illustrated in Figure 8. The cases shown correspond to perfect contact between the electrode and electrolyte, i.e., every granule in a close-packed array makes contact.

It may be noted that the polarization curves are readily translated to different values of P, N, r, and X. Thus, the current density at which an equivalent polarization is obtained is proportional to P, N and X. For close-packed array of contacts it is also proportional to r_1. For the same number of contacts/cm^2 it is inversely proportional to r_1.

The experimental results with the hydrogen nickel electrode showed that the polarization voltage was less than .08 volts at temperatures above 700°C. It is seen from Figure 8 that such a result can reasonably be achieved with the permeation mechanism cited although the case is far from proven.

The permeation rate, as noted above, goes down with temperature. Thus at 600°C it is lower by a factor of 3 and consequently only 1/3 as much current could be drawn before an equivalent amount of polarization sets in. The earlier onset of polarization at lower operating temperatures has been noted in our work and by others.

The polarization curves shown in Figure 8 correspond to rather perfect contact between electrode and electrolyte. The effective resistance ratio may be estimated as discussed above. Take for example, the case shown for $\psi = 5°$, the values of Δ/d, and ℓ/d in this case are .02 and 30 respectively. Referring to Figure 4 the calculated $R_{eff}/R = 2.5$ which is considerably smaller than the observed value of 7. In actuality, less than perfect contact may be anticipated. The case is also illustrated in Figure 8 where only one in two particles at the electrode surface actually make contact. The predicted polarization in this case is in accord with that observed while R_{eff}/R rises according to Figure 4 to 3.5 which is closer to the observed ratio.

One must make one important qualification, however, since it can be shown that for high values of (k_1/D) the current is concentrated over a relatively small fraction of the total contact area. Thus the effective resistance ratio would actually be greater than the value estimated above.

As a matter of fact, a peculiar feature of this treatment of the electrode process is that an extremely rapid electrode reaction causes it to be concentrated in a small area and thus increases the effective internal resistance of the cell.

The iron electrode may be evaluated in a similar fashion. The permeability of hydrogen through iron from the data of Smithells and Ramsley[13] may be described by the following equation

$$P_o = 2.01 \times 10^{-7} \; e^{\frac{-9800}{RT}} \quad \text{mols/cm}^2 \text{ sec/cm.}$$ Thus,

P_o at 750°C is equal to 1.8×10^{-9} which is very close to the value for the permeability of nickel. On this basis its performance as a hydrogen electrode should be very similar to nickel which is in accord with the facts.

The relatively poor performance of carbon monoxide electrode may be ascribed to its low permeability through the metal electrodes.

We will now turn our attention to a discussion of the silver electrode. This electrode was used both as a hydrogen and air electrode in the form of wire gauze. We therefore use equation (15) to discuss this case. The variation of the flux factor X with $(\frac{k_1}{D})$ using the contact angle as parameter is shown in Figure 8. Again the flux factor may be extrapolated to higher values of $(\frac{k_1}{D})$ by means of the empirical equation

$$X_2 = A \left(\frac{k_1}{D} \right)^n$$

The justification again is the behavior of equation (15) which shows that X increases indefinitely as $(\frac{k_1}{D})$ increases. As a matter of fact it may be shown that equation (15) takes the form

$$X_2 = \frac{4}{\pi} \sum_{n=1}^{\infty} \frac{\sin^2 n\psi}{n} \qquad (16)$$

as $\left(\frac{kr_i}{D}\right) \rightarrow \infty$. The above series diverges and thus X_3 becomes infinite. Likewise it may be shown the current is concentrated in an infinitely small area.

The permeability of oxygen through silver was measured by Johnson and LaRose. Their results may be expressed by the equation

$$P_o = 6.2 \times 10^{-6} e^{-\frac{22600}{RT}}$$

and shows a value for P_o of 9.3×10^{-11} mols/cm^2 sec at 750° C. The diffusion coefficient may be obtained by combining the solubility data of Steacie and Johnson[15] with the above permeability data. Thus the value of D at 750° C is 9.5×10^{-6} cm^2 sec^{-1}. By the same argument as was developed previously for nickel we find than the maximum possible value of $\frac{kr_i}{D} \cong 7 \times 10^7$. The maximum current that can be drawn in air under the assumption that all wires contact the electrolyte matrix throughout their length can now be computed for various assigned values of $\left(\frac{kr_i}{D}\right)$. These figures are shown in the table below:

Short Circuit Current For
30 Mesh Silver Wire Gauze Electrode $r_1 = 7 \times 10^{-3}$ cm

Contact Angle	$\frac{kr_i}{D}$	Short Circuit Current ma/cm^2
12.8°	2000	5.0
1.28°	2000	2.8
1.28°	7×10^7	42.0

It is now seen that permeation through a silver air electrode is nowhere sufficiently fast to explain its performance.

Similar considerations may be made with regard to the silver hydrogen electrode. Accurate data are not available for the permeation rate of hydrogen through silver. The indications again are, however, that it would be insufficient to explain its performance as a hydrogen electrode.

To resolve these discrepancies, it is necessary to assume that the permeation rate through a thin surface layer of the metal is much greater than through the metal in bulk. Equations may be derived for this case in a similar manner to the bulk permeation case treated above. The result, for example, for rapid permeation through a thin surface spherical shell of thickness Δ is given below

$$F = \pi r_1 D (c_g - c_1) X_3 \tag{17}$$

$$X_3 = \left(\frac{kr_1}{D}\right) \sum_{m=1}^{\infty} \frac{m\left[P_{m-1}(k) - P_{m+1}(k)\right]^2}{(2m+1)\left(m + \frac{kr_1^2}{\Delta D(m+1)}\right)} \tag{18}$$

Thus, the form of the equation is identical to that for bulk diffusion with the only change being in the flux factor X_3. The dependence of the polarization voltage on the system variables is thus identical.

In conclusion, the performance of the nickel and iron electrodes can be explained on the basis of the bulk permeation rate through the metal. The silver electrode performance required the introduction of the concept of accelerated surface diffusion. Further experimental data are required to determine whether variation of cell performance with system variables such as gas concentration behaves in the predicted fashion.

Literature Cited

1 G. E. Evans

Proceedings of the 12th Annual Battery Research and Development Conference (U.S. Army Signal Corps Research and Development Laboratories Publication) May 1958.

2 F. T. Bacon

The Beama Journal, 61, 2-8 (1954).

3 J. H. McKee

The Production of Electricity From Coal, British Coal Utilization Research Association Bulletin 9, No. 7 193-200 (1945).

A. M. Adams

Fuel Cells II Low Temperature Cells, Future Development, Chemical and Process Engineering, 35, 238-240, 1954.

4 J. A. A. Ketelaar

Die Ingenieur 66, 34 E 88-91 (August 20, 1954).

5 G. H. J. Broers

"High Temperature Galvanic Cells" Thesis, University of Amsterdam, 1958.

6 E. Gorin and H. L. Recht

A. Mechanical Engineering, 81, No. 3, 63 (1959).

B. Chemical Engineering Progress in Press. 55, 51-8 Aug 1959

7 E. Gorin and H. L. Recht

Proceedings of the Tenth Annual Battery Conference, May, 1956.

Proceedings of the Twelfth Annual Battery Conference, May, 1958.

Quarterly Reports 1 - 17 to the
Signal Corps Engineering Laboratories
Fort Monmouth, New Jersey, 1954-1958

8 E. Gorin and H. L. Recht

U. S. Patent Application Pending.

9 H. Eyring, S. Glasstone and K. J. Laidler

Theory of Rate Process - McGraw-Hill, 1941.

10 V. Ipatieff and V. I. Tikhomirov

J. Gen. Chem. USSR 7, 736-9 (1931).

11 M. Armbruster

J. Am. Chem. Soc., 65, 1050 (1943).

12 A. G. Edwards

Brit. Jour. of Applied Physics, 8, 406 (1957).

13 C. J. Smithells and C. B. Ramsley

Proc. Roy. Soc. London A, 157, 292 (1936).

14 F. Johnson and P. LaRose

J. Am. Chem. Soc., 46, 1377 (1924).

15 Steacie and Johnson

Proc. Roy. Soc. A, 112, 542 (1926).

Table I

Summary Fuel Cell Performance Data

A. CONDITIONS OF RUNS

Run No.	Temp., °C	Fuel Electrode	Air Electrode	Fuel Gas Comp.	% CO_2 in Air
Ag-2a	700	"D" Porosity Porous Nickel	80 Mesh Silver Gauze	97% H_2-3% H_2O	16.6
Ag-2b	750	"	"	"	11.1
Ag-2c	800	"	"	"	18.2
Ag-12	750	"	"	"	11.1
Ag-13	800	Fe Powder on "D" Porosity Stainless Steel	"	"	11.1
N-6	700	"D" Porosity Porous Nickel	Lithiated Nickel Oxide	"	11.1
N-16	750	"D" Porosity Porous Nickel	Lithiated Nickel Oxide	"	11.1
Ag-7B	825	80 Mesh Silver Gauze	80 Mesh Silver Gauze	"	16.6
Ag-7C	825	"	"	2 CO - 1 CO_2	16.6

Table I

Summary Fuel Cell Performance Data

B. CURRENT DRAIN BEHAVIOR

Run No.	Current Density ma/cm²	Voltage		Specific Resist. ohm cm	
		Measured	Calc. Open Circuit	Measured	Calculated
Ag-2a	0	1.216	-	6.4	9.1
	30	0.918	1.191	↓	↓
	65	0.578	1.170	↓	↓
Ag-2b	0	1.250	-	5.2	5.3
	30	1.012	1.180	↓	↓
	65	0.781	1.128	↓	↓
	100	0.572	1.100	↓	↓
	127	0.426	1.076	↓	↓
Ag-2c	0	1.170	-	7.6	-
	65	0.625	1.191	↓	-
	100	0.418	1.160	↓	-
Ag-12	0	1.180	-	7.4	-
	35	.923	1.184	↓	-
	65	.680	1.145	↓	-
Ag-13	0	1.143	-	4.2	-
	32*	0.832	1.206	↓	-
Ag-7B	0	0.181	0.931	-	-
	10*	0.140		-	-
N-6	0	1.230	-	7.3	11.1
	30	0.872	1.212	↓	
	65	0.440	1.165	↓	
	100	0.030	1.138	↓	

* Actual experimental points.

Figure 1

Cell Performance at 750°C

Porous Nickel — Fuel Electrode
Silver — Air Electrode
H_2 — Fuel Gas

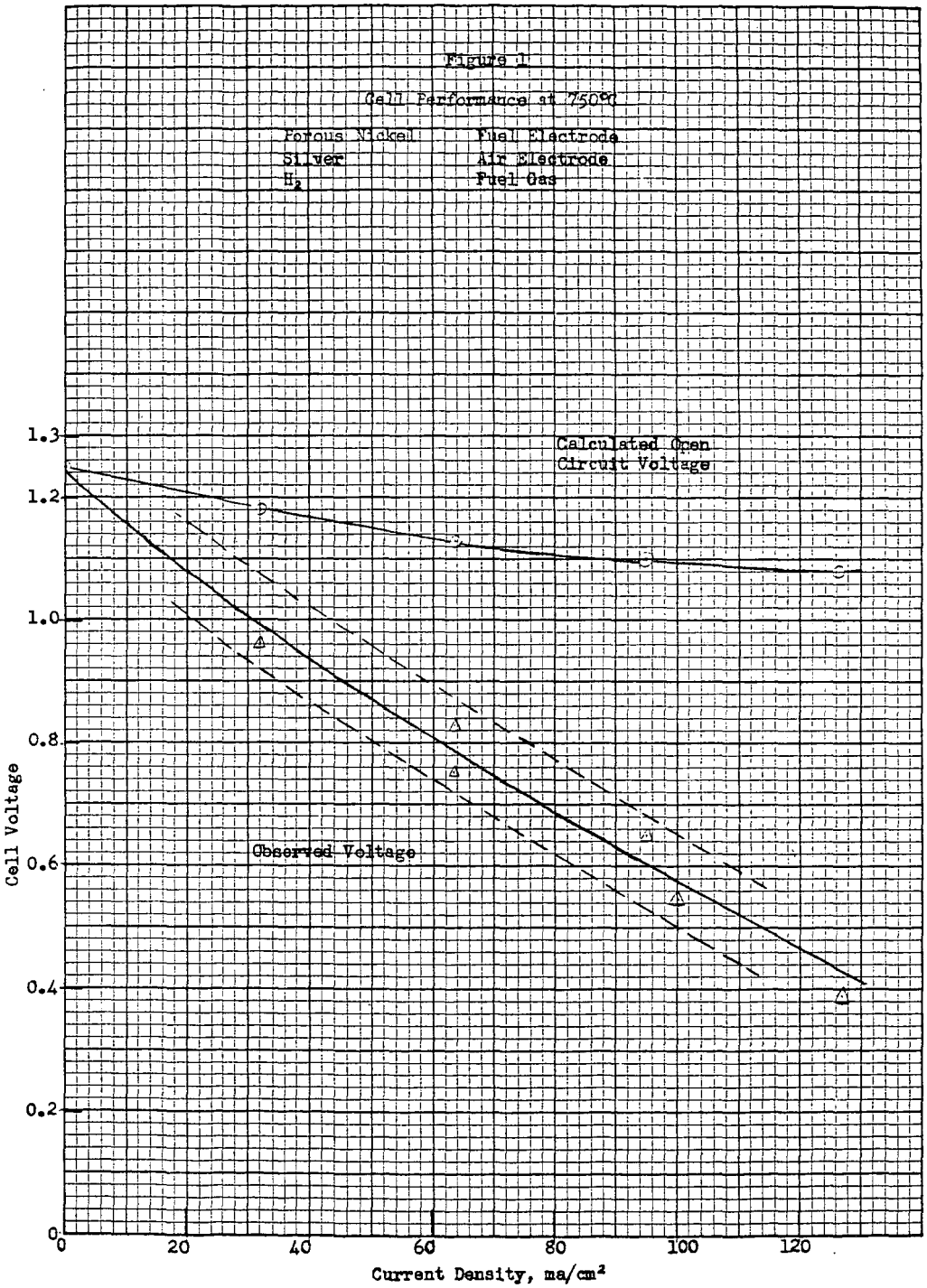

Figure 2

Cell Performance at 700°C

Porous Nickel — Fuel Electrode
Lithiated Nickel Oxide — Air Electrode
H_2 — Fuel Gas

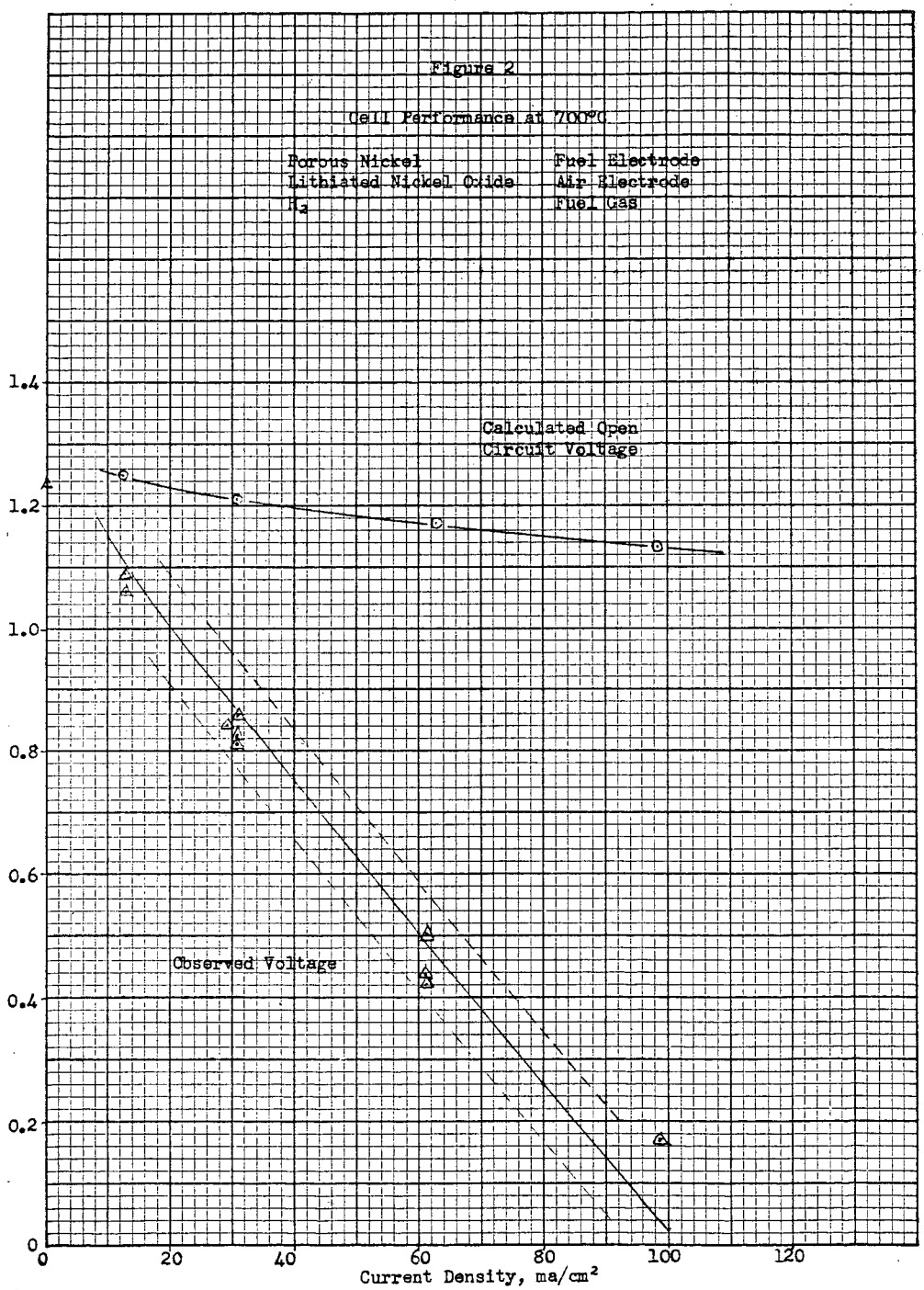

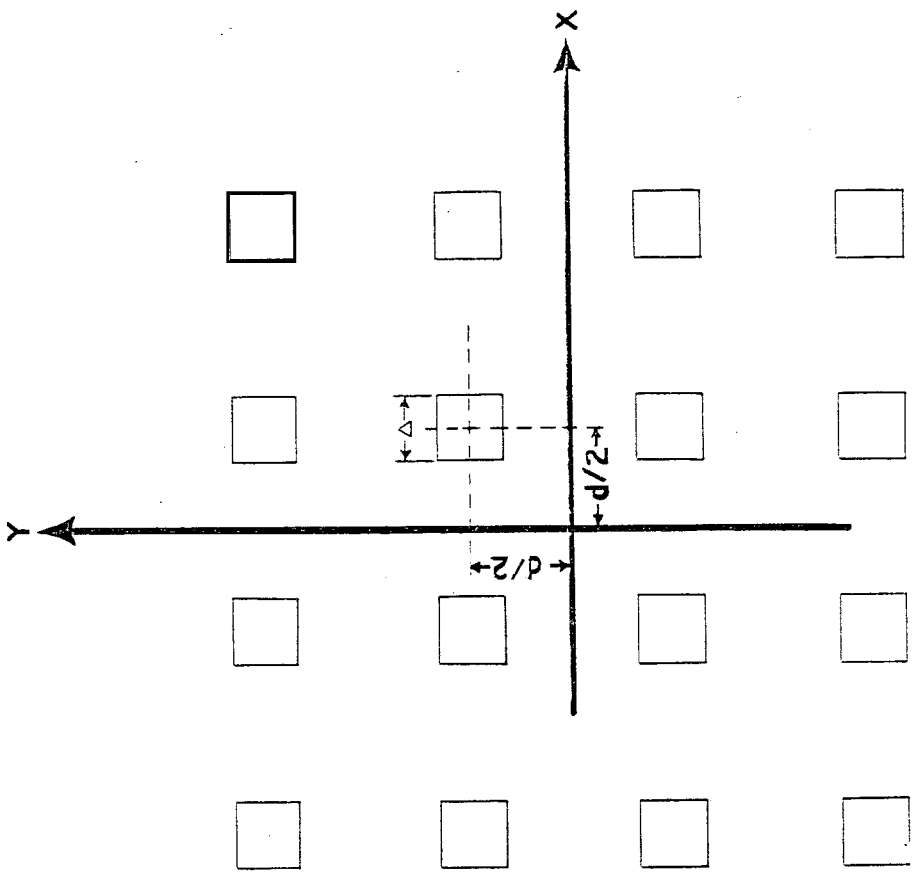

Figure 3

Diagram of Square Mesh Electrode

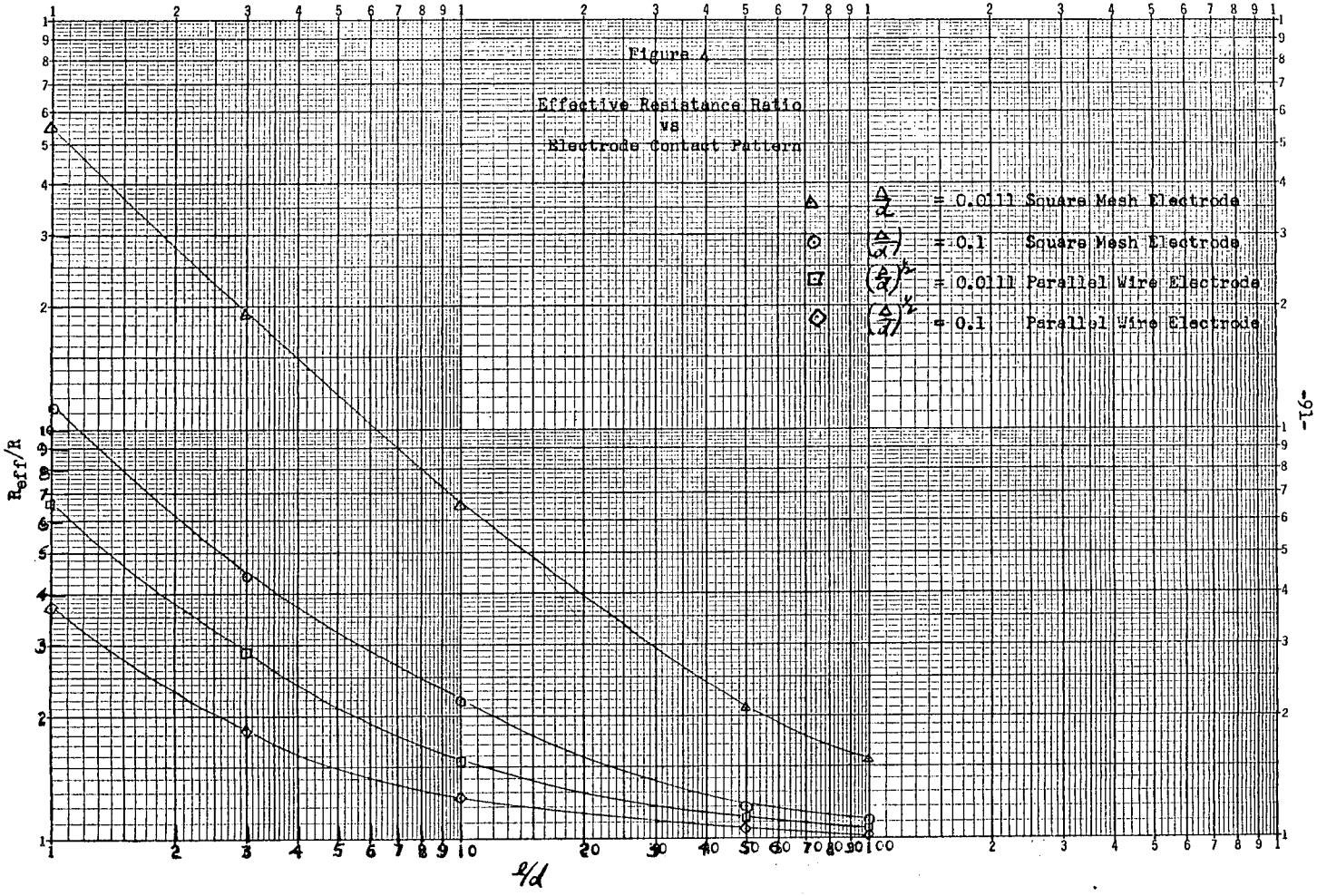
Figure 4
Effective Resistance Ratio
vs
Electrode Contact Pattern
Δ/d = 0.0111 Square Mesh Electrode
(Δ/d)' = 0.1 Square Mesh Electrode
(Δ/d)' = 0.0111 Parallel Wire Electrode
(Δ/d)' = 0.1 Parallel Wire Electrode
Reff/R
ℓ/d

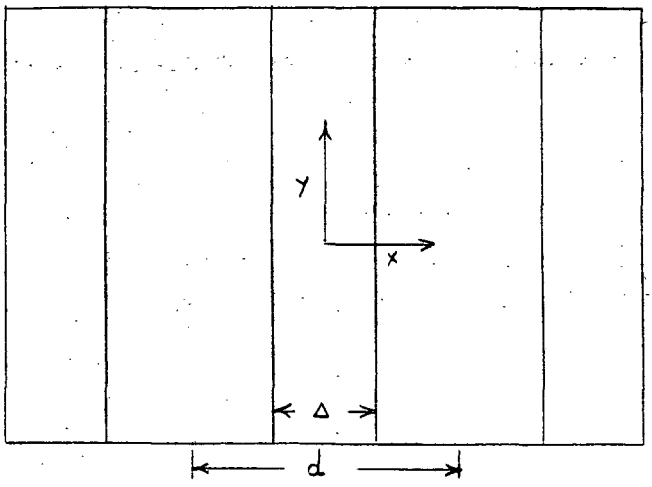

Figure 5. Diagram of Parallel Wire Type Electrode

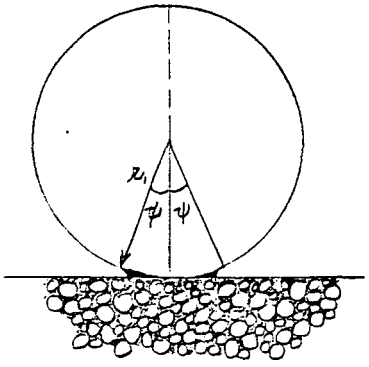

Figure 6. Diagram of Electrode Contact

Figure 7

Flux Factor For Spherical Electrode

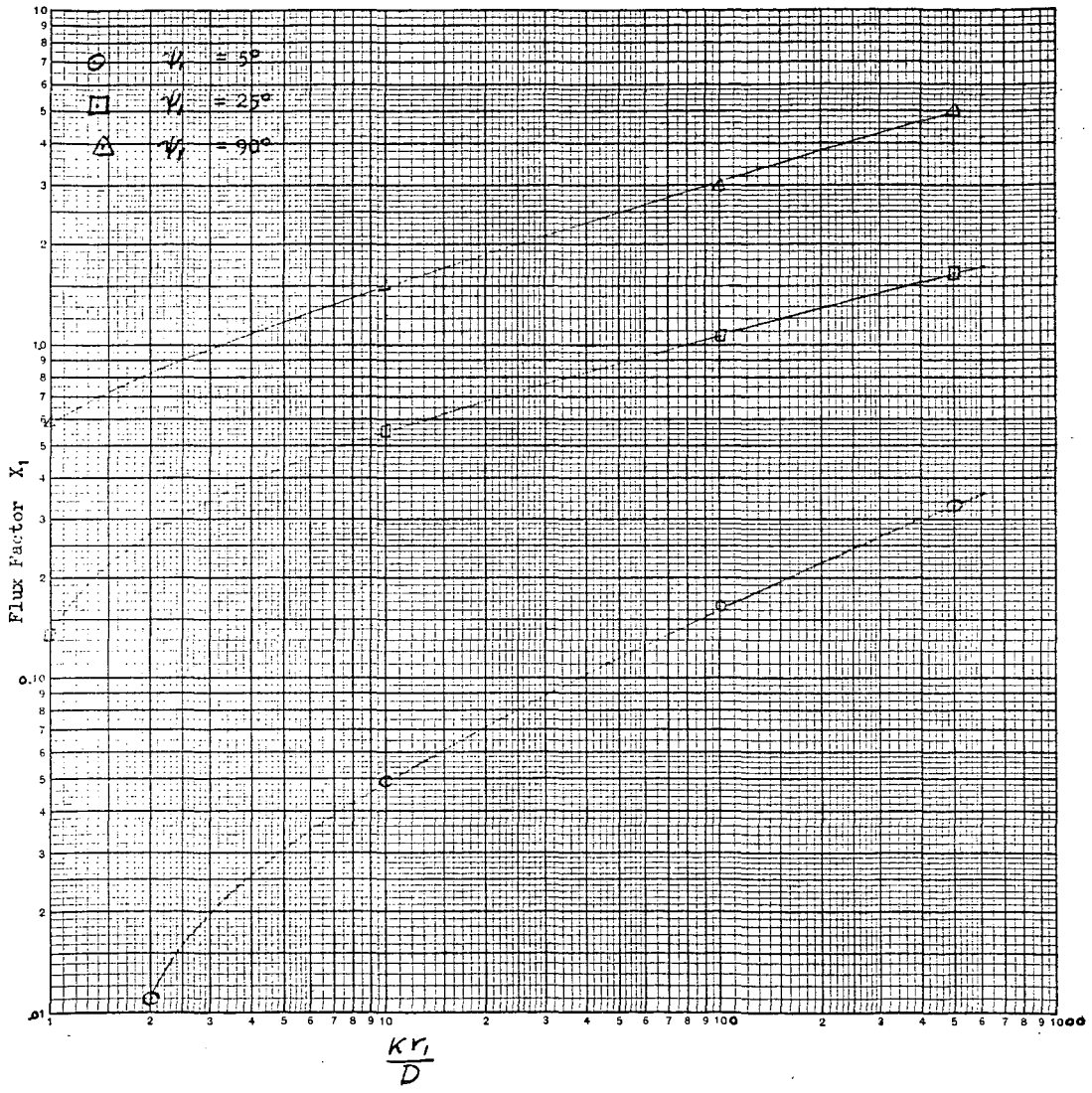

Figure 8

Polarization Due to Slow Formation
Through Spherical Hydrogen Electrode

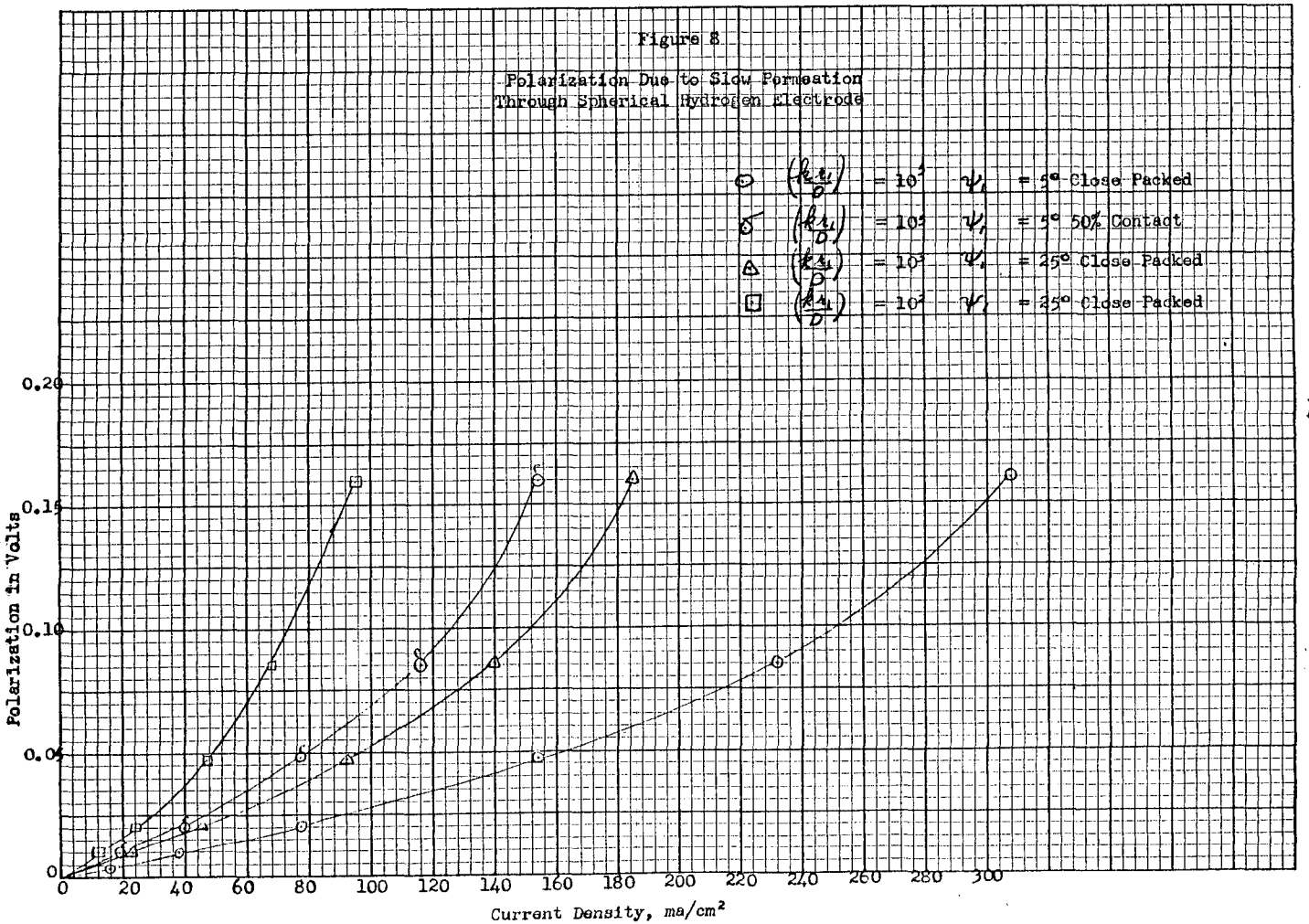

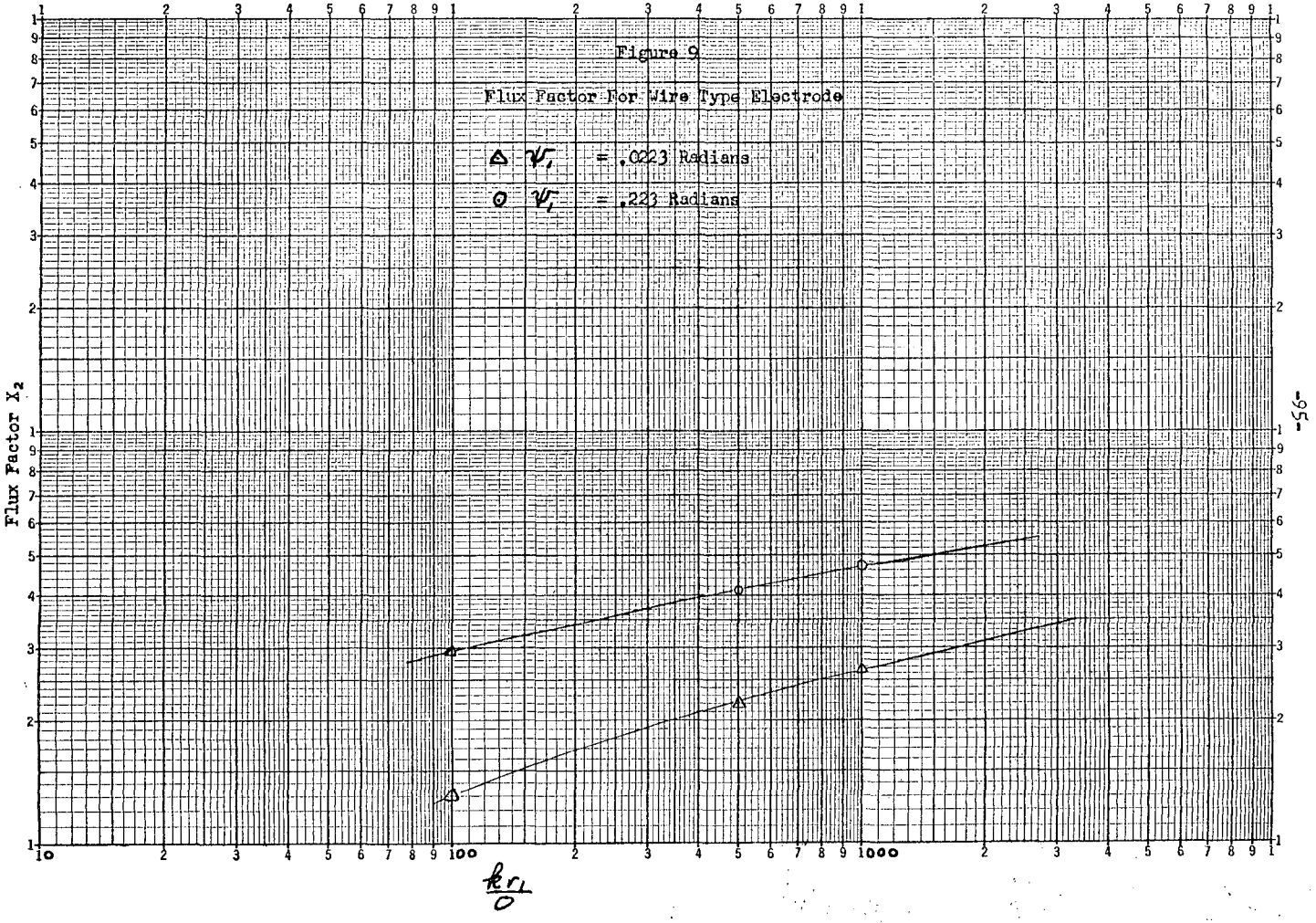
Figure 9
Flux Factor For Wire Type Electrode
Δ ψ₁ = .0223 Radians
○ ψ₁ = .223 Radians
Flux Factor X₂
kr₁/0
10
100
1000

MOLTEN ALKALI CARBONATE CELLS WITH GAS-DIFFUSION ELECTRODES*

by

David L. Douglas
Research Laboratory, General Electric Co.
Schenectady, New York

ABSTRACT

The application of gas-diffusion electrodes to high temperature fuel cells offers the possibility of obtaining the large current densities associated with such electrodes in low temperature cells. In addition the high internal resistance, electrolyte contamination and fragility encountered in the magnesia diaphragm cells are avoided. The problems which arise in connection with design and construction of gas-diffusion electrodes are control of pore size distribution and selection of materials.

An apparatus has been assembled to study the performance of small gas-diffusion electrodes immersed in a molten mixture of lithium, sodium and potassium carbonates. A reference electrode, consisting of a porous plug of gold sintered into a gold tube, permits study of the polarization characteristics of the individual electrodes. This is operated as an unloaded cathode (oxygen electrode). Gas-diffusion electrodes have been fabricated successfully using commercially available porous nickel and stainless steels and various sintered silver powders. Nickel shows very little polarization as a hydrogen electrode at temperatures above 500 C. Porous 431 stainless steel as a carbon monoxide electrode shows comparable polarization losses at 600 C. The data suggest that both the hydrogen and carbon monoxide electrodes suffer some activation polarization. In agreement with other workers we have found that silver makes an oxygen electrode showing negligible polarization above 600 C.

The cell assembly, although having large electrode separation, yields power densities at 600-650 C. comparable to those obtained from magnesia diaphragm cells operated at higher temperatures. It is anticipated that these will improve greatly when parallel close-spaced electrodes are used. No life tests have been carried out, but cells have been operated continuously for 100 hrs. Individual electrodes have operated without failure for several hundred hours. It appears that the operating life of electrodes will be limited by corrosion processes at the electrodes.

* Manuscript not received in time for preprinting.